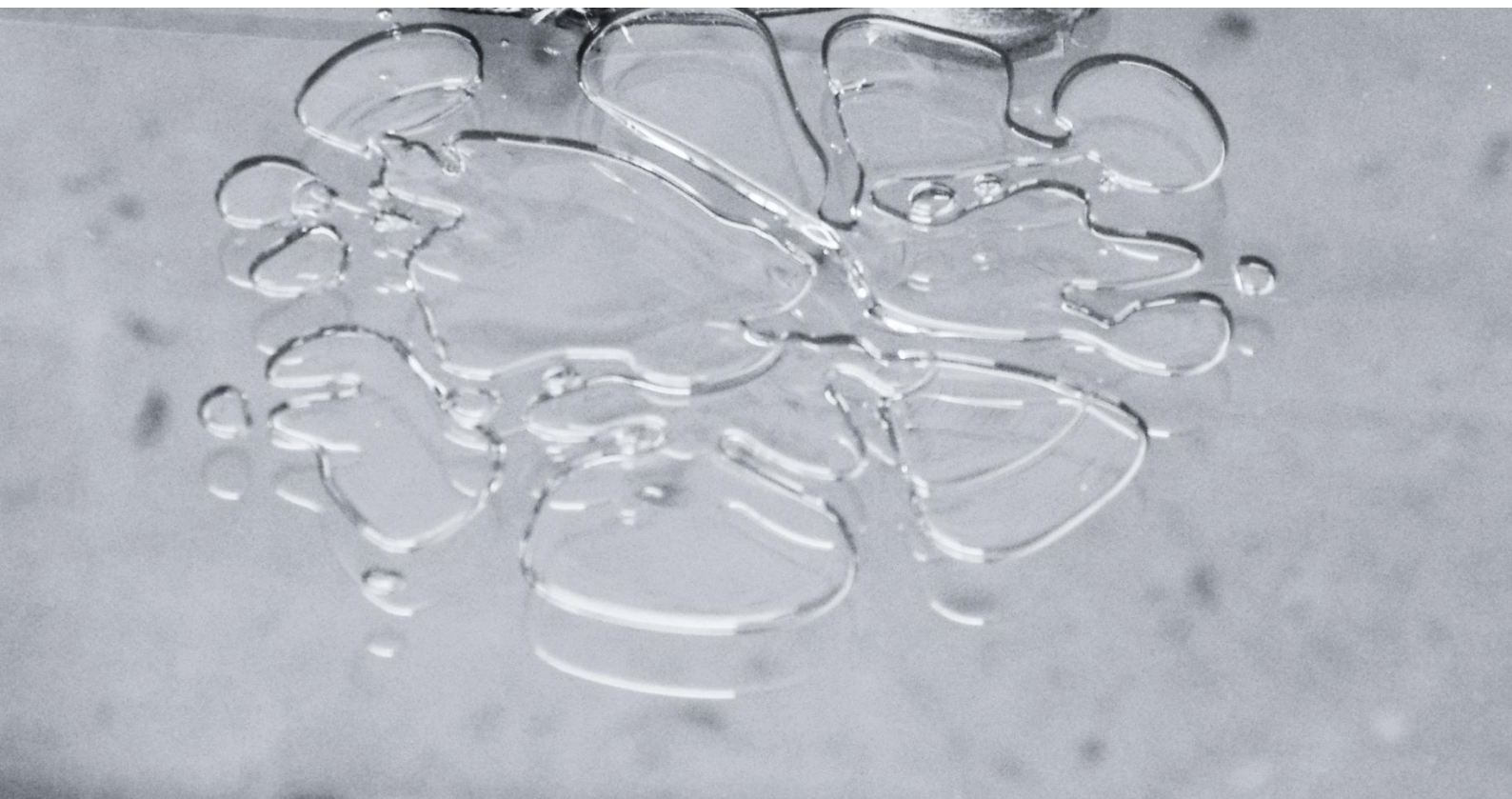# Performance of structural glass at elevated temperatures

A research into the Young's modulus of glass and the effect of coatings on laminated glass panels at elevated temperatures

A. A. C. Loman

Performance of structural glass at elevated temperatures

A research into the Young's modulus of glass and the effect of coatings on laminated glass panels at elevated temperatures

By

A.A.C. Loman

in partial fulfilment of the requirements for the degree of

Master of Science

in Civil Engineering, Building Engineering,

Faculty of Civil Engineering and Geosciences
Delft University of Technology

September 2019

TUDelft

Thesis Committee

Prof. ir. R. Nijsse	TU Delft, faculty of Civil Engineering and Geosciences
Dr. ir. H.R. Schipper	TU Delft, faculty of Civil Engineering and Geosciences
Dr. ir. F.A. Veer	TU Delft, faculty of Architecture and the Built Environment

An electronic version of this thesis will be available at *http://repository.tudelft.nl/*.

Cover image: bubble formation in interlayer laminated glass panel

Preface

I am grateful to present you my Master thesis about the performance of structural glass at elevated temperatures. It has been written to fulfil the requirements for the degree of Master of Science in Building Engineering at the Technical University of Delft. I learned a lot during this challenging period; conducting experimental research was completely new to me.

Therefore, I would like to thank my graduation committee for guiding me through this process. First of all my daily supervisor Fred Veer, for his experimental and material knowledge and always providing patient advice. Roel Schipper for his valuable feedback and problem-solving approach and Rob Nijsse for his practical approach and for inspiring me to choose the topic of structural glass. I would also like to thank Christian Louter for introducing me into the topic of fire safety of structural glass and his guidance in the first period of my graduation.

Furthermore, I would like to express my gratitude to Hans Brouwer, who enabled me to make use of the tube furnaces and assisted me during the experiments. Albert Bosman for his assistance in preparing the ultrasonic measurements. And Kees van Beek for his guidance during the experiments with the laminated glass panels. Additionally, I would like to thank AGC for providing me the laminated glass panels for the experiments.

Finally I would like to thank my boyfriend, friends and family for their unconditional support and understanding during my graduation.

Anouk Loman,
Delft, September 11, 2019

Abstract

Nowadays glass is more commonly applied as structural element, either as a replacement for, or in collaboration with conventional building materials such as steel, aluminium, timber and concrete. Key arguments to opt for glass in structural design are sustainability, aesthetics and transparency. As for all structural elements, glass elements are required to be structurally safe, even in extreme conditions such as during a fire. Building regulations demand a structural element to be able to withstand a fire for at least 30 minutes. There is however a lack of experimental results on the material properties and performance of structural glass elements at elevated temperatures.

One of the key material properties that determines the performance of glass at elevated temperatures is its stiffness (Young's modulus). In this research the Young's modulus of both Sola Lime Silica (SLS) and Borosilicate (BS) glass is experimentally determined for temperatures up to 700°C. The transmittance time of high-frequency sound waves (ultrasound) is measured for both BS as SLS glass rods during heating in a tube furnace. From this data the Young's modulus has been derived mathematically.

Additionally, the effect of a low-E coating and an intumescent coating on the performance of laminated glass panels is experimentally determined and assessed. During heating of only one side of the laminated glass panels, the time until the interlayer starts to form gas bubbles is recorded, whereas the temperature of the glass has been measured on both sides of the glass panels.

From the experiments it is observed that glass performs well up to temperatures of 500 °C, provided there are no distributed thermal stresses present in the glass. Given this condition, the remaining stiffness at a temperature of 500 °C is 90% for SLS glass and 102% for BS glass. As for structural steel this is only 60%, it is concluded that both SLS and BS glass outperform steel in terms of relative stiffness at elevated temperatures. Between 500 and 600 °C a sudden deformation is observed. Therefore the structural safety of a glass element cannot be guaranteed for temperatures beyond 500 °C.

The heating of a glass element can be delayed by the application of an intumescent coating. For low-E coating, an improvement in fire resistance is however not proven in this research. Instead, a negative effect has been observed and therefore the application of low-E coating is not recommended.

It was shown that the PVB interlayer is the weakest point of the glass element. At temperatures of 200 °C the PVB interlayer is already completely molten, while at 500 °C the glass is still intact. The fire resistance can be improved by applying glass without an interlayer.

Table of Contents

III EXPERIMENTAL TESTING

IV CONCLUSIONS & RECOMMENDATIONS

x

I
Introduction

1. Introduction

Glass is an interesting material, with impressive properties. It has a high transparency, which makes it perfect to look through it, but yet water and other aggressive substances cannot pass through it. Glass is also known for its brittle behaviour. It has a high resistance against compression, but yet a limited tensile resistance, which can cause breakage into large sharp pieces. This makes glass not the first material to think of as a structural load-bearing material. The question that arises is, how was glass introduced into the building industry?

The first discovery of glass was in the form of the rock crystals that were found in mountain caves. It looked like ice, but did not melt. To the primitive men this must have been magic. Then people learned how to make glass. The story of a Roman writer goes that one day a ship belonging to traders in soda entered the shore of the sandy beach and spread out along the shore to make a meal. Since they needed supports for their cooking-pots, they placed chunks of soda on the sand. When these became hot by the cooking-pots it fused with the sand and chalk (seashells) and streams of an unknown translucent material flowed. It didn't take long for the traders to realize the commercial potential of this shimmering, transparent material, now known as glass.

Different techniques were developed to shape and manipulate this material. The blowpipe is probably one of the most intelligent ones, which gave the opportunity to make bottles, cups, vases and ornaments. This technique led also to the production of round glass plates by quick rotation of the blowpipe after a large glass bubble was pricked open. Even plates up to a diameter of 1 m were possible. This plate could be divided into smaller rectangular parts and the glass window was born.

Figure 1 Production of glass plates by quick rotation (retrieved from http://www.londoncrownglass.f9.co.uk/History.html)
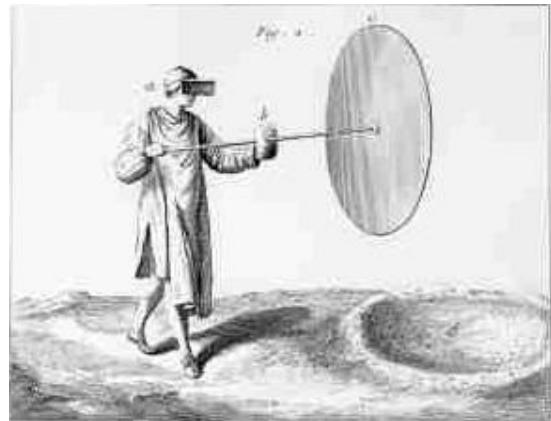
These glass parts were limited in size to 400 x 300 mm and were set in a wooden or bronze frame. These "windows" allowed the entrance of daylight, while wind, rain or cold stayed outside.

In the 14th century a change in architecture was provided by the possibility of blowing a cylinder instead of a sphere. This allowed for larger planes of glass. Around 1900 the industrial process of pulling of glass was developed and made it possible to produce wide plates. This created a striking effect on the creation of large windows in buildings in the newly built towns. In the mid-fifties of the 20th century the latest improvement in the technology of glass production was made in England. The float glass method was created: floating/pouring still liquid glass on a bed of molten tin. Glass panels with two smooth surfaces were now able to be produced. The impact of this new technique was huge. Large walls/façades were made of glass panels and almost all glass currently produced is float glass. This is the starting point for the structural design in glass. (Nijsse, 2003) (Bedon, 2017)

1.1 Relevance

Nowadays glass is widely used as a construction material, either as a replacement for or in collaboration with conventional building materials such as steel, aluminium, timber and concrete. Important reasons to use glass as a building material are related to the aesthetics, transparency, lighting and insulation properties. In this way innovative and iconic designs can be made with glass.

Nevertheless, fail-safe designs with structural glass require good knowledge of theory and practice. Glass structures need to perform well, both under standard and extreme loading conditions, such as fire conditions. Special safety levels should be guaranteed to allow evacuation of buildings, especially in case of fire accidents. (Bedon, 2017)

In a conversation with James O'Callaghan, widely acknowledged as an authority on structural glass, it appeared that nowadays only one-storey buildings are built with structural load-bearing glass elements. This is because there are no specific fire safety requirements for these one-storey buildings. Building regulations prohibit the use of load-bearing structural glass elements in buildings higher than one level, because the glass elements are unable to provide the fire resistance demanded. The iconic Apple Cube in New York or the Apple IFC at Shanghai are example of these one-storey structures (Figure 2).

Figure 2 Left: Apple Cube New York, right: Apple IFC Shanghai
(both retrieved from https://www.eocengineers.com/en/projects)

The demand for these special glass structures is not high, but there is also a lack in knowledge. If a client asks for a special glass structure which requires a certain fire resistance, the demand has to be turned down. However, if there would be more knowledge about these structures and their fire safety, the possibilities for the use of structural glass elements would be larger and as a result more will be built with structural glass.

1.2 Problem statement

Various researches have already been carried out on glass and glazing systems subject to fire. The total fire performance of a structural glass system is dependent on several factors. These factors include the brittle behaviour, the high sensitivity of the mechanical properties to temperature, the geometry, glass type and the cooperation between the various components of a system.

A specific problem in the determination of the fire behaviour of glass systems is that the fire performance is not easy to determine with only analytical derivations, but needs fire testing. Although various research studies have been done on the thermal performance of glass systems, little experimental research has been done on the performance of structural glass elements under fire loading, such as beams or floors.

Finite Element Modelling could in this case be a good alternative to time- and cost-consuming tests. The most important problems with Finite Element Modelling, however, arise from the lack of general rules and guidelines, but also from the lack of experimental results to the mechanical and thermal properties under fire circumstances of the used materials.

1.3 Research questions

From the problem statement the following research question is formulated:

How does structural glass perform at elevated temperatures and how can the fire resistance be improved?

Subsequently the following sub-questions are defined:

- *Which types of structural glass are relevant to investigate?*
- *What are the current rules and regulations regarding structural glass systems and fire safety?*
- *What are the relevant properties of structural glass at elevated temperatures and how can these properties be assessed?*
- *What research has been carried out on structural glass elements at elevated temperatures?*
- *What is the effect of coatings on the performance of laminated glass panels at elevated temperatures?*

1.4 Research methodology and outline

In order to answer the stated research question a qualitative study to recent literature on (structural) glass is performed which is presented in chapter 2. This concerns amongst other topics the production process; physical and chemical properties of glass; processing and glass products. Chapter 3 more specifically explains the state-of-the-art on structural glass at elevated temperatures and current regulations for structural glass systems.

The experimental research is presented in chapter 4 and 5. Section 4.1-4.4 presents the reader with the theoretical framework and test methodology adopted for the performed ultrasonic measurements, whereas the results, analyses, validation and discussion are provided in section 4.5-4.8. Tests on coated laminated glass panels are elaborated in chapter 5; results and discussion are given in section 5.3 and 5.4 respectively. In the Appendices specific measurement results are presented for both of these tests.

The results of both of the experiments are discussed in chapter 6. Overall conclusions of this research are presented in chapter 7. Chapter 8 provides the reader with recommendations on how to improve the fire resistance and recommendations for future research.

II
Literature review

2. Glass – the material

In order to get a better understanding of the behaviour of glass as a material, the chemical composition, production process, material properties and processing and glass products will be discussed in the following paragraphs.

2.1 Chemical composition

Glass is a non-crystalline inorganic solid material. It is a product of fusion, which has been cooled to a rigid condition without crystallization. Crystallization is the process by which a solid forms, where the atoms or molecules are ordered into a structure known as a crystal. So glasses do, in contrast to most other materials, not consist of a geometrically fixed network of crystals, but of an irregular network of silicon and oxygen atoms with alkaline parts in between, which can be seen in Figure 3.

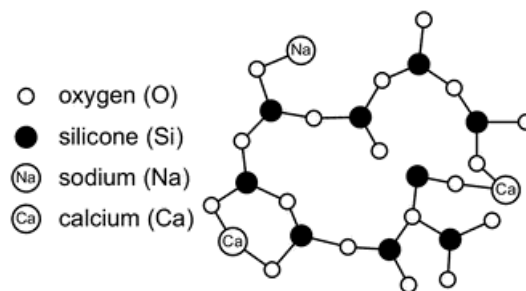○ oxygen (O)
● silicone (Si)
Ⓝ sodium (Na)
Ⓒ calcium (Ca)

Figure 3 Schematic view of the irregular network of soda lime silica glass (Haldimann, et al., 2008)

Soda lime silica glass (SLS) is the most common type of glass used in construction. This glass consists of about 70 to 75 % SiO_2 (silica, also known as sand) plus Na_2CO_3 (sodium carbonate, soda), CaO (calcium oxide, lime) and other additions that influence either the melting point during the production process or the mechanical and optic characteristics of the final glass product. A translucent glass product is created by melting the ingredients and cooling them down rapidly. (Schipper, 2011) For some special applications, such as fire protection glazing and heat resistant glazing, borosilicate glass (BS) is used. This type of glass has a very high resistance to temperature changes and also a very high hydrolytic and acid resistance. In Figure 3 the chemical composition of SLS and BS glass is shown according to European standards. (Haldimann, et al., 2008)

Table 1 Chemical composition of SLS and BS glass (Haldimann, et al., 2008)

		Soda lime silica glass	Borosilicate glass
Silica sand	SiO_2	69–74%	70–87%
Lime (calcium oxide)	CaO	5–14%	–
Soda	Na_2O	10–16%	0–8%
Boron-oxide	B_2O_3	–	7–15%
Potassium oxide	K_2O	–	0–8%
Magnesia	MgO	0–6%	–
Alumina	Al_2O_3	0–3%	0–8%
Others		0–5%	0–8%

6

2.2 Production process

In Figure 4 an overview is given of the most common production processes, processing methods and products of glass. The most important production steps are always the same: melting at 1600-1800°C, forming at 800-1600°C and cooling at 100-800°C.
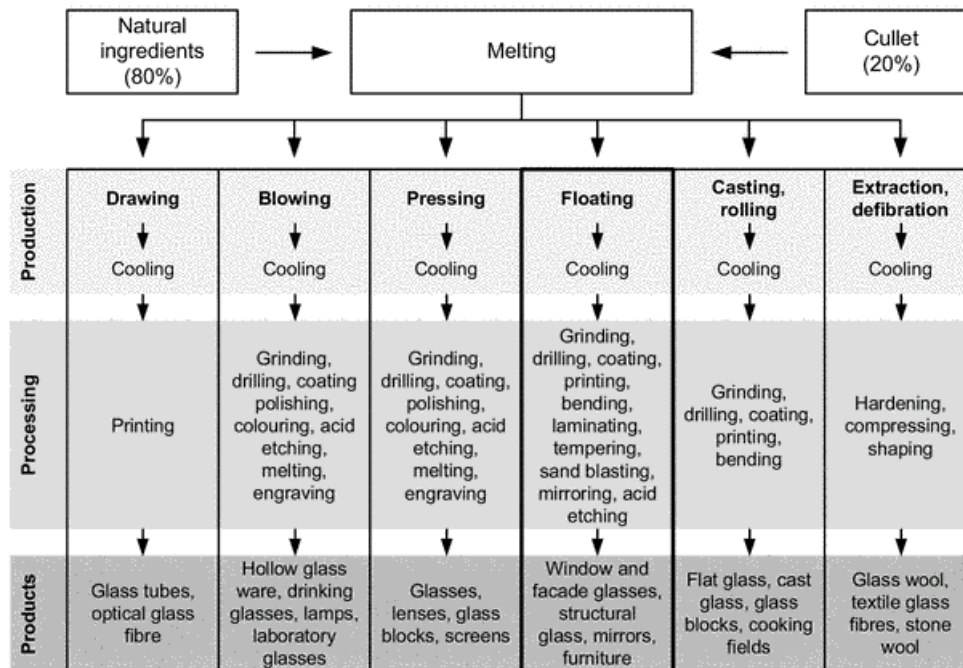
	Drawing	Blowing	Pressing	Floating	Casting, rolling	Extraction, defibration
Production	Drawing ↓ Cooling	Blowing ↓ Cooling	Pressing ↓ Cooling	Floating ↓ Cooling	Casting, rolling ↓ Cooling	Extraction, defibration ↓ Cooling
Processing	Printing	Grinding, drilling, coating polishing, colouring, acid etching, melting, engraving	Grinding, drilling, coating, polishing, colouring, acid etching, melting, engraving	Grinding, drilling, coating, printing, bending, laminating, tempering, sand blasting, mirroring, acid etching	Grinding, drilling, coating, printing, bending	Hardening, compressing, shaping
Products	Glass tubes, optical glass fibre	Hollow glass ware, drinking glasses, lamps, laboratory glasses	Glasses, lenses, glass blocks, screens	Window and facade glasses, structural glass, mirrors, furniture	Flat glass, cast glass, glass blocks, cooking fields	Glass wool, textile glass fibres, stone wool

Natural ingredients (80%) → Melting ← Cullet (20%)

Figure 4 Overview of production processes and products of glass (Haldimann, et al., 2008)

The most prevalent primary manufacturing process at the moment is the float process, which accounts for about 90 percent of the current flat glass production worldwide. This process is commercially introduced by the Pilkington Brothers in 1959 and its low costs, wide availability, the remarkable optical quality of the glasses and the large size of panes which can be achieved reliably are the most important benefits. Over the last 50 years the mass production, but also the finishing and refinement technologies improved, so that glass was made cheap enough to use it in large amounts in the construction industry. Because of more improvements in the field of refinement technologies (tempering, laminating) and the help of structural analysis methods (finite element method) for the last 2-3 decades it was possible to use glass for structural building elements.

In Figure 5 a schematic overview is shown for the production process of float glass. This glass is made in large manufacturing plants, which work continually 24 hours a day, 365 days a year. The process works as follows: the raw materials, described in the previous paragraph, are melted in a furnace at temperatures up to 1550°C. Then at approximately 1000°C, the molten glass is poured continuously on to a shallow bath of molten tin. To prevent the oxidation of this tin, an internal atmosphere consisting of hydrogen and nitrogen is created. The choice for tin is because of the large temperature range of its liquid physical state (232-2270°C) and its high specific weight compared to glass. The glass flows on the tin surface and spreads outwards forming a smooth flat surface at an even thickness.
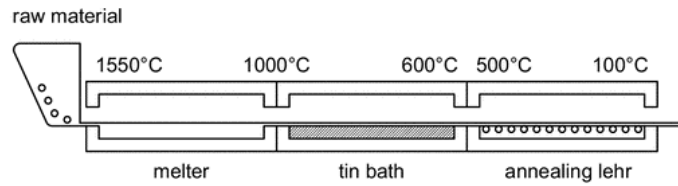
raw material

1550°C   1000°C   600°C 500°C   100°C

melter   tin bath   annealing lehr

Figure 5 production of float glass (Haldimann, et al., 2008)

As the glass flows it is gradually cooled and pulled off the bath by rollers at a controlled speed, before entering a long oven, called a lehr, at around 600°C. By adjusting the speed of the rollers, the thickness of the glass can be changed within a range of 2 to 25 mm. This means that if the speed will be reduced the glass thickness increases and the other way around. In the annealing lehr the glass will slowly be cooled, preventing the forming of residual stresses within the glass. Automated machines will inspect the float glass after annealing, so that obvious visual defects and imperfections can be removed during cutting. At the end of the process, the glass is automatically cut to a typical size of 3.21 x 6.00 m before it will be stored. To reduce waste, the unwanted or broken glass is collected and brought back into the furnace. (Haldimann, et al., 2008)

2.3 Material properties

2.3.1 Chemical properties

The chemical composition of glass, as described in an earlier section, has an influence on the properties of glass. These properties are the viscosity, the melting temperature T_s and the thermal expansion coefficient α_T of glass. For pure silica oxide, the melting point is about 1710 °C, but due to the addition of alkali this temperature will drop to 1300-1600 °C. The thermal expansion coefficient is about $0.5 \cdot 10^{-6}$ K^{-1} for pure silica glass and $9 \cdot 10^{-6}$ K^{-1} for soda lime glass, this is about three quarters of that of structural steelwork. This coefficient expresses the relative longitudinal expansion of a component per degree of temperature rise. (Wurm, 2007) Since the viscosity is dependent on temperature, this will be discussed in the next chapter.

Another quite important property of glass is the outstanding chemical resistance to a lot of aggressive substances, which makes glass popular for the chemical industry and also makes it one of the most durable materials in construction. Table 2 gives an overview of the chemical resistance of soda lime silica glass. (Haldimann, et al., 2008)

Table 2 Chemical resistance of SLS glass (Haldimann, et al., 2008)

Substance	Resistance
Non-oxidant and oxidant acids	+
SiO_2-solving acids	0/−
Salt	+
Water	+
Non-oxidant and oxidant alkalis	0/−
Aliphatic, aromatic and chlorinated hydrocarbons	+
Alcohol	+
Ester	+
Ketones	+
Oil and Fat	+

+: resistant, 0: partly resistant, −: not resistant.

2.3.2   Physical properties

Next to the chemical properties, glass also has some interesting physical properties. The most important properties of soda lime silica and borosilicate glass are summarized in Table 3. The glass thickness, chemical composition and the applied coatings influence the optical properties. The very high transparency within the visible range of wavelengths ($\lambda \approx 380 - 750$ nm) is the most obvious property. The exact profiles of the non-transmitted (that means absorbed and reflected) radiation spectrum are usually in the wavelengths outside the visible and near infrared band, although there will be a variation between the different types of glass. A big part of the UV radiation will be absorbed due to the interaction with O_2-ions in the glass. The Si-O-groups absorb the long-wave infrared radiation ($\lambda > 5000$ nm), causing it to be blocked. This also explains the greenhouse effect: the visual light passes through the glass and heats up the interior, while the emitted long-wave thermal radiation cannot escape. The reflection of visual light by normal SLS glass is 4% per surface. With a refractive index of about 1.5, this gives a total of 8% for a glass pane. This will reduce the transparency, but special coating can be applied to avoid this. (Haldimann, et al., 2008)

Table 3 physical properties of SLS and BS glass (Haldimann, et al., 2008)

			Soda lime silica glass	Borosilicate glass
Density	ρ	kg/m^3	2 500	2 200–2 500
Knoop hardness	$HK_{0,1/20}$	GPa	6	4.5–6
Young's modulus	E	MPa	70 000	60 000–70 000
Poisson's ratio	ν	–	0.23*	0.2
Coefficient of thermal expansion[†]	α_T	10^{-6} K^{-1}	9	Class 1: 3.1–4.0
				Class 2: 4.1–5.0
				Class 3: 5.1–6.0
Specific thermal capacity	c_p	J kg^{-1} K^{-1}	720	800
Thermal conductivity	λ	W m^{-1} K^{-1}	1	1
Average refractive index within the visible spectrum[‡]	n	–	1.52[§]	1.5
Emissivity (corrected[¶])	ε	–	0.837	0.837

* EN 572-1:2004   gives 0.2. In research and application, values between 0.22 and 0.24 are commonly used.
[†] Mean between 20 °C and 300 °C.
[‡] The refractive index is a constant for a given glazing material, but depends on the wavelength. The variation being small within the visible spectrum, a single value provides sufficient accuracy.
[§] EN 572-1:2004   gives a rounded value of 1.50.
[¶] For detailed information on the determination of this value see EN 673:1997   .

Glass is known for its almost perfectly elastic, isotropic behaviour and its brittle character at failure. Since glass does not yield plastically, it is not possible to reduce local stress concentrations by redistribution, which is the case for other construction materials like steel. Figure 6 shows the stress-strain diagrams for glass (this accounts for compression) in comparison with other materials, like steel and concrete. The ratio between the stress and the strain is given by the stiffness. It can be seen that glass is relatively stiff compared to other materials. (Schipper, 2011)
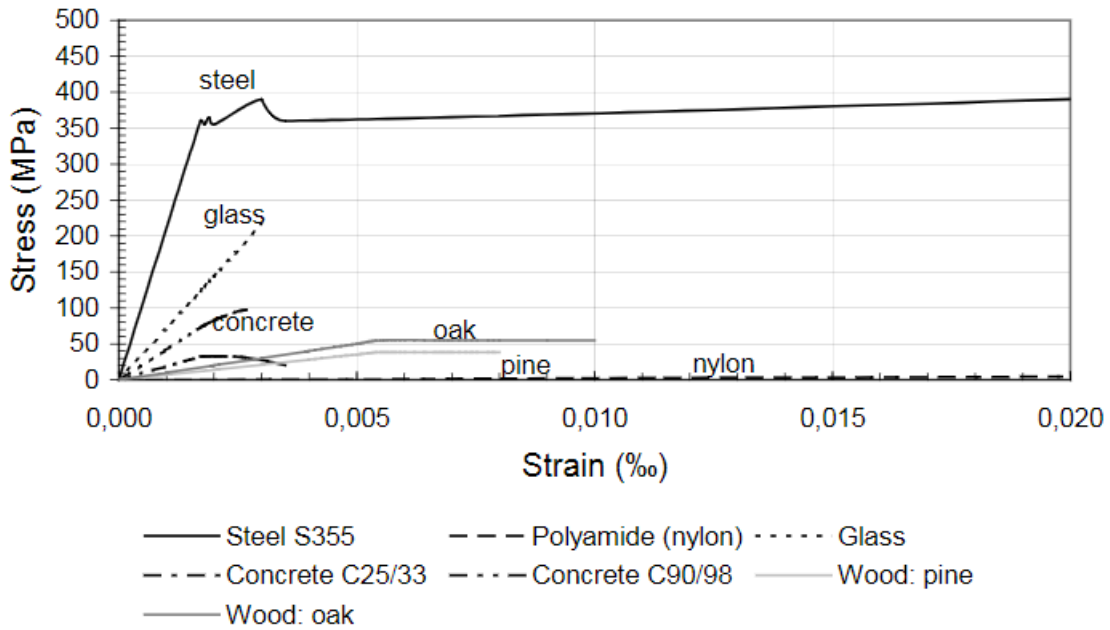
9

Figure 6 Stress strain diagram glass and other materials (Schipper, 2011)

The theoretical tensile strength (based on molecular forces) of glass may reach 32 GPa, which is very high. Of course, the actual strength which could be used for engineering will be much lower. This is caused by the mechanical flaws on the surface that affect the tensile strength of the glass. This applies for all brittle materials. These flaws do not have to be visible to the naked eye. Glass panes mostly contain a large number of relatively severe flaws at the surface, but the surface of glass fibres have minor and less deep surface flaws. This is the reason why glass fibres have much higher strength than glass panes. In Figure 7 a rough overview of typical strength values for different flaw depths is given.
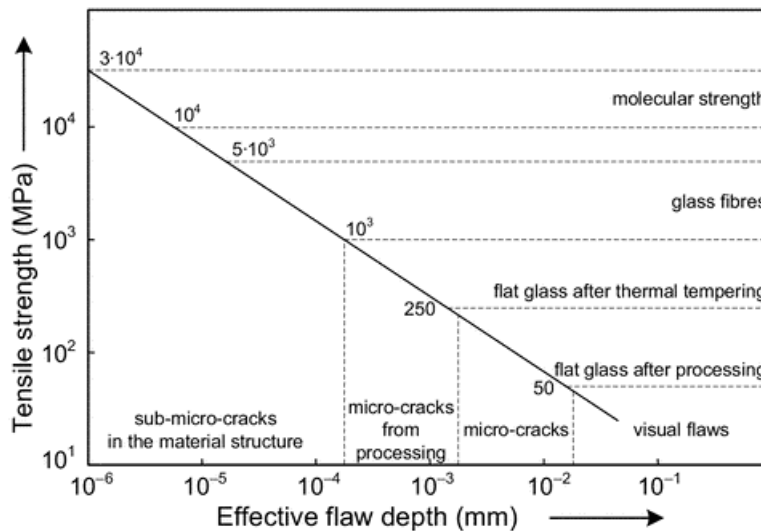

Figure 7 short-term strength as a function of the flaw depth (Haldimann, et al., 2008)

When the critical value for the stress intensity due to tensile stress at the tip of one flaw is reached, a glass element will already fail. It can be concluded that the tensile strength of glass is not a material constant. Various factors influence this strength, especially the condition of the surface, the size of the glass element, the load history (intensity and duration), the residual stress and the environmental conditions. The effective tensile strength will be decreased by higher loads, longer load durations and deeper initial surface flaws.

In contrast to the tensile strength, the compressive strength of glass is much larger. This has to do with the fact that surface flaws do not become bigger or fail when in compression. Though, the compressive strength is not relevant for every structural application, because tensile stresses can develop in different situations. For example due to buckling in the case of problems with stability or because of the Poisson's ratio effect at load introduction points. In these two examples, the tensile strength will be exceeded long before the element is loaded to its compressive strength. (Haldimann, et al., 2008)

2.4 Processing and glass products

After the production process, flat glass usually goes through post processing steps to reach the characteristics needed for different glass products. This secondary processing include for example: cutting, edge working, coating, curving, laminating, thermal treatment and assembling. A few of the relevant processes for this thesis will be explained below.

2.4.1 Thermal treatment

For structural reasons and safety, glass will often be tempered (heat treated) after manufacturing. The principle of heat strengthening is based on changing the internal stress distribution in the glass layer, so higher loads can be taken by the glass. (Schipper, 2011) To be more specific, a favourable residual stress field is made, at which tensile stresses arise in the core and compressive stresses on and near the surfaces. Since there are no flaws present in the core, it will be suitable to resist tensile stresses. There will always be flaws on the surface, but they can only grow if they are exposed to effective tensile stress. This means that if the surface stress by loads is smaller than the residual compressive stress, there will be no tensile stresses that can cause the cracks to grow. This principle is explained by Figure 8 below.
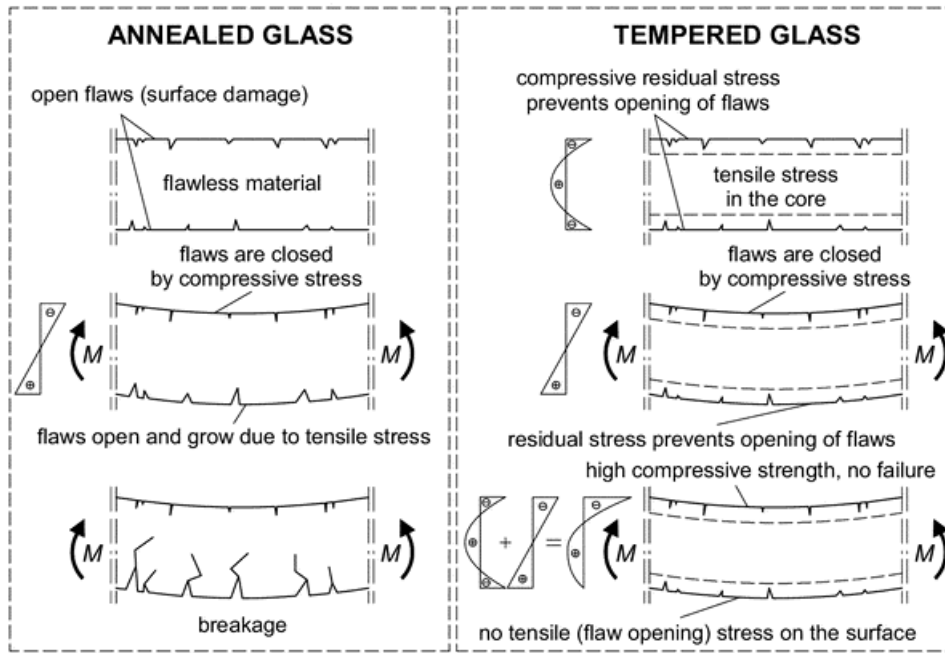
Figure 8 Tempering of glass, effect on stresses (Haldimann, et al., 2008)

The fracture pattern of the glass pane is dependent on the residual stress and the stress due to loads. It holds that *fully tempered* glass will have the highest residual stress level and will break into small, relatively harmless fragments of about 100 mm^2. This is also the reason why fully tempered glass is called "safety glass". Though, this glass is not always safe, because even small pieces can cause injury when falling from several meters high. Above that, when a fully tempered glass panel fails, the structural performance is quite low due to the little fragments, even though it had the highest structural capacity due to tempering.

In contrast to tempered glass, *heat strengthened* glass breaks into sharp pieces, which are little smaller than those of annealed glass. The strength of heat strengthened glass is to be found between annealed and tempered glasses. (Schipper, 2011) This type of glass is produced according to the same process as for fully tempered glass, but the cooling rate is lower. This results in lower residual stress and lower tensile strength. When heat strengthened glass is used in laminated elements, after failure there will be some meaningful load-bearing capacity.
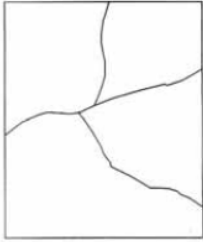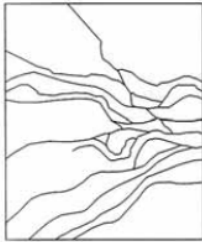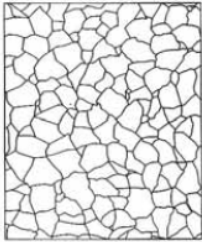
Prestress level	(almost) none	medium	high
Fracture pattern			
Terminology	**Annealed glass** (ANG) (float glass) ≈ 45 MPa	**Heat strengthened glass** (HSG) (partly toughened glass) ≈ 70 MPa	**Fully tempered glass** (FTG) (tempered glass) ≈ 120 MPa

Figure 9 Fracture pattern for different prestress levels (Louter, 2017)

The standard float glass, produced after the float process is also called *annealed* glass. This glass is not exposed to the tempering process and will normally break into large sharp pieces. However, if this glass gets to endure high (especially in-plane) loads, a fracture pattern similar to heat treated glass can be formed. This is caused by the elastic energy stored in the material due to elastic deformation. In Figure 9 the different fracture patterns discussed are shown.

Regarding borosilicate glass, this type of glass is harder to temper because of its low thermal expansion coefficient. (Haldimann, et al., 2008)

2.4.2 Laminating

Laminated glass is formed by two or more panes, bonded together by some transparent plastic interlayer. The panes can be of various thicknesses and heat treatments. This type of safety glass will be held together in the event of breaking, due to the bonding effect of the interlayer. (Schipper, 2011) Therefore laminated glass is of great interest for structural applications, since a certain remaining structural capacity is obtained after breaking. Since this capacity depends on the fragment size (capacity increases with increasing fragment size), annealed and heat strengthened glass are suitable if a high

Figure 10 Behavior of laminated glass after breaking with different types of glass (Haldimann, et al., 2008)

remaining capacity needs to be reached. Figure 10 shows the post breakage behaviour for the different types of glass. (Haldimann, et al., 2008)
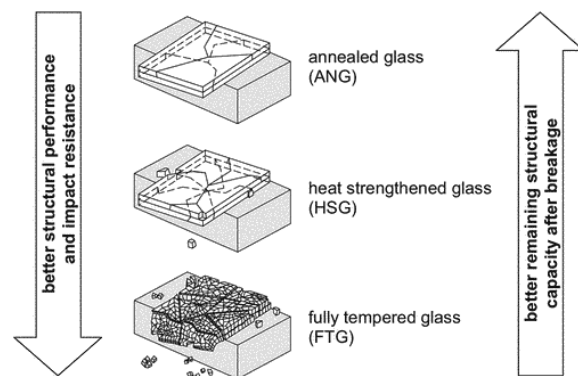
It is important that the broken, more or less flexible panes, stay in their position. This can be done by clamping the glass panel strongly to the supports or gluing the glass for example. (Schipper, 2011)

The behaviour after breaking also depends on the interlayer material. PVB (polyvinyl butyral) is the most commonly used material, because it blocks UV radiation almost completely. A single PVB foil has a thickness of 0.38 mm. In laminated glass, usually two or four foils form one interlayer. Since PVB is a viscoelastic material, the physical properties will depend highly on the temperature and load duration. PVB is able to transfer the full shear stress between two panes at temperatures well below 0 °C. Though, the shear transfer will be reduced significantly for higher temperatures and long loading times. In Table 4 the typical material properties of PVB are given. (Haldimann, et al., 2008)

<div align="center">Table 4 Material properties of PVB (Haldimann, et al., 2008)</div>

Property	Symbol	Unit	Value
Density	ρ	kg/m^3	1070
Shear modulus	G	GPa	0–4
Poisson's ratio	ν	–	≈ 0.50
Coefficient of thermal expansion	a_T	K^{-1}	$80 \cdot 10^{-6}$
Tensile strength	f_t	MPa	≥ 20
Elongation at failure	ε_t	%	≥ 300

Also other alternative interlayer materials have been created with the goal to reach higher stiffness, temperature resistance, tensile strength or resistance to tearing. SentryGlas® from DuPont is one of those alternatives. The interlayers can be five times stronger and up to 100 times stiffer than common laminating materials. It also retains its transparency after years of service. (Trosifol, 2014) However, lamination of those interlayers can be more difficult due to the high stiffness. In Table 5 below some typical physical properties of the SentryGlas® interlayer are given.

<div align="center">Table 5 Physical properties of SentryGlas interlayer (Trosifol, 2014)</div>

Property	Symbol	Unit	Value
Density	ρ	g/cm^3	0.95
Young's Modulus	E	MPa	300
Tensile Strength	f_t	MPa	34.5
Elongation	ε_t	%	400
Flex Modulus 23°C	E_{bend}	MPa	345
Heat Deflection Temperature at 0.46 MPa		°C	43
Melting Point		°C	94
Coefficient of Thermal Expansion (-20°C to 32 °C)	a_T	10^{-5} cm/cm °C	10 - 15

Laminated glass is also used for fire protection functions. The so-called fire protection glass is a form of laminated glass with one or more special transparent intumescent interlayers. When such a panel will be exposed to fire, the panel which is facing the fire will break, but stays in place. The interlayers will foam up and in this way a non-transparent insulating shield protects the rest of the glass against the flames. (Haldimann, et al., 2008)

2.4.3 Coatings

The chemical composition of glass is not the only factor that determines the thermal, optical or durability characteristics of a glass pane. These characteristics can be changed by applying coatings on the glass afterwards (online, directly after the float process or offline, on the cut glass panels). To improve the thermal performance, commonly metal oxides or nitrides are applied to the glass, using the magnetic sputtering process. If the glass has to be more durable, hard coatings (pyrolytic coatings) can be applied.

Online coating (pyrolytic coatings)

These types of coatings are suitable for thermal processes, like bending, tempering etc. and are used as coatings for solar control, thermally insulating and self-cleaning glass. During the production of float glass, a coat of metal oxide is applied on the upper surface of the glass, while it is still hot. This results in a firmly bonded coating to the glass, which reduces the amount of light and energy transmitted through the glass. This can be selectively or over the whole solar spectrum. A layer of tin oxide coating can be applied to improve the thermal insulation. This coating reduces the emissivity (heat radiation) of the glass from about 90 to approximately 15 percent, also called low-E coating.

Offline coating (magnetron sputtering)

High performance soft coatings for solar control and heat insulation applied by the magnetron sputtering process are the most important coatings to the construction industry. Magnetron sputtering is a physical coating process and happens after production and cutting to size. The glass is coated with metal oxides and this process involves the acceleration of free electrons in an electric field which then collide with gas molecules. These gas molecules will subsequently take on a positive charge and, accelerated by the electric field, bombard a negatively charged cathode. This cathode is provided with the coating material which throws off particles and these attach themselves to the surface of the glass. The process described, repeats millions of times. The glass which is passing through the coating plant will be continuously coated in this way.

These offline (soft) coatings haven't yet reached the durability of float glass itself or online coatings. Glasses coated by the magnetron sputtering method can mainly be left outside for a limited period (approximately three months). Therefore, these coatings are only used on surfaces within the cavity of an insulating unit. (Schipper, 2011) (Schittich, et al., 2007) (Wurm, 2007)

3. Glass at elevated temperatures

Since the 1950s, the use of glazing panels in windows and fenestrations was very high and therefore research studies to the performance of glass under high temperatures and fire loading gained more attention. Thermal shock is one of the aspects that is studied most, but also the thermal properties in general of soda lime silica glass, including the variating modulus of elasticity and resistance with high temperatures. However, there are just few studies known about composite glass systems and assemblies under fire or fire and mechanical loads acting together.

3.1 Material properties

In this paragraph key influencing properties of glass under high temperatures will be given on the basis of some researches.

3.1.1 Viscosity and glass transition temperature

For the viscosity (a measure of the resistance of a liquid to shear deformation) it holds that during the cooling of the liquid glass, its viscosity increases constantly until the material solidifies at 10^{14} Pa s. The temperature at which this solidification takes place is described as the glass transition temperature T_g and is about 530°C for SLS glass. The transition between liquid and solid states does not occur at one specific temperature, but over a temperature range, in contrast to crystalline materials. This property is shown in Figure 11. The dashed part of the curve indicates the glass transition range. In Table 6 the typical viscosities and corresponding temperatures for SLS and BS glass are given. (Haldimann, et al., 2008)
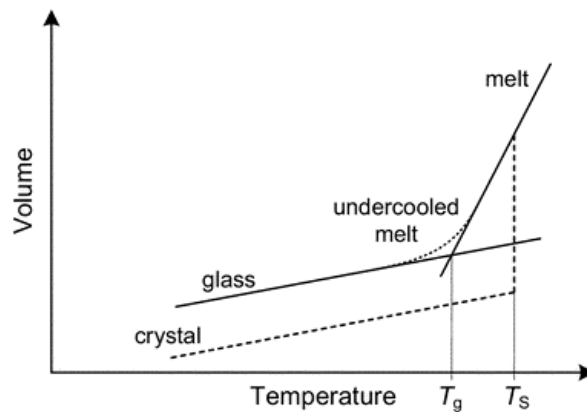

Figure 11 schematic comparison of the volume's dependence on temperature for a glass and a crystalline material (Haldimann, et al., 2008)

Viscosity	State	Temperature	
		SLSG	BSG
(dPa s)		(°C)	(°C)
10^5	Working point	1040	1280
$10^{8.6}$	Softening point	720	830
10^{14}	Annealing point	540	570
$10^{14.3}$	Transition temperature T_g	530	560
$10^{15.5}$	Strain point	506	530

These important reference points can be defined as follows (Brow, sd):

- *Working point:* The temperature at which molten glass can be formed/manipulated. The viscosity is low enough for some shear processing like pressing, blowing, etc., but high enough to retain some shape after shear is removed.
- *Softening point:* The temperature at which glass will deform under its own weight.
- *Annealing point:* The temperature at which "stress is substantially relieved" in a few minutes.
- *Strain point:* The temperature at which "stress is substantially relieved" in several hours.

As already mentioned, the glass transition temperature of soda lime glass is 530°C according to design standards (Table 6). Nevertheless, different experiments on soda lime glass that has carried out in the last decades gave high variations in this temperature for annealed glass. These differed in the order of 283°C, 400°C and 550°C. (Bedon, 2017)

One of the experiments is from Rouxel and Sangleboeuf (Rouxel & Sangleboeuf, 2000). They measured values for the transition temperature comprised between 450°C and 600°C on soda lime silica glass samples.

It is known, by the characteristics of soda lime silica glass, that the behaviour of glass will become gradually time-dependent if the service temperature will reach up to the transition temperature. This goes together with a fast increase of permanent deformations. The standard annealed glass has a typical brittle-to-ductile (BTD) transition at high temperatures, with better toughness compared to other glass types. However, the same BTD behaviour seemed strongly dependent on the imposed strain rate according to Rouxel and Sangleboeuf. This means that if the strain rate increases, the BTD behaviour and the transition temperature increase. (Bedon, 2017)

3.1.2 Modulus of elasticity

Rouxel not only investigated the glass transition temperature, but also studied the elastic properties of standard glass at elevated temperatures, by processing the experimental data which were available in literature after the 1950s and determining the E-modulus by an ultrasonic echography method. He thereby proved the temperature sensitivity of soda lime glass in comparison with other glass types as can be seen in Figure 12. Until the temperature reaches the transition temperature, the modulus of elasticity behaves rather linear dependent and has limited decrease. After the transition temperature a sudden loss of stiffness can be noticed. (Rouxel, 2007)

Kerper and Scuderi also investigated the E-values of soda lime silica and borosilicate glass specimens in previous experiments by a dynamic method, based on resonance frequencies (Kerper & Scuderi, 1966). In this study, chemically strengthened and fully tempered soda lime silica glass and thermally semi-tempered borosilicate glass were tested in the range of 0-560°C. Almost stable E-values were found, even after consecutive heating and cooling cycles. For temperatures higher than 400°C the values were generally found to be completely relaxed. (Bedon, 2017) (Kerper & Scuderi, 1966)
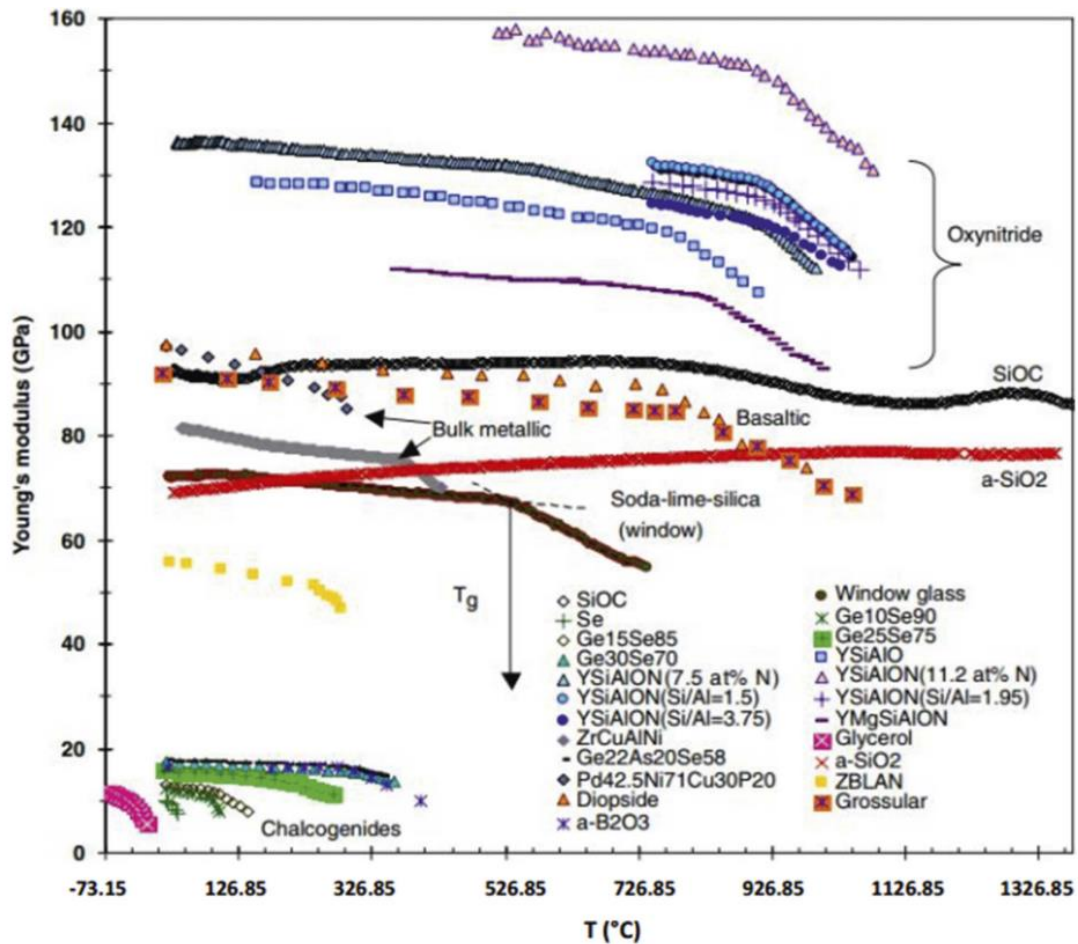
Figure 12 Variation of modulus of elasticity of different glass types as a function of temperature (Rouxel, 2007)

A similar relationship between the different experiments can be seen for the E-values of standard annealed glass samples in relation to temperature. In Figure 13 the aforementioned test results with addition of those from Shen et al (based on a resonance method) (Shen, et al., 2003) are shown. Those show an almost linear decrease of E-modulus as temperature increases. It can also be seen that the E-modulus for borosilicate glass increases with increasing temperature.

Another interesting aspect for the purpose of structural design is the evaluation of Kerper and Scuderi into the resistance variations in soda lime silica glass at high temperatures. For thermally fully tempered soda lime silica glass specimens no resistance losses were mentioned for temperatures up to 375°C (less than 5% losses, compared to room temperature). Significant decrease of resistance was reported only for temperatures higher than 500°C and 550°C. However for chemically strengthened soda lime glass a distinct decrease of resistance was noticed with the increase of the

temperature. At 204°C 5% loss, at 260°C 5.8% and 100% at 600°C. (Kerper & Scuderi, 1966) (Bedon, 2017)
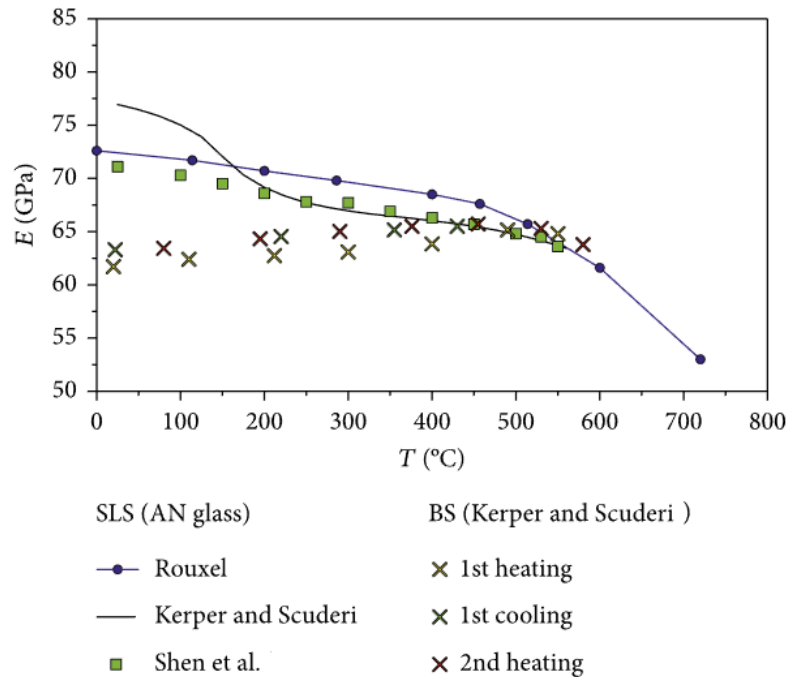

Figure 13 Variation of E-modulus as a function of temperature for SLS annealed and borosilicate glass (Bedon, 2017)

3.1.3 Thermal shock

Thermal shock is the most important cause of glass cracking for windows and therefor a big number of researches on the performance of soda lime silica glass focused on this phenomena. Thermal shock is the cracking due to the temperature gradient between heated and unheated glass areas, but also due to the relatively low thermal expansion coefficient of glass. This cracking is typically expected to occur when the temperature gradient of the different types of glass lies in the order of:

- 40°C for annealed glass
- up to 100°C for heat strengthened glass
- 200-250°C for fully tempered glass

Various experiments proved the edge and boundary condition effects on the thermal response and breakage of standard window glass panes. A research by Malou et al. on the thermal shock resistance documented a quite constant value for the tensile strength of annealed glass up to a temperature increase of 270°C. A sharp decrease however is noticed in the measured resistance (more than 50% of the reference value at room temperature) at higher temperatures. This gives evidence of the thermal shock effects and propagation of damage in glass samples, but also of the limited performances of annealed glass. Besides, a rather smooth (without any sudden
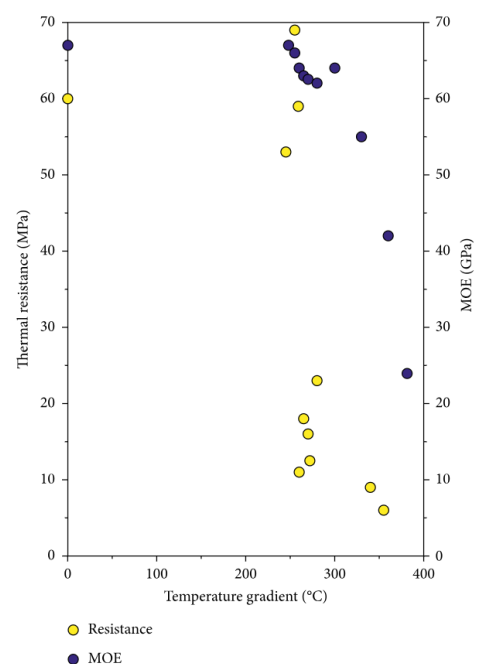

Figure 14 Variations of resistance and E-modulus under thermal shock (Bedon, 2017)

19

change) decrease of the modulus of elasticity could be seen. In Figure 14 the discussed results can be seen.

There are various experiments done, but from those experiments, different and opposite results can be derived, which proves the high scatter and sensitivity of the thermal resistance of glass to elevated temperatures. (Bedon, 2017)

3.1.4 Thermal performance of interlayers

Regarding laminated glass systems, the thermal performance of the interlayers also have to be investigated. Debuyser et al. researched the behaviour of monolithic and triple-layer laminated glass samples of standard annealed glass exposed to radiant heating. The laminated glass was bonded by both PVB and SG layers. Also Low-E coated, monolithic specimens were tested.

They performed radiant as well as transmittance tests, which gave evidence of the relatively limited resistance and low thermal performance of annealed glass, caused by the premature occurrence of thermal cracks. Besides, the bonding interlayers had a poor thermal reaction. The behaviour for both the SG- and PVB-laminated specimens were quite the same. The most exposed glass pane started cracking before gas bubbles were formed in the first, respectively the second interlayer. However, for the SentryGlas specimens, the gas bubbles were mostly smaller and limited the transparency more significantly. The formation of these bubbles happened at an interlayer temperature of about 90°C for PVB and 150°C for SG. The cracking occurred at a temperature difference of approximately 50°C over the thickness of the exposed glass pane.

Furthermore, the low-E coating causes more reflectance of the specimens, resulting in a reduction of the absoptance and transmittance. This implies that the application of a pyrolytic low-E coating has advantages for the behaviour of a structural glass element in a fire. The decrease in absorptance reduces the magnitude of the in-plane thermal gradients and of the thermal gradients over the thickness of the glass. The thermal fracture as mentioned in the previous part, is therefore delayed or even completely avoided. (Debuyser, et al., 2017)

In the figure below the thermal properties are presented for annealed glass, and both PVB and SG foils. The results of the test, even limited to maximum temperatures of 340°C, give close similarities with earlier literature as can be seen in Figure 15. (Bedon & Louter, 2018)
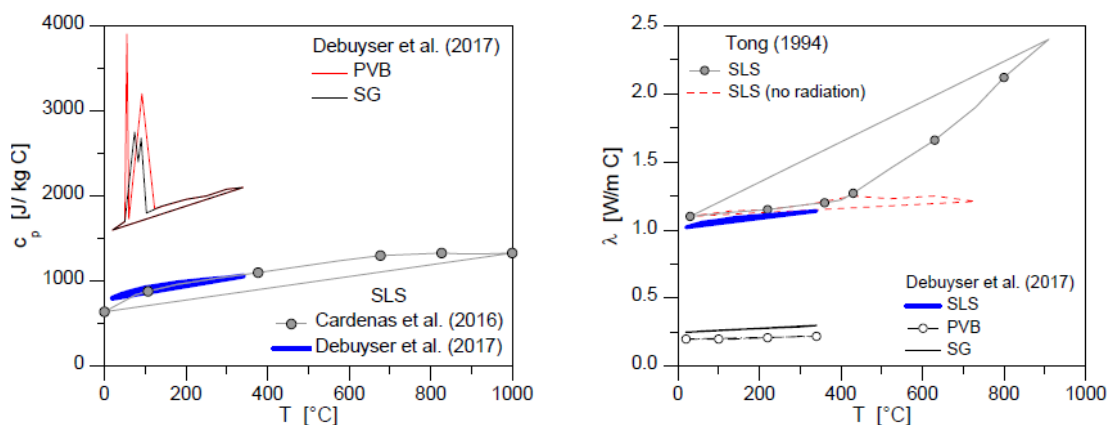
Figure 15 thermal properties as function of temperature. Left: specific heat. Right: conductivity (Bedon & Louter, 2018)

The modulus of elasticity will be a good parameter, if we consider the stiffness of both types of interlayers with respect to the temperature. Figure 16 shows a graph of DuPont in which can be seen that a SentryGlas interlayer acts stiffer than a PVB interlayer when temperature increases. However, this is only considered at temperatures up to 60°C, while in fires temperatures will increase much more.
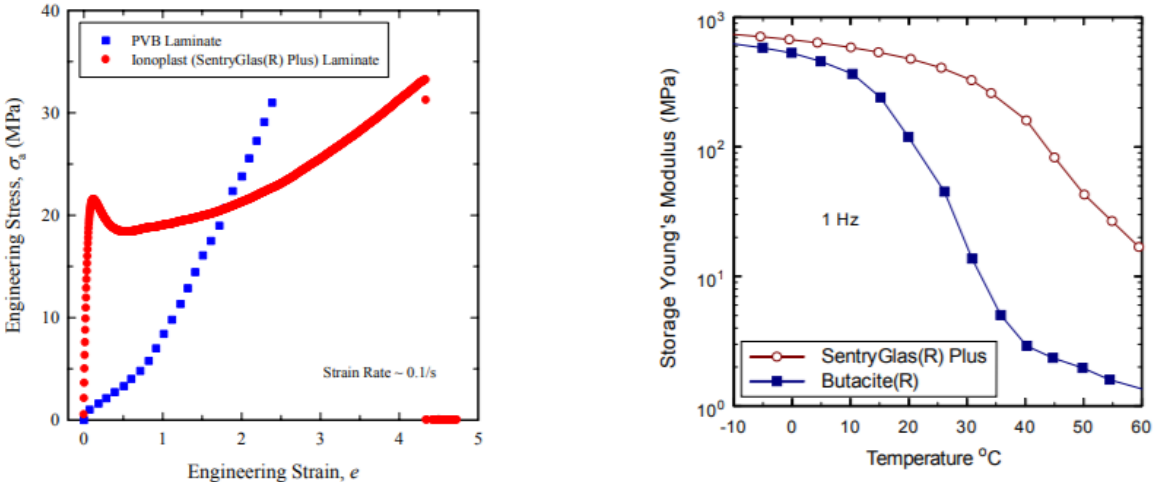
SentryGlas® Plus vs. PVB for Laminated Glass

- SentryGlas® Plus is elasto-plastic, high tear energy (5 x PVB).
- Glass transition temperature ~ 55° C. (Stiffness 30 – 100 x PVB).

Figure 16 SentryGlas vs. PVB stress-strain relationship and Young's Modulus dependence on temperature (DuPont, 2018)

3.2 Rules and regulations

3.2.1 Structural glass systems under standard loads

The characteristic properties of glass will affect the design and verification of structural glass elements. During the service life of glass, there is a possibility of unexpected breakage of a structural glass element, even without the designer's fault. However, in case of such an event, the structural integrity of the whole construction must be guaranteed. Eurocode EN 1990: 2002 (Basis of structural design) states that the design have to fulfil the requirements for both the ultimate limit state (ULS) and the serviceability limit state (SLS). (NEN, 2002)

To guarantee the structural safety of a structural glass element, the ULS verifications have to be met. To verify the ULS, the design resistance of glass must not be exceeded. Therefore the maximum principal stresses have to be calculated under relevant load combinations. Though, the design value of glass resistance can be influenced by several aspects, for example the function of glass type, loading, loading time, edge effects and treatments, glass surface treatments, profile, etc. In Europe, the same design rules are adopted by several national codes.

As regards the verification of the SLS, the calculation focuses on limiting the deflections. These maximum values for deflection will vary due to the specific applications or support conditions and can be found in standards. A last limit state that has to be verified is the so called collapse limit state (CLS) according to the CNR guidelines. This means that there has to be enough redundancy in the case of accidental cracking of a structural glass element. This is expressed in the residual CLS resistance and maximum deformations of the partially damaged system. (Bedon, 2017)

3.2.2 Structural glass systems under fire loading

A fire loading is a form of an extreme loading, which not only applies for glass structures, but also generally for all constructions. To be sure that the construction functions as desirable, specific measures should be taken into account.

For glazing systems which are exposed to fire, three classification levels are defined to ensure the performance in case of fire (NEN, 2016):

- Integrity (classification "E"): glass prevents flames, smoke and hot gases from passing through. It does not prevent the transfer of heat in the event of a fire.;
- Limiting radiation ("EW"): glass restricts the amount of heat passing through it to the side which is to be protected;
- Thermal insulation ("EI"): the highest level of protection against flames, smoke and heat. The average temperature of glass on the protected side remains below 140°C; hence, the risk of self-combustion of exposed materials (due to either radiation or convection) can be minimized, and buildings can be evacuated safely and calmly.

The aforementioned classification levels for fire safety can only be determined by performing fire tests. The typical fire resistant rating classes are based on a performance of 30, 60 or 120 minutes. The Bouwbesluit states different requirements for the duration of fire resistance with regard to failure in minutes, depending on the function of the building (residential or non-residential) and the height of the building. (Bouwbesluit , 2018)

In Europe, the relevant standards that are being used for fire testing are:

- EN 1361-1: Fire resistance tests – Part 1: General requirements (NEN, 2012);
- EN 1364-1: Fire resistance tests for non-loadbearing elements – Part 1: Walls (NEN, 2015);
- EN 1634: Fire resistance and smoke control tests for door and shutter assemblies, openable windows and elements of building hardware (NEN, 2004);
- EN 1365-2: Fire resistance tests for loadbearing elements – Part 2: Floors and roofs (NEN, 2014);
- EN 13501-2: Fire classification of construction products and building elements – Part 2: Classification using data from fire resistance tests, excluding ventilation services (NEN, 2016)

The American Underwriters Laboratory standard has, besides the regulations in Europe, another requirement for a fire safety glazing system. The system must be resistant against the so-called "hose-stream" test. This means that in case of a fire, the glazing system has to stay intact after a jet of water has been blasted onto the surface. (Bedon, 2017)

3.3 Existing experimental research

As mentioned before, a large number of experimental studies is done regarding the thermal performance of glass as a construction material. However, still limited research is carried out on the fire performance of full glass systems and assemblies. There are some studies done to, among others, glass beams, which will be described below.

3.3.1 Glass beams

Since the interest and ask for the evaluation of the exposure and protection of structural glass elements under fire loading is only relatively recent, not much experimental literature information is available.

Using transparent intumescent coatings to increase the fire resistance of glass and glass laminates – 2001 - Veer et al.

One of the researches into the fire resistance of glass and glass laminates is done by Veer et al. (Veer, et al., 2001). Intumescent coatings are already used at steel, aluminium and wood to improve the fire resistance. Veer et al. researched the effects of intumescent coatings by testing beams of annealed float glass, chemically toughened glass, chemically toughened glass laminated with polycarbonate foil and a special laminate with insulating cavity in a 4-point bending test using weights. The fire loading was applied as a constant flame of 650°C at a fixed distance from the lateral surface of the beams. The test setup is shown in Figure 17.
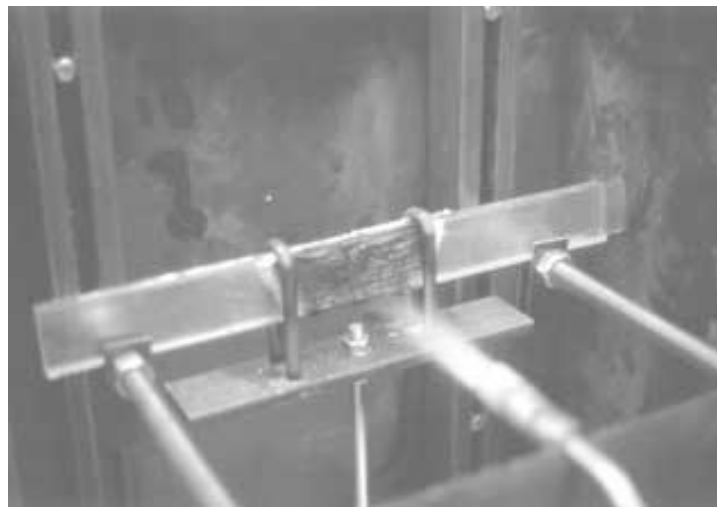

Figure 17 Four point bending test setup (Veer, et al., 2001)

The tests were carried out on beams with a length of 400 mm and a height of 40 mm and different thicknesses. Five types of configurations were tested both with and without the application of intumescent coating. For this coating was chosen for Flameguard HCA-TR.

One of the results showed that annealed float glass is a very unsafe structural material with regard to fire safety. The inhomogeneous thermal strain caused by relatively small exposure to heat will result in failure. Glass beams that are toughened will have a higher strength and therefore are more resistant in case of fire. It is also stated that continuous laminates made from toughened glass should be resistant to fire as long as a large enough region is not exposed to high temperatures. This is subject to that the mechanical safety is available to prevent the glass plies from rotating and

buckling. However, some serious damage to the interlayer of polycarbonate should be expected. This means that after fire, the complete beam should be replaced.

As far the transparent intumescent coatings are concerned, they will improve the fire safety of glass structures. They reduce the heat build-up and thus slow down the growth of thermal strain in both the glass and adhesive layer. For short duration and/or low temperature fires it will increase the safety. However, only using intumescent paint will not provide fire safety for a structural member which will not have enough build in fire safety. (Veer, et al., 2001)

Fire resistance of glass – 2003 – Bokel et al.

A few years later, Bokel et al researched beams of the same geometry as well as the same test setup as mentioned above. Commercially available Pyroguard™ (fire resistant glass) and a laboratory made alternative of 3 mm glass bonded with a cheap, clear epoxy resin were compared to each other. Both type of beams showed limited fire performance, because after several seconds the interlayer of both the Pyroguard™ and the laboratory alternative started charring. This gives evidence of the need for further research. (Bokel, et al., 2003)

Fire Testing of Structural Glass Beams; Initial Experimental Results – 2016 – Louter & Nussbaumer

Louter and Nussbaumer carried out experiments on larger soda lime silica glass beams composed of three glass layers of 10mm each laminated with PVB interlayers. The glass beams were 1m long and had a height of 100mm. Three beams with different glass types were tested: annealed (AN), heat-strengthened (HS) and fully tempered (FT) glass.

The three 1m glass beams where spanned over a small-scale fire testing furnace and were loaded in in-plane bending with a fixed load of about 115 kg each. In between the glass beams, 3cm thick fire protective panels were placed to close the top of the furnace. This left the lower part of the beams exposed to the standardized fire loading. During the test the temperature in the oven, the temperature within the beam laminate and the vertical deformation of the beams have been measured. In Figure 18 a schematic representation of the test setup is shown.
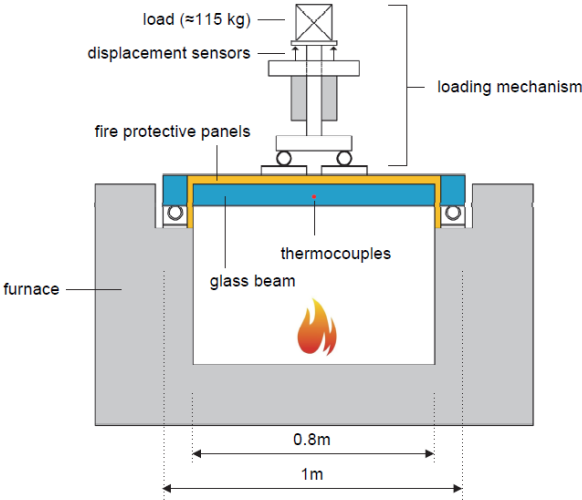

Figure 18 Schematic cross section of the fire testing setup (Louter & Nussbaumer, 2016)

It was observed that the PVB interlayers melted and leaked out of the laminated beams. Though, none of the glass beams broke during the test, but at the end of the fire testing, the mid-spans of the beams were completely molten. Yet, the non-exposed ends of the beams were still intact. The beams displaced gradually in vertical direction over time, until in the end a rapid increase in beam displacement was seen. This fast increase could be explained by the full melting of the mid-span of the glass beams. In Figure 19 an example of a glass beam after testing is shown.

Figure 19 Glass beam with molten mid-span and disappeared PVB interlayer after testing (Louter & Nussbaumer, 2016)

The order of the beam collapse was as follows, first the annealed glass beam, following by the heat-strengthened beam and finally the fully tempered beam. This order is mostly related to the rate of temperature increase of the glass beams. It was observed that the annealed glass beam heated up faster than the heat-strengthened beam, which again was faster in heating up than the fully tempered glass beam. If this is directly related to the level of pre-stress in the glass beams needs to be investigated in detail. At a temperature of about 780 °C, all three of the glass beams fully collapsed.

Though the times before collapse exceeded 30 minutes, the beneficial testing conditions could be the reason for these positive results. These conditions regarded the relatively low in-plane loading and a non-exposed laterally supported top part of the glass beams. (Louter & Nussbaumer, 2016)

Fire Resistant Structural Glass Beams – 2018 – Jelle Sturkenboom
For his master thesis, Jelle Sturkenboom continued with testing laminated beams as mentioned in the previous research by Louter and Nussbaumer. The 4-point bending test set-up was based on the previous test, but since some conditions might have been in favour of the test, one aspect has changed. Now the top 3 cm of the beams are not protected anymore by the fire protective panels, since they are placed on top of the beams. In Figure 20 the test setup above the oven is shown schematically.
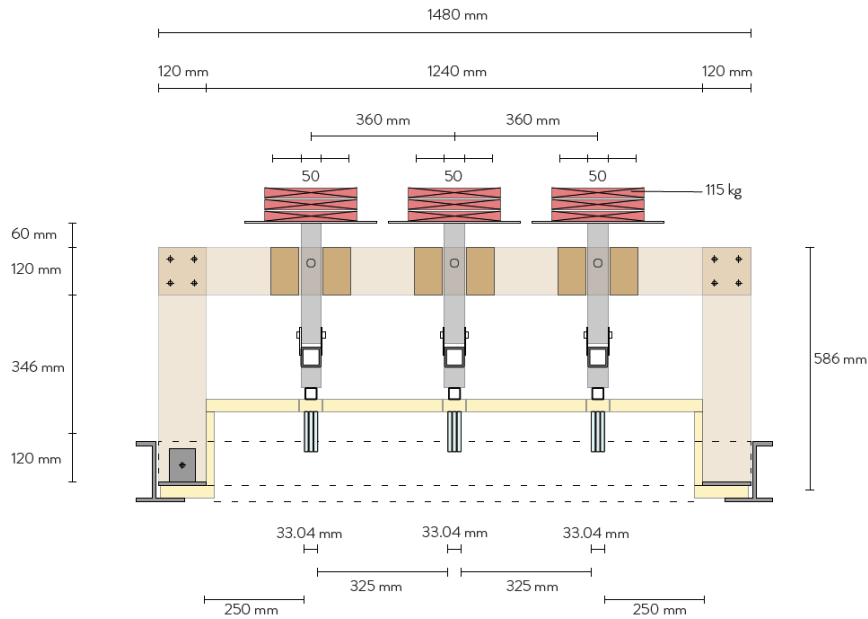
The beams that are used for this test are of standard soda lime silica glass, laminated with either PVB or SentryGlass (SG) interlayers. Again, annealed, heat strengthened and fully tempered glass were tested with the different interlayers in between. Two sets of three beams were tested first. The dimensions of the glass beams were equal to the test of Louter and Nussbaumer: 1m long and 100mm high beams consisting of panels with a width of 10mm each. The tests were performed at a certified oven at Efectis were a standard fire curve was simulated. During the test the temperature of the beams, the oven temperature and the displacement of both the beams and the set of weights are measured.

In a third series of tests also the weight on top of the beams was adjusted to 250 kg per beam. This was done because the research of Louter and Nussbaumer stated that the relatively low loading might be in favour of the outcome of the test. The tensile bending stress is now increased to approximately 11 MPa instead of the 5 MPa caused by the 115 kg of weight. Only the beams with interlayers of SentryGlas were used.

There are some interesting results from the tests. First of all, the three series of tests did not meet the requirement of a fire resistance of 30 minutes before failure. The protected 3 cm at the top of the beam as seen in the tests of Louter and Nussbaumer performed better in time. What corresponded with the previous research is the order of failure of the beams. This was also in the order of the treatment of the beams. Another similar event is the melting of the interlayers. Striking is the fact that the PVB laminates started to decompose and burn at an earlier stage than the SG laminates. This corresponds to the finding of Debuyser and the specifications of DuPont. The increasing of the load did not seem to have an influence on the time to failure. It might have an effect when a more critical load is applied on top of the beams.

During the last series of tests the beams were modified to perform better in the fire test. It was chosen to apply the intumescent paint FlameGuard HCA-TR (also used in the research of Veer et al.) onto the beams in two different ways on the surface area. One beam was coated along the bottom

3cm on the side and the full bottom of the beam. The other beam was fully coated on the three sides that are directly heated during the test. A third adjustment was the protection of the bottom edge of the beam by adding additional glass at the bottom of the glass beam.

It can be concluded that also with this test, the minimal requirement of 30 minutes fire resistance was not met. The best result was 23.5 minutes before failure. Adding the additional glass at the bottom of the beam resulted in additional strength after fracture of the glass at high temperatures. Besides, the glass seems to postpone the burning of the interlayer by protecting it from direct heating.

Applying the coating on the surface of the beam improved the performance of the glass beam. It has to be mentioned that a full protection of three sides of the beam resulted in a better performance than only coating the bottom 3cm.

However, due to the limited number of tests it is hard to draw strong conclusions based on the test data. A larger number of tests would prevent the effect of coincidence. Of course more research has to be done on this subject to really create fire resistance glass beams. (Sturkenboom, 2018)

3.4 Discussion

If the material level and its properties at elevated temperatures are considered, it can be concluded that a large number of researches can be found in literature which focus on the effects of the modulus of elasticity, tensile resistance and the thermal cracking of standard glass. Most of them seem to agree regarding the variations with temperature, but some also give a high scatter in the observed results, for example for the thermal resistance.

However, despite the agreement on the changing values of the modulus of elasticity with increasing temperature, Sturkenboom (2018) stated that above the temperature of 700°C there was a lack of data for the modulus of elasticity of soda lime silica glass. This was, as he mentioned, already stated in the master thesis of Nodehi (2016), where higher Young's modulus values had to be extrapolated above that temperature for finite element modelling purposes. It can be seen in section 3.1.2 that even for borosilicate glass the values stop at 600°C. It might be interesting to see what happens at the area above 600°C for the modulus of elasticity, as an input modelling. After all, the temperatures in fire conditions will rise above the 700°C.

Regarding the research to the fire performance of full glass systems and assemblies, it is stated that much less literature is available, especially in case of structural glass elements under fire loading. It can be concluded that not only the glass itself is important to look at, but also the connection details and restraints play an important role in the performance of the system. For structural glass beams specifically one can say that laminated beams have the potential to withstand fire loading for a significant time, however still further research has to be carried out, not only into the supports, but also into the interlayers. This also applies for the use of special coatings; they have potential to increase the fire resistance, but the right application needs further research to optimize the effects.

III
Experimental testing

4. Ultrasonic testing

From the literature review it appeared that there is a lack of data on the Young's Modulus of glass for temperatures above 600°C. This accounts for both soda lime silica and borosilicate glass. An interesting observation from literature is that the Young's modulus decreases with temperature for soda lime silica and increases for borosilicate glass. This experiment therefore aims to determine the values for the Young's modulus at temperatures beyond 600 degrees Celsius, also with the aim for better modelling. After all, the temperature of a fully developed fire can rise to between 800°C and 1200°C. (Breunese & Maljaars, 2014)

4.1 Theoretical background

4.1.1 Principle of ultrasonic testing

In earlier experiments by Rouxel, the Young's modulus was determined by the Ultrasonic Echography Method (USE). This method seems the most accurate if compared to the more dynamic methods based on resonance by Kerper and Scuderi and Shen et al. Ultrasonic testing is a form of non-destructive testing, meaning that the tested object will not be harmed while testing. With this testing method, high-frequency sound waves (ultrasound) are transmitted into a material mostly in order to detect imperfections or locate changes in material properties. (NDT Resource Center, 2014)

The principle of the USE method used by Rouxel is well described in the article of Huger et al. (2002) and is based on calculating the E-modulus from the velocity of an ultrasonic pulse transmitted in a long, thin, and refractory wave-guide sealed to a (in this case glass) specimen (Figure 21). The Young's modulus (E) then can be calculated from the density (ρ) and the longitudinal wave velocity (V_l) according to:
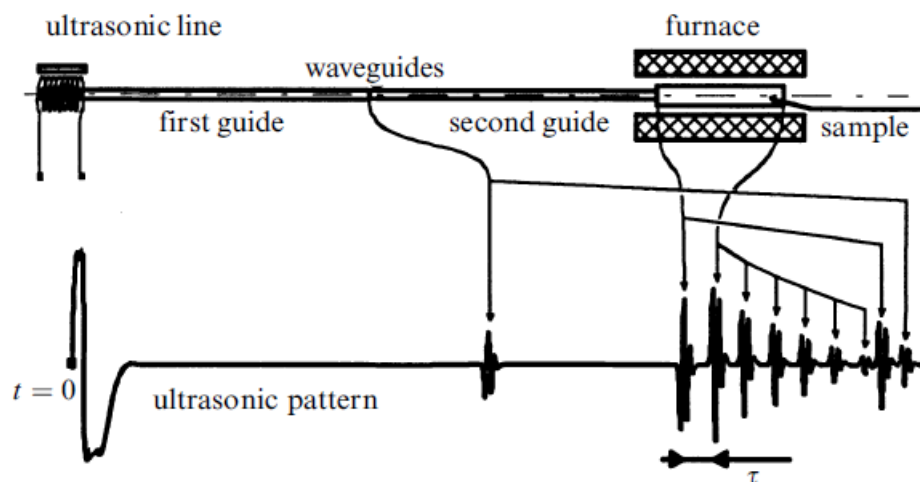
$$E = \rho \cdot V_l{}^2$$

Figure 21 Principle of the experimental setup for ultrasonic velocity measurements at high temperature in LBM ('long bar' mode) propagation mode (Huger, et al., 2002)

The condition for this LBM (Long Bar Mode) setup is that the diameter D of the tested specimen must be smaller than the wavelength λ of the sound:

$$D \ll \lambda$$

30

4.1.2 Speed of sound

To get a better understanding of the theory of sound through materials, first the speed of sound in materials will be discussed shortly. Also the material properties from which this speed depends will be explained.

The speed of sound is not always the same. Sound can be described as a "mechanical wave": it is a vibration of kinetic energy transferred from one particle (molecule or atom) to the next. When the particles are closer to each other and their bonds are thus stiffer, it will take less time to pass the sound from one particle to another. This means that the sound will travel faster through the material. This explains why it is easier for sound waves to travel through solids than through liquids, because in solids the particles are closer together and bonded stronger. The same regards to the relationship between liquids and gases. Sound will pass easier through liquids than through gases.

The velocity of a sound wave is determined by two material properties, namely the elastic properties and the density. The relationship is described as follows:

$$V = \sqrt{\frac{C_{ij}}{\rho}}$$

In this equation the elastic properties are represented by C_{ij} is ρ stands for the density of the material.

Elastic properties

Since the elastic properties are different for different types of materials, so will be the speed of sound. The elastic properties are related to the change of shape and deformation of a material when a force is applied to it. More rigid materials like steel will deform less than more flexible materials like rubber.

If the particle level is considered, the atoms and/or molecules from a rigid material have strong bonds with each other. These strong forces that exist between the particles can be seen as springs that control how fast the particles return to their original positions. The faster this happens, the quicker they are able to move again and thus they can vibrate at higher speeds. This explains why sound can travel faster through materials with higher elastic properties.

Although the density of a material also will affect the speed of sound that travels through it, the elastic properties will have a larger influence on the wave speed.

Density

The other property that has an influence on the speed of sound is the density. The density of a material can be described as the mass per volume. A material that is more dense per volume, has more mass per volume. Mostly, larger molecules have more mass, so if a material is more dense because its molecules are larger, it will pass the sound slower. This can be explained by the fact that it will take more energy to make large molecules vibrate than it does with smaller molecules. Resulting, sound will travel slower in the more dense material, while having the same elastic properties. (NDT Resource Center, 2014)

Temperature

The speed of sound in a material is also dependent on the temperature. If the temperature will increase, the particles will move faster and sound waves will travel more quickly. However, this accounts for gases. In liquids and solids the density differences as result of the high temperature are negligible and therefore the speed of sound will barely change with an increasing temperature. (CMA, sd) However, this should not be confused with the effect of the changing elastic properties at high temperatures.

4.2 Test set-up

4.2.1   Test approach

Now that the theory behind ultrasonic testing is known, the test approach can be determined. Since the testing is dependent on the available equipment and materials, some considerations have to be made. First of all, tube ovens are available at the 3ME faculty which are particularly suitable for this experiment. These ovens differ in tube length, inner diameter, maximum temperature and hotzone (length where the temperature is homogeneous). Secondly, the ultrasonic measurement equipment available has two transducers, meaning that the sound will be transferred from A to B (see Figure 22). This is in contrast with the pulse echo as described before, which is transmitted back to the same point. Finally, there are glass rods available with a maximum length of 1.5m and different diameters.

Figure 22 Pundit 200 ultrasonic equipment from Proceq as used in this test

As a first approach to determine the Young's modulus at high temperatures, it was chosen to simplify the test set up with the least possible disturbances. The principle described by Huger et al. uses a waveguide which is sealed to the glass specimen. However, the extra transitions that are involved with the use of a waveguide can lead to inaccuracies in the measurements, due to the impedance differences between the materials. To exclude these inaccuracies, measurements will be made directly on the glass. This means that the glass rod has to protrude from the oven on both sides.

For the first experimental step, the small tube oven will be used. The tube has a length of 80 cm and an inner diameter of 25mm. The hotzone of this oven is 12cm. To be sure the transducers of the ultrasonic measurement equipment will not be influenced by the heat of the oven, the length of the

glass rod is kept at 1.5m. The diameter of the glass rod used is 20 mm and the glass type is soda lime silica. Besides, to avoid that the ultrasound signal might choose the fastest route through the material of the oven, the glass rod is supported by two steel frames. In this way the glass is not in contact with the oven, which ensures the sound will go through the glass. The set-up is shown in Figure 23.

The transducers are placed on both ends of the glass rod to measure the time the sound travels from one end to the other. This time is measured at different temperatures to see the effect of temperature on time. Steps of 50 degrees Celsius have been taken up to 500 degrees Celsius.
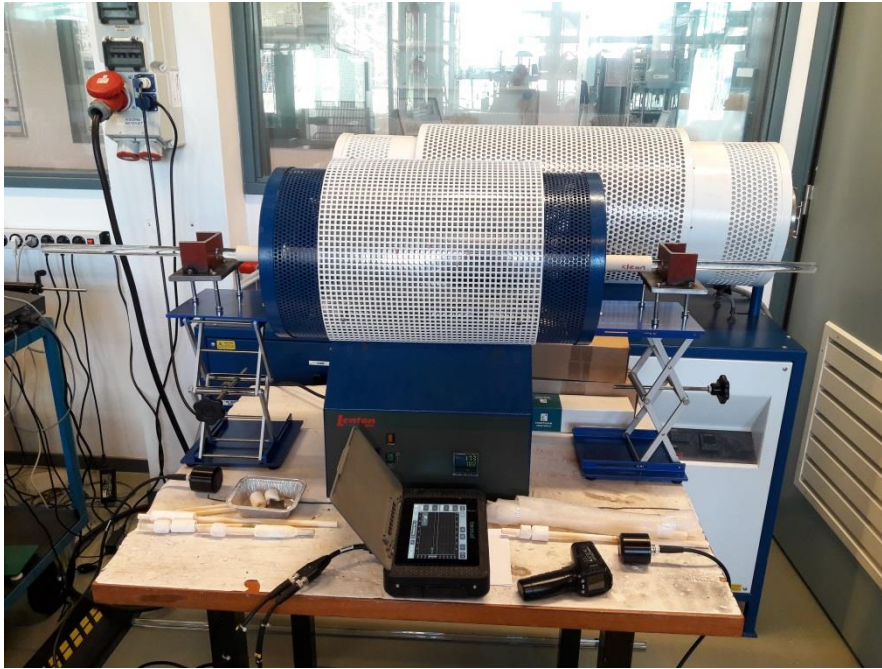
Figure 23 Test set up experimental test small oven

This first experiment was especially intended to find out if it is possible to make measurements in such a test set-up and to see if there are any weak points which could be improved. Before increasing the temperature, the ultrasonic device was tested on the glass rod at room temperature. This measurement gave a logical value for the velocity of sound through glass, thus indicating that it is at least possible to measure the time of the soundwave. Also the condition D « λ is met. At room temperature the longitudinal wave velocity was measured to be 5535 m/s and the sound was produced with a frequency of 54kHz. It follows that the wavelength is 102 mm, which is greater than the diameter of the rod.

The measurements at higher temperatures showed an increase in transmission time from approximately 250°C and higher, meaning that the velocity decreases with higher temperatures. This is in accordance with the theory. It is expected that the Young's modulus will decrease, because the stiffness of the glass will decrease due to the less stiffer bonds between the atoms at higher temperatures. For this reason the sound will travel slower through the glass and so the velocity will decrease too.

However, this increase in time is rather small, due to the small part of the glass which is heated homogeneously compared to the whole length of the rod. The outer ends of the glass stay on room

temperature, while the middle of the glass may already has risen to 400°C. A larger hotzone is preferable to improve the measurements and to eliminate that the results are influenced by noise. It will also be important to measure the temperature at different points over the length of the rod, to find out the variations of temperature. This could be done with the use of thermocouples.

To achieve a larger hotzone, the most logical step would be to change to a bigger tube furnace. The bigger available furnace has a hotzone of 60 cm and a tube length of 150 cm. The inner diameter of the tube is 70 mm. Since the maximum length of the glass rod is 150 cm, which is the same as the tube length, other supports for the rod must be devised. The deflection at room temperature is also calculated and result in a value of 0.6mm. This is assumed to be negligible. To prevent that the transducers not work properly anymore at too high temperatures, it is also important that the outer ends of the glass will not heat up too high. In Figure 24 the test set-up for the bigger tube furnace is shown.
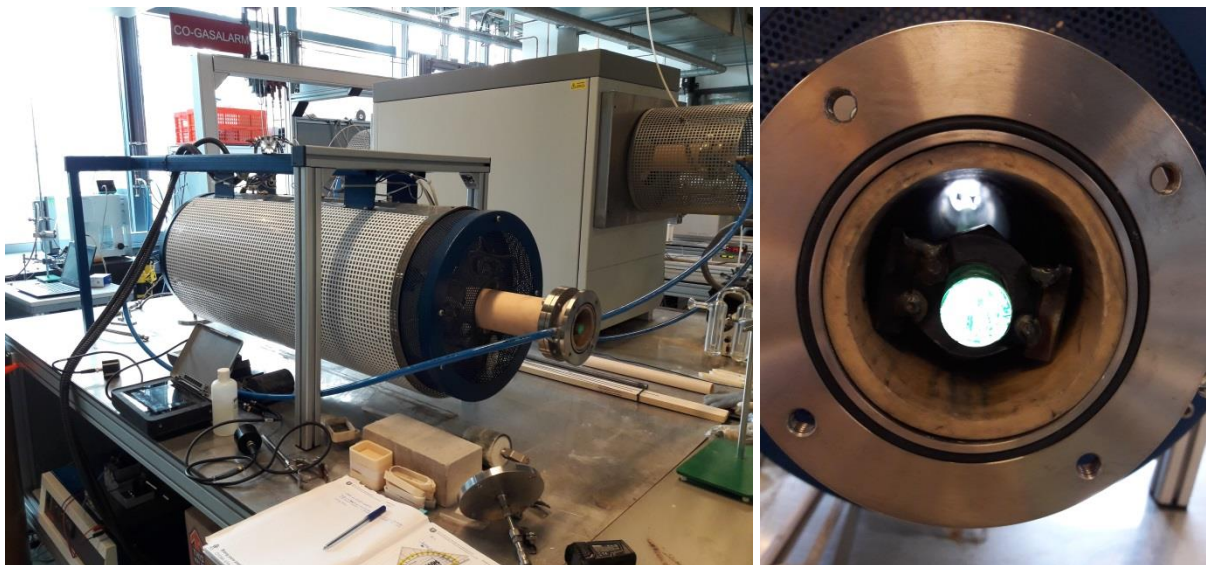
Figure 24 Test set up experimental test large tube oven

The temperature of the oven was set to different setpoints, starting at room temperature and increasing in steps of 100 degrees Celsius to a maximum of 500°C. Each setpoint was kept constant for an hour to be sure the glass rod adapted to the temperature of the oven. Besides, the temperature inside the oven was measured with a thermocouple. This temperature will always be a little bit lower than the set temperatures. Also the temperatures at the ends of the glass rod were measured to be sure they did not heat up too quickly.

It could be concluded after the test that this set up as such was not perfect either. First of all, the glass rod easily shifts position. In addition, the rod is exactly as long as the tube, which makes the workspace very small. It is not possible to hold the glass firmly to press the transducer against the glass. Besides, the transducer easily shifts position too when pressed against the glass. This is due to the limited workings space, but also due to the fact that the person holding one of the transducers has to check the result on the ultrasonic equipment at the same time. The final setup needs some improvements.

4.2.2 Final setup

For the final tests it was decided to improve the setup in the big tube oven. To prevent the rod from shifting position, the steel profiles were provided with screws to fix the glass rod. Besides, alumina felt was placed between the tube wall and the profiles to keep the profiles in place. Also alumina felt was used to cover the ends of the tube to prevent airflows through the tube as much as possible (Figure 25). These airflows could influence the temperature in the oven.
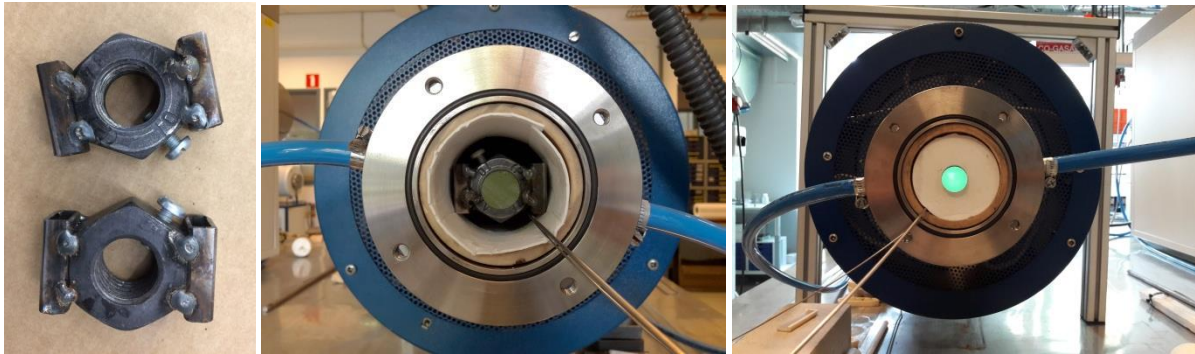

Figure 25 Test set up SLS glass in tube oven

To measure the temperature of the glass more precisely, five thermocouples of type K were placed on the glass rod at different positions. One thermocouple is placed in the middle of the rod. Two other thermocouples are placed at the ends of what is supposed to be the "hotzone": 30 centimetres at each side from the middle. The last two are placed in the middle of the remaining length between the aforementioned thermocouples and the ends of the rod (Figure 26). The temperature at the end of the glass rod is measured with a laser device.

| 22,25 | 22,20 | 30,00 | 30,00 | 22,20 | 22,25 |

Figure 26 Locations thermocouples

To prevent the shifting of the sensors while watching the result on the ultrasonic device, the measurement is done with three people. Two holding each of the sensors and one reading the measured time on the ultrasonic device. Before each measurement the ends of the glass rod are cleaned and provided with new contact fluid to ensure a good transfer of the ultrasound.
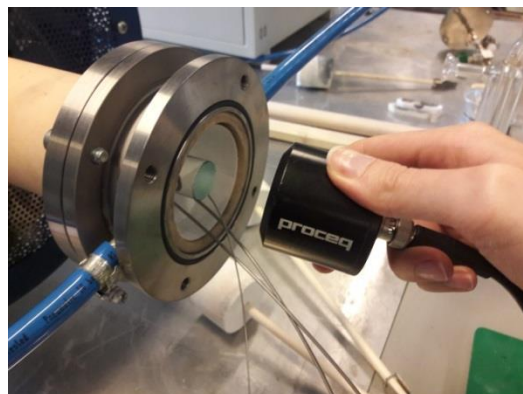

Figure 27 Measurement at the end of the glass rod with the sensor of the ultrasonic device

4.3 Results

In this paragraph the measurement results of the thermocouples and the ultrasonic device will be presented, both for the soda lime silica and the borosilicate glass rod. For the soda lime silica rod, AR-GLAS® is used and for the borosilicate rod DURAN®. Both glass types are from SCHOTT. The ends of the rods are made as smooth as possible. For this reason, the lengths of the rods are a little less than 1.5m.

4.3.1 Soda Lime Silica

As was described in the paragraph before, the temperature of the glass is measured with thermocouples at different points along the rod. The thermocouples are constantly measuring the temperature during the test. The results of this measurement are shown in Figure 29 below. For clarity, Figure 28 shows the locations of the various thermocouples.
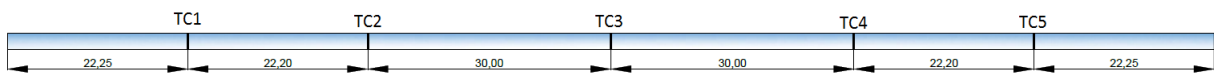
Figure 28 Locations thermocouples SLS glass
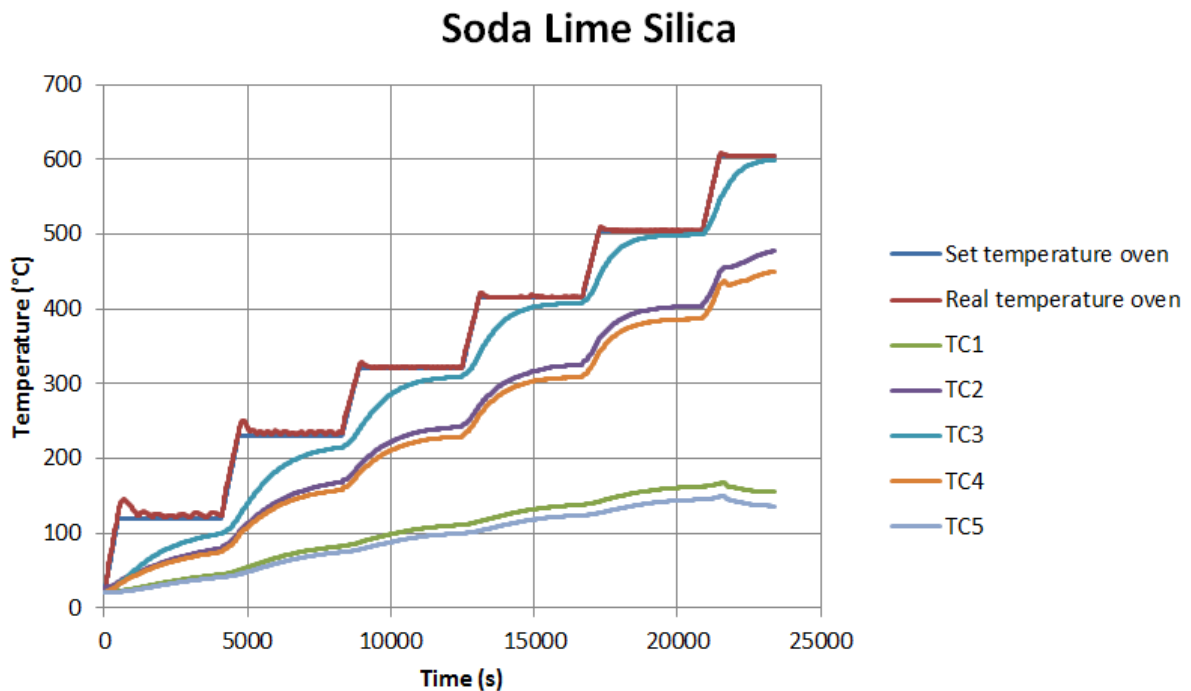

Figure 29 Temperature thermocouples SLS glass rod during test

At the horizontal axis the time (in seconds) of the test is given, the vertical axis shows the measured temperatures in degrees Celsius. The test starts at time 0 on room temperature. In 10 minutes the temperature of the oven will rise to the first setpoint and will be kept at that point for an hour. In this way there will be enough time for the glass to adapt to the temperature, since glass does not conduct heat very well. After that hour the temperature rises for about 100 degrees Celsius in ten minutes and is kept stable again for an hour. This process repeats until the test comes to an end.

36

The transmission time of the ultrasound is measured at the end of each temperature step, right before the setpoint rises to the next value. In this way, the glass is heated up as much as possible, to get a measurement as accurate as possible. For every measurement made, a different temperature curve along the rod could be derived. Each of the curves shown in Figure 30 are related to a measured transmission time.
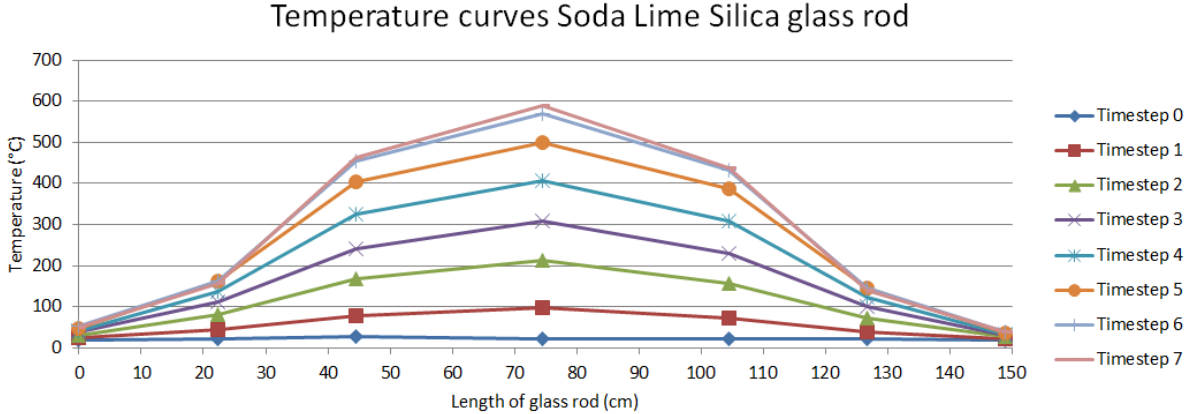

Figure 30 Temperature curves soda lime silica glass rod

It could be noted from the graph that the hotzone, which is supposed to be the zone with a homogeneous temperature over the middle 60 cm, is not quite constant in temperature. This could be related to the fact that the oven is not completely closed off during the test. Normally, this kind of tube furnace is closed on both sides during experiments. In this case however, some warmth could escape through the glass and small gaps between the alumina felt and the glass rod /tube wall.

The exact values of the measured temperatures, corresponding to the measured transmission times can be found in Appendix A: Measurement results ultrasonic testing. To get a clear picture of the change of the measured transmission time against the temperature, the highest measured temperature of the glass rod (middle value in Figure 30) is plotted against the transmission time in Figure 31.
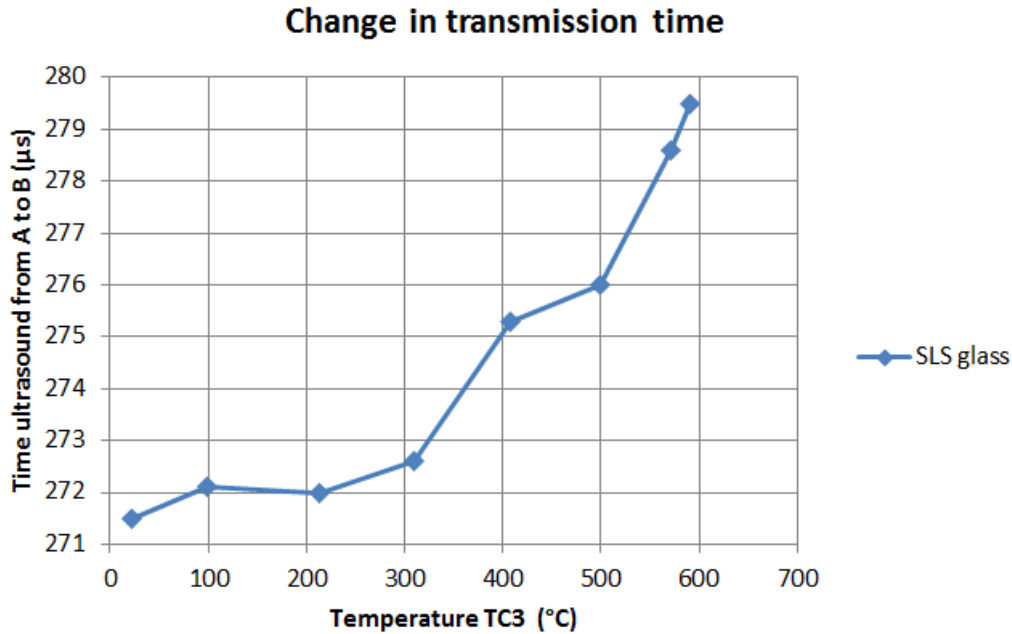
Figure 31 Change in transmission time over temperature of SLS glass

It can be clearly seen that the transmission time increases with the rising temperature. This means that the longitudinal velocity of the soundwave decreases with increasing temperature, indicating that the Young's modulus will decrease as expected.

It can be noted that the measurement ends at 600 °C. This is due to the deflection of the glass rod, which started around 21600 seconds after the start of the test. This has been observed by moving aside the alumina felt a little. In Figure 29 this could be noticed by a small drop in temperature, probably caused by some colder air flow due to the removal of the alumina felt on both sides to have a better observation. When the first small deflection was noticed around 21600 seconds, the maximum temperature in the middle of the glass rod was around 554°C. After 21780 seconds, which is only 3 minutes later, the rod already deflected quite a lot. Yet the rod did not reach the bottom of the furnace. At 23250 seconds the middle of the glass rod lay on the bottom of the oven. The ultrasound measurement at that time gave an unrealistic value, indicating that the sound chose the fastest way through the wall of the oven. Therefore the test came to an end at that time and the temperature of the oven could return to room temperature. The last useful measurement was done at 22400 seconds, with a maximum temperature of 590°C of the glass rod.

The observed deflection results in a slight increase of the length of the glass rod. The maximum increase is equal to 4 mm. How this is of influence on the result will be elaborated in section 4.4.

4.3.2 Borosilicate

Also borosilicate glass is tested in the same test setup. It must be noted that the available diameter of the rod is slightly bigger than for the soda lime silica: 24 mm. Though, the condition D « λ is still being met. It should also be mentioned that the steel profiles must be replaced by bigger ones to fit the rod. These larger profiles however obstructed the view in the oven quite a lot.

Just like the soda lime silica the temperature is measured along the rod according to Figure 32. Figure 33 shows the results of these thermocouples.
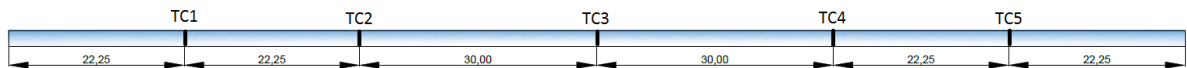
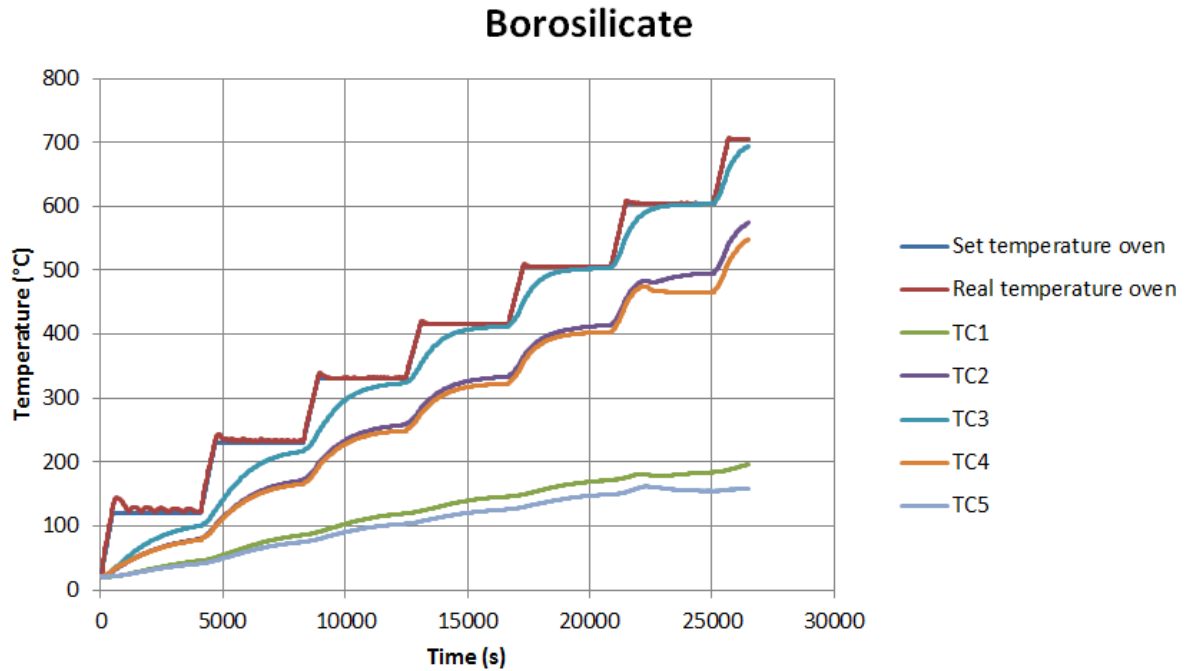**Figure 32 Locations thermocouples BS glass**

Figure 33 Temperature thermocouples BS glass rod during test

At the horizontal axis the time (in seconds) of the test is given, the vertical axis shows the measured temperatures in degrees Celsius. Equal to the test for the soda lime silica, the test starts at time 0 on room temperature. In 10 minutes the temperature of the oven will rise to the first setpoint and will be kept at that point for an hour. After that hour the temperature rises for about 100 degrees Celsius in ten minutes and is kept stable again for an hour. This process repeats until the test comes to an end.

Again, the transmission time of the ultrasound is measured at the end of each temperature step, right before the setpoint rises to the next value. For every measurement made, a different temperature curve along the rod could be derived. Each of the curves shown in Figure 34 are related to a measured transmission time.
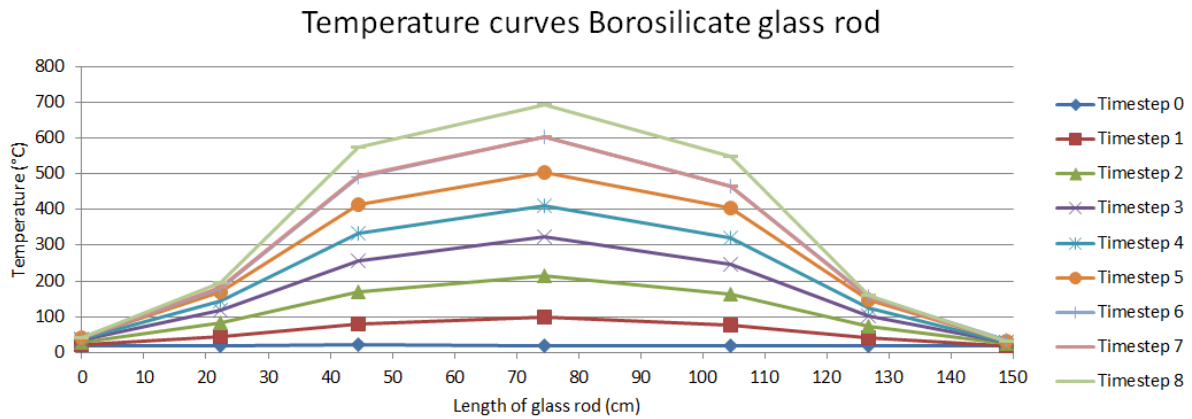
Figure 34 Temperature curves borosilicate glass rod

What has been mentioned previously for the soda lime silica glass, is logically also the case here: the hotzone again is not quite constant in temperature. The exact values of the measured temperatures, corresponding to the measured transmission times can be found in Appendix A: Measurement results ultrasonic testing. To get a clear picture of the change of the measured transmission time against the temperature, the highest measured temperature of the glass rod (middle value in Figure 34) is plotted against the transmission time in Figure 35.
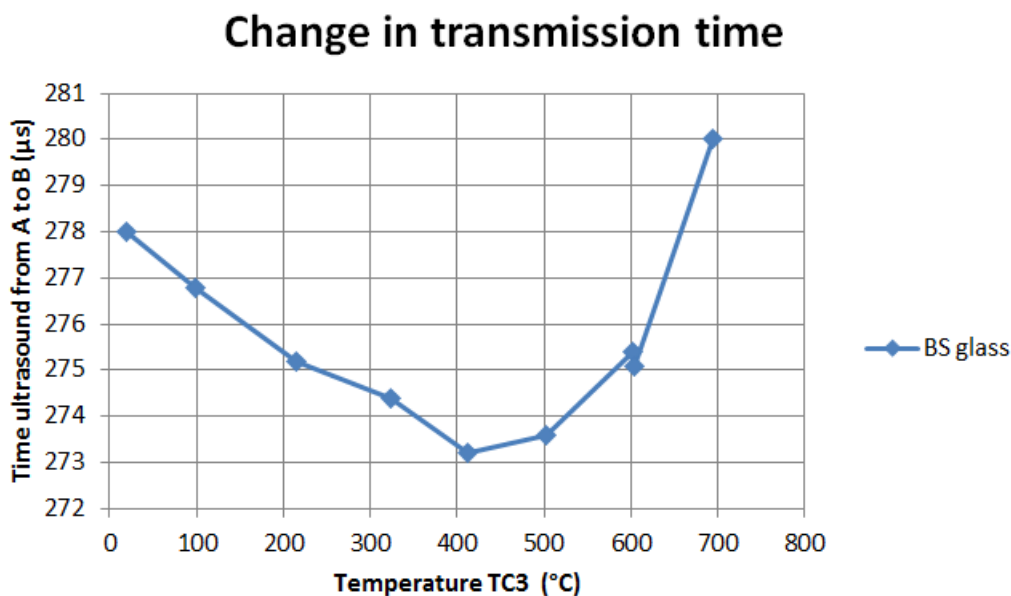

Figure 35 Change in transmission time over temperature of BS glass

In contrast to the soda lime silica glass rod, the transmission time for the borosilicate glass rod first decreases with the rising temperature. This indicates that the longitudinal velocity will increase with higher temperatures and so will the Young's modulus. This observation was already noticed in literature (Kerper & Scuderi, 1966). However, at one point the transmission time starts to increase with rising temperature, indicating a decrease for the modulus of elasticity for borosilicate glass.

For this test the measurement ends at 700 °C. Again the deflection was tried to be watched above the 500 °C, since Table 6 shows some critical points for these temperatures. Also in this case a drop in temperature for the thermocouples TC4 and TC5 can be seen. This is caused by removing the

40

alumina felt at the side of these thermocouples to have a good view in the oven. Unfortunately it was difficult to observe the beginning of the deflection due to the bigger sight blocking profiles which supported the glass rod. At 23500 seconds the borosilicate glass rod was already deflected quite a lot. The temperature in the middle of the glass is then measured at 601 °C. In comparison with the soda lime silica rod, the temperature was 570 °C with comparable deflection. The temperature of the borosilicate glass is around 30 °C higher and also the time at which this deflection occurs is later after starting time. The last relevant measurement was done at 26477 seconds at a maximum temperature of 694 °C in the middle of the glass rod.

The observed deflection results in a slight increase of the length of the glass rod. The maximum increase is equal to 1 mm. How this is of influence on the result will be elaborated in section 4.4.

4.4 Analysis

To retrieve the values of the modulus of Elasticity of the glass rods at different temperatures, the following formula will be used:

$$E = \rho \cdot V_l{}^2$$

Where E is the Young's modulus, ρ the density and V_l the longitudinal wave velocity.

The density of glass changes with temperature, however, this change is very small over the range of this experiment. For example the density of soda lime silica glass at 500 °C is still 2474 kg/m^3 and at 700 °C 2438 kg/m^3. (Kozlowski, et al., 2018) Since this does not vary more than a few percent, the velocity changes recorded are mainly due to the effect of temperature on the modulus of elasticity. This was also mentioned in the experiments of Rouxel, based on earlier findings. (Rouxel, 2007)

It can be said that the longitudinal velocity does change significantly as was seen in the results by looking at the changing transmission time. However, this velocity cannot directly be calculated from the transmission time and the length of the rod, due to the varying temperature over the length of the rod. This means that the velocity will also change over the length of the rod. In the warmer areas the velocity will probably be smaller than in the colder parts. The problem that arises is that this change of the velocity is not known. Therefore an approximation for the variation of the velocity has to be found.

When looking at the change of the transmission time, the assumption is made that the longitudinal velocity can be approximated with a polynomial function in the form of:

$$V_l(T) = A + B \cdot T + C \cdot T^2 + D \cdot T^3$$

This is a polynomial of the third degree with 4 unknown coefficients: A, B, C and D. These coefficients can be solved by using the values that are known, like the measured total transmission time, length of the rod and the corresponding temperatures. These values relate to each other in the following way:

$$l_{tot} = \sum \Delta l_i = \Delta l_1 + \Delta l_2 + \Delta l_3 + .. + \Delta l_i$$

$$t_{tot} = \sum \Delta t_i = \Delta t_1 + \Delta t_2 + \Delta t_3 + .. + \Delta t_i$$

Where l_{tot} is the total length of the glass rod and t_{tot} is the total transmission time, measured from one end to the other. The sum of the total transmission time can also be described as the sum of the length parts divided by the sum of the mean velocities per length of the rod:

$$t_{tot} = \frac{\sum \Delta l_i}{\sum \Delta V_{l,mean,i}}$$

For every mean velocity over a small part of the beam applies:

$$\Delta V_{l,mean,i} = A + B \cdot T_i + C \cdot T_i^2 + D \cdot T_i^3$$

Filling in this formula in the aforementioned formula for the total transmission time, you get:

$$t_{tot} = \frac{\sum \Delta l_i}{\sum (A + B \cdot T_i + C \cdot T_i^2 + D \cdot T_i^3)}$$

Since the length of the rod is known, as well as the measured transmission times, the above equation can be filled in for every timestep as presented in Figure 30 for soda lime silica and Figure 34 for borosilicate glass. The coefficients A, B, C and D will be the only unknowns, therefore only 4 equations are needed to solve the problem.

Due to mathematical solvability reasons, the length of the rod will be divided in four parts according to the places of the thermocouples (Figure 36). Over each part of the length the mean temperature will be calculated and entered in the formula together with the corresponding value for the measured transmission time. Besides, the temperature curve over the length of the rod will be assumed to be symmetrical, to be able to solve the formulas.
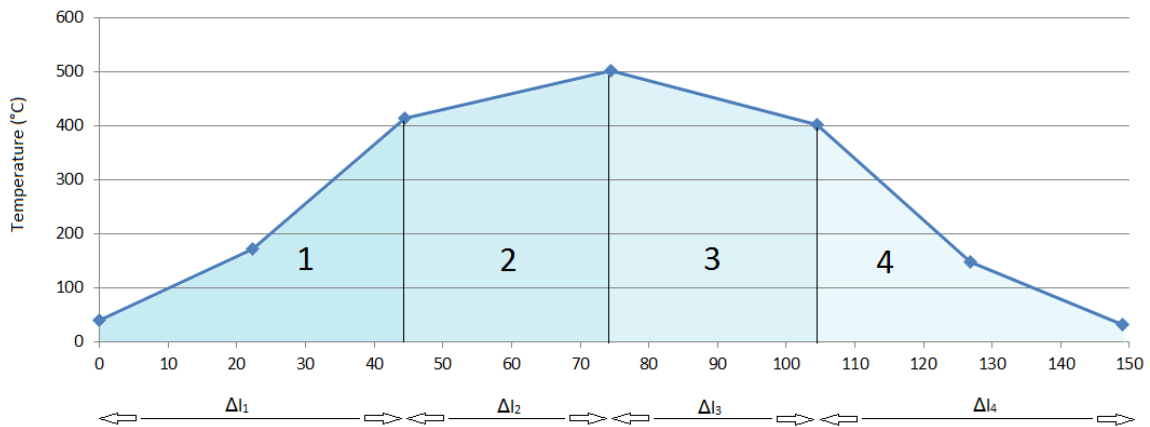

Figure 36 Example division of the length of the rod at one timestep

The solutions for these equations will be presented in the next two paragraphs for the soda lime silica glass rod and the borosilicate glass rod. Maple, software for mathematics, will be used to solve the equations with the four unknowns. The aforementioned analysis will be validated by means of an experiment on aluminium, of which the results for the Young's Modulus at elevated temperatures are known in the standards. (NEN, 2011) This will be elaborated in section 4.5.

4.4.1 Soda Lime Silica

After solving the equations in Maple, the formula for the longitudinal velocity of the soda lime silica glass rod can be written as follows:

$$V_{l,SLS}(T) = 0.55 - (4.35 \cdot 10^{-5}) \cdot T + (2.73 \cdot 10^{-7}) \cdot T^2 - (6.17 \cdot 10^{-10}) \cdot T^3$$

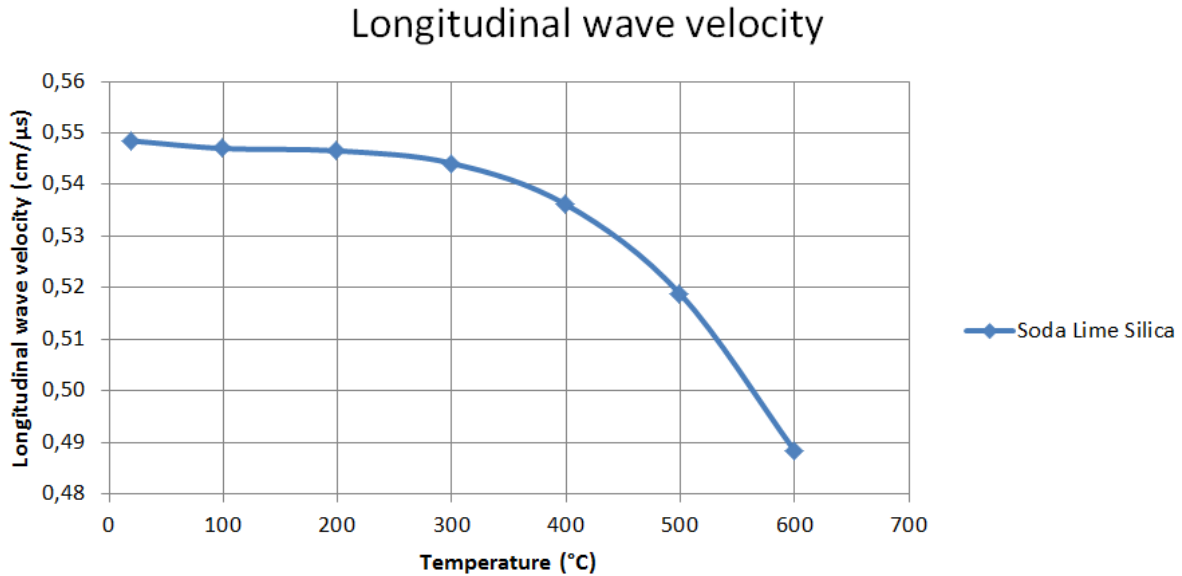The curve for this longitudinal velocity then can be shown as follows:

Figure 37 Longitudinal wave velocity soda lime silica glass

Figure 37 shows that the velocity will decrease with increasing temperature. With the values for the longitudinal wave velocity, the Young's modulus can be calculated with the earlier mentioned formula:

$$E = \rho \cdot V_l^{\,2}$$

The density (ρ) of soda lime silica glass is 2500 kg/m^3 and will be used to calculate the value for E. The resulting values are presented in Figure 38. The exact values can be found in Appendix B: Young's modulus values at elevated temperatures.
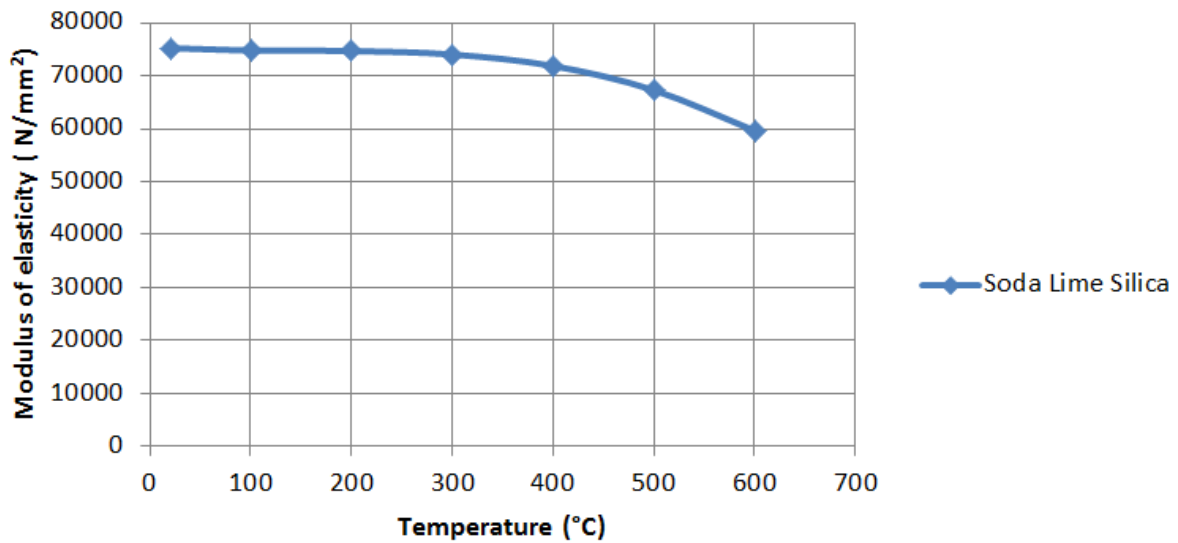
Modulus of Elasticity

Figure 38 Modulus of Elasticity soda lime silica glass

Figure 38 shows that the modulus of elasticity is decreasing almost linearly until a temperature of 400 degrees Celsius. Then the decrease is becoming larger and a more steeper decline can be noticed. It looks like the stiffness will decrease more quickly with increasing temperature from then. This change is in correspondence with previous experiments found in literature.

Since the Young's modulus is derived using equation $E = \rho \cdot V_l^2$, where the longitudinal wave velocity depends on the length of the rod, a length increase results in an overestimation in the decrease of E at temperatures where the deflection is clearly present. This change of E for the last temperature step is calculated and results in a change for E of 4.5%. This percentage is assumed to be not negligible and should be taken into account.

Figure 39 shows the modulus of elasticity for the Soda Lime Silica glass, including the effect of the change of length of the rod. The exact values can be found in Appendix B: Young's modulus values at elevated temperatures.
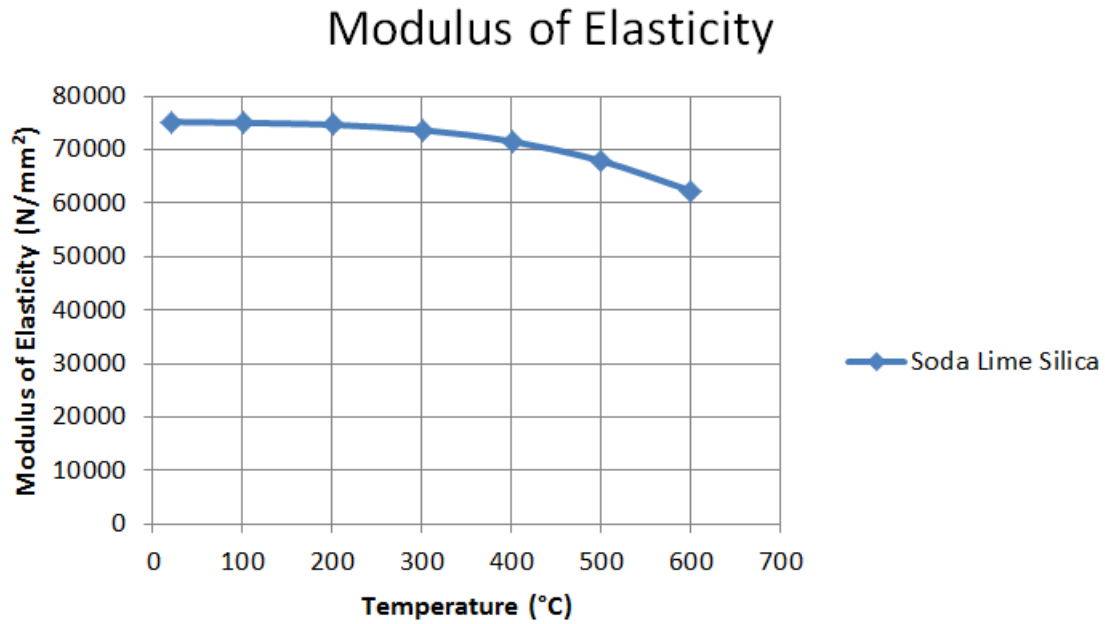
Modulus of Elasticity

Figure 39 Modulus of Elasticity Soda Lime Silica glass including change of length

Plastic deformation

During the experiments a maximum deformation of 25 mm was observed for the SLS glass rod. This deformation consists of an elastic and plastic part. The elastic deformation is calculated with the following equations:

$$w = \frac{5}{384}\frac{q\ell^4}{EI} \qquad \text{(for pinned support)}$$

$$w = \frac{1}{384}\frac{q\ell^4}{EI} \qquad \text{(for fixed support)}$$

In this equation w represents the elastic deformation, q is in this case the self- weight, ℓ the length between the supports and EI the bending stiffness of the glass rod. The assumption is that the support situation of the glass rod lies between a pinned support and a fixed support.

The elastic deformation therefore will be between 0.13 mm and 0.66 mm at 600 °C. This means that the plastic deformation is about 98.4% of the total deformation at 600 °C.

4.4.2 Borosilicate

After solving the equations in Maple, the formula for the longitudinal velocity of the borosilicate glass rod can be written as follows:

$$V_{l,SLS}(T) = 0.54 + (1.04 \cdot 10^{-6}) \cdot T + (3.39 \cdot 10^{-7}) \cdot T^2 - (6.44 \cdot 10^{-10}) \cdot T^3$$

The curve for this longitudinal velocity then can be shown as follows:

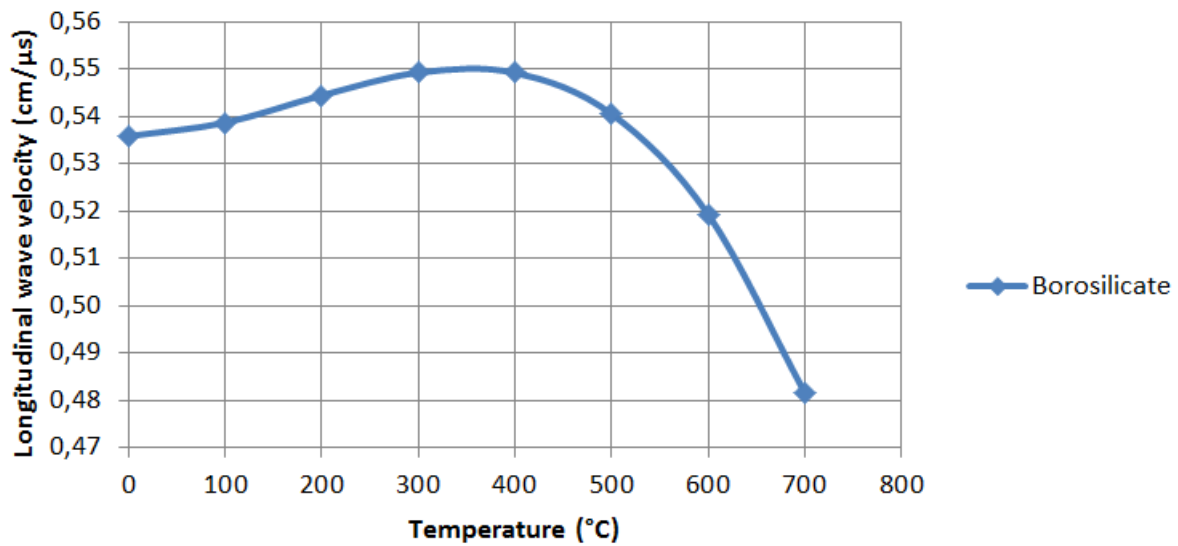Figure 40 shows that the longitudinal velocity first will increase with increasing temperature. After 400 degrees Celsius however the turning point takes place and the velocity will decrease. With the values for the longitudinal wave velocity, the Young's modulus can be calculated with:

$$E = \rho \cdot V_l^{\,2}$$

The density (ρ) of borosilicate glass is 2230 kg/m^3 and will be used to calculate the value for E. The resulting values are presented in Figure 41. The exact values can be found in in Appendix B: Young's modulus values at elevated temperatures.

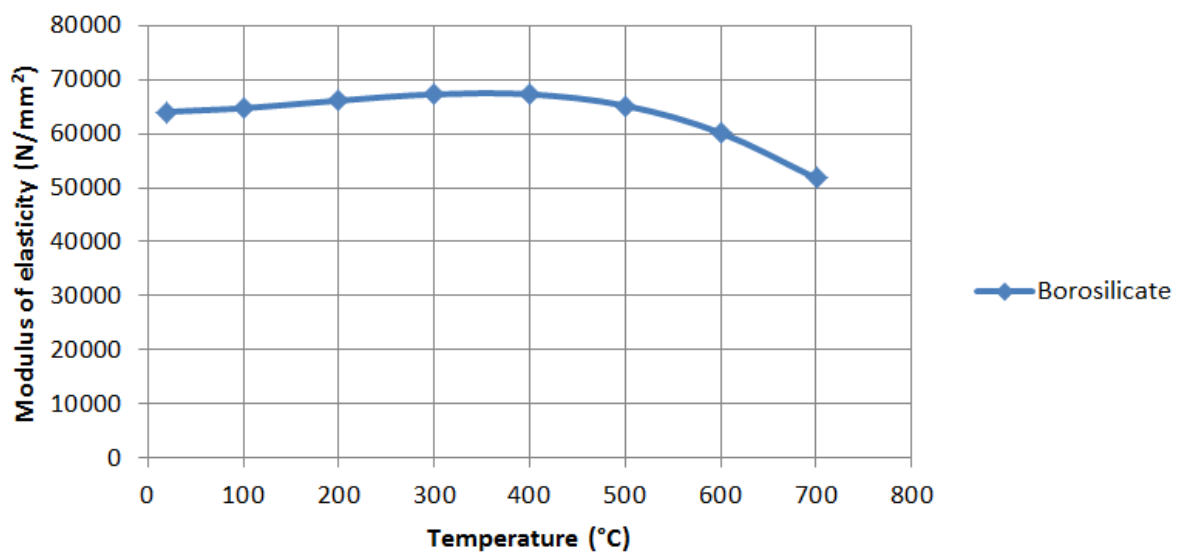Figure 41 shows that the modulus of Elasticity first increases almost linearly with increasing temperatures until 400 degrees Celsius. This indicates that the stiffness of borosilicate glass first becomes larger with increasing temperatures. However, after 400 degrees Celsius, the Young's modulus decreases and so the stiffness becomes smaller with increasing temperatures. Also in earlier experimental results (Kerper & Scuderi, 1966), it is observed that the stiffness of borosilicate glass first increased with higher temperatures.

Since the Young's modulus is derived using equation E = ρ · V$_l^2$, where the longitudinal wave velocity depends on the length of the rod, a length increase results in an overestimation in the decrease of E at temperatures where the deflection is clearly present. This change of E for the last two temperature steps is calculated and results in a change for E of 0.9%. This percentage is assumed to be negligible.

Plastic deformation
During the experiments a maximum deformation of 23 mm was observed for the BS glass rod. This deformation consists of an elastic and plastic part. The elastic deformation is calculated with the following equations:

$$w = \frac{5}{384}\frac{q\ell^4}{EI} \qquad \text{(for pinned support)}$$

$$w = \frac{1}{384}\frac{q\ell^4}{EI} \qquad \text{(for fixed support)}$$

In this equation w represents the elastic deformation, q is in this case the self-weight, ℓ the length between the supports and EI the bending stiffness of the glass rod. The assumption is that the support situation of the glass rod lies between a pinned support and a fixed support.

The elastic deformation therefore will be between 0.10 mm and 0.49 mm at 700 °C. This means that the plastic deformation is about 98.7% of the total deformation at 700 °C.

4.4.3 Comparison SLS and BS glass
The following graph compares the results of the analysis for both the soda lime silica as the borosilicate glass to each other.
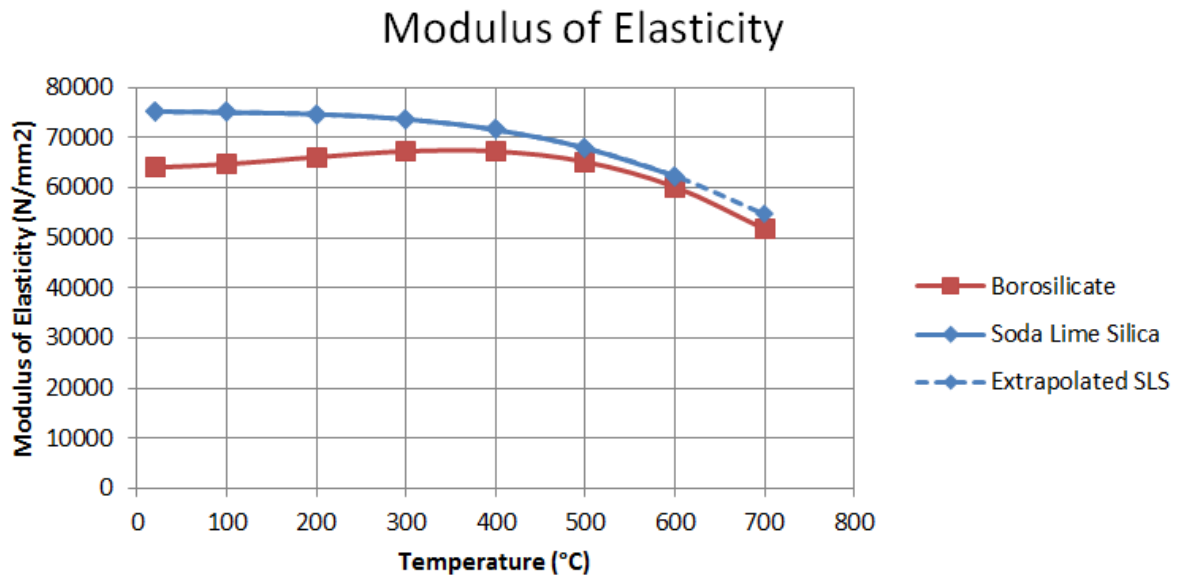
Figure 42 Comparison modulus of elasticity SLS and BS glass

There are a few aspects that can be noticed from Figure 42. First of all there is an obvious difference in the initial values for the Soda Lime Silica and the Borosilicate glass. The Soda Lime Silica glass starts at a stiffness of $75 \cdot 10^3$ N/mm^2 at room temperature and the Borosilicate glass at $64 \cdot 10^3$ N/mm^2. According to the specifications of the manufacturer the Young's modulus for the soda lime silica glass rod should be $73 \cdot 10^3$ N/mm^2 and for the borosilicate glass rod $63 \cdot 10^3$ N/mm^2 at room temperature. So there is a slight difference between the analysed values and that of the manufacturer. A likely explanation is that a different measurement method is used for the determination of the values of the manufacturer. The differences lie within the measurement error of both techniques and are negligible.

Secondly, it can be observed that initially a decrease of the modulus of elasticity for Soda Lime Silica glass can be noted, while an increase of E for Borosilicate glass can be seen with increasing temperature, as was already noted from Figure 39 and Figure 41. However, from 400 degrees Celsius, both of the glass types show a decrease in the Modulus of Elasticity. The Soda Lime Silica glass and the Borosilicate glass are practically running parallel to each other.

4.4.4 Comparison with steel

Steel is widely applied in structural elements which are required to be structurally safe during a fire. To visualise the performance of structural glass at elevated temperatures a relative comparison with structural steel is presented. The relative stiffness loss has been plotted against the temperature for both steel (Bouwen met Staal, 2019) as SLS and BS glass in Figure 43.
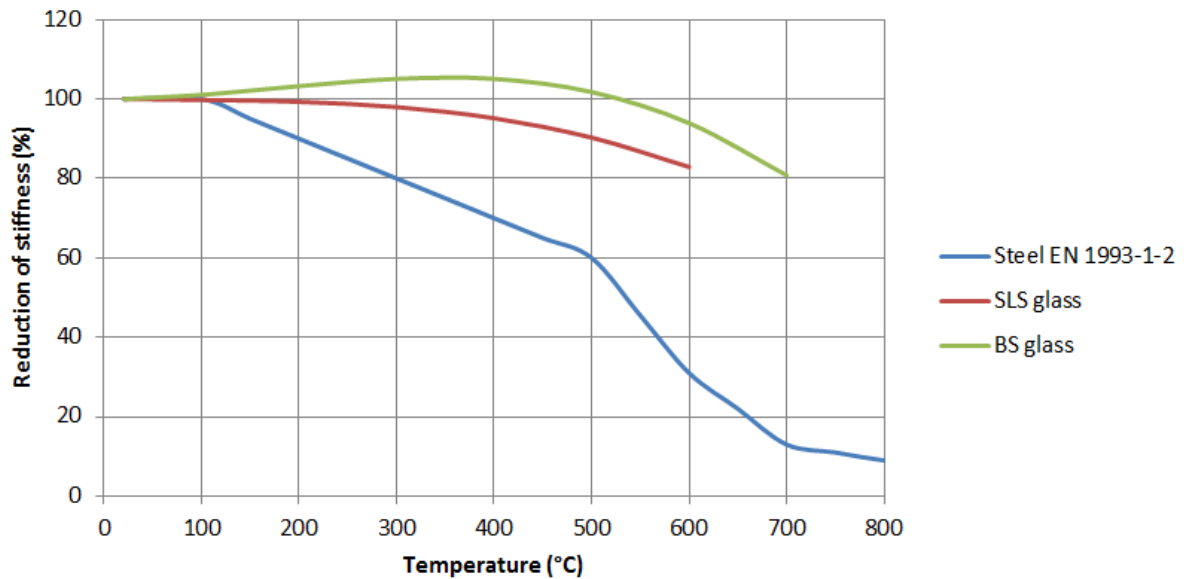
Stiffness loss at elevated temperatures

Figure 43 Comparison of stiffness loss at elevated temperatures

From the graph it can be observed that the stiffness loss at 500 °C for steel is already 40%, which is significantly higher than the stiffness loss for SLS glass (10%). For Borosilicate glass there is even a stiffness increase of 2% at 500 °C. For both steel and glass, the stiffness reduction is more significant for temperatures beyond 500 °C. For steel a more sudden stiffness loss beyond 500 °C is observed, whereas for glass the stiffness decreases more gradually. Therefore, it can be concluded that glass outperforms steel in terms of relative stiffness within the measured temperature range.

4.5 Validation

To validate the results and the analysis of the conducted experiments, an aluminium rod is tested and analysed in the same way as was done for the glass rods. Since the values for the changing Modulus of Elasticity for aluminium are known in the standards (NEN, 2011), the measurement error and the accuracy of the 3rd order polynomial approximation can be determined.

For this test, the same experimental setup is used as described for the glass rods. An aluminium rod (aluminium alloy EN-AW 6082-T6) with a length of 1.5 m and a diameter of 20 mm is used for this experiment. In this case also the condition D « λ is met: 20 mm is much smaller than 95.7 mm for the calculated wavelength of the ultrasound, using a frequency of 54 kHz.

4.5.1   Results

The measurement results of the thermocouples are presented in Figure 44. It should be noted that the ultrasonic device could only handle temperatures up to 60 degrees Celsius. That is the reason why the test had to stop when the ends of the rod reached that temperature (temperatures ends only pictured in Figure 45). The tube furnace unfortunately was not the most accurate in controlling the temperature in the temperature range shown in the graph. This is the reason why some overshoot can be noticed. Though, the aluminium rod heated up gradually.
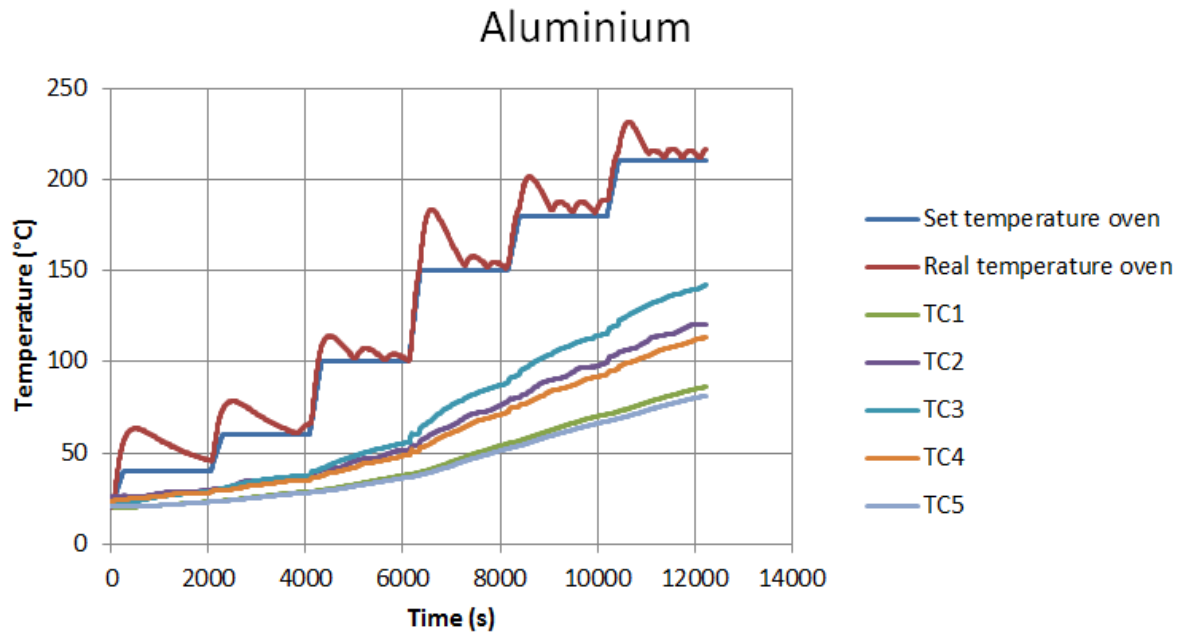
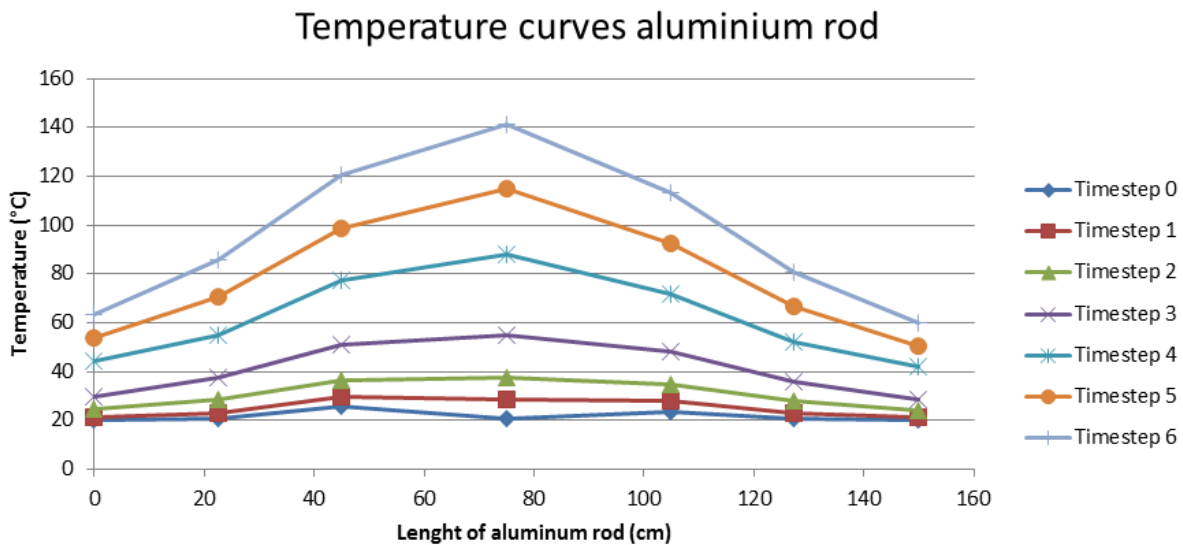Figure 44 Temperature thermocouples aluminium during test

Figure 45 Temperature curves aluminium rod

The transmission time of the ultrasound is measured at the end of each temperature step, right before the setpoint rises to the next value. For every measurement made, a different temperature curve along the rod could be derived. Each of the curves shown in Figure 45 are related to a measured transmission time.

The exact values of the measured temperatures, corresponding to the measured transmission times can be found in Appendix A: Measurement results ultrasonic testing. In Figure 46 the highest measured temperature of the rod (TC3) is plotted against the transmission time.
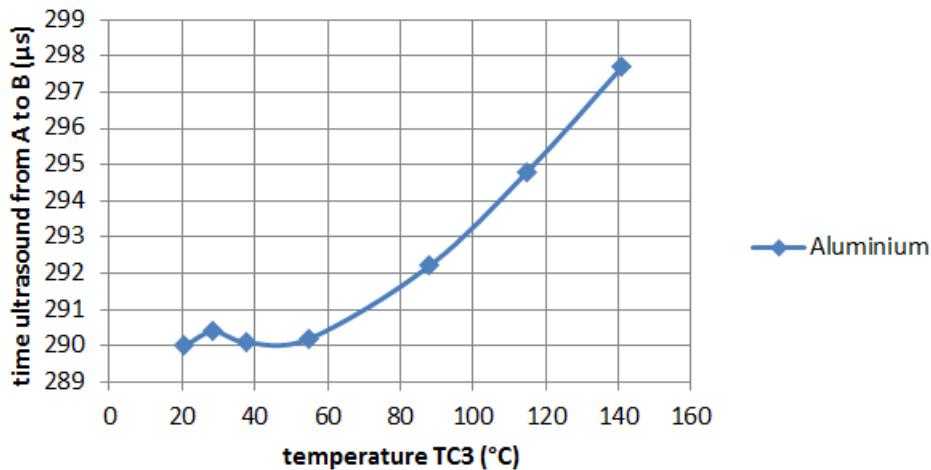
Change in transmission time

Figure 46 Change in transmission time aluminium

4.5.2 Analysis

For the analysis of the aluminium rod, the same mathematical equations and method of analysis described in section 4.4 are used to derive the Young's modulus. Figure 47 shows the change of the E-modulus over the temperature. The exact values can be found in Appendix B: Young's modulus values at elevated temperatures.

Modulus of Elasticity
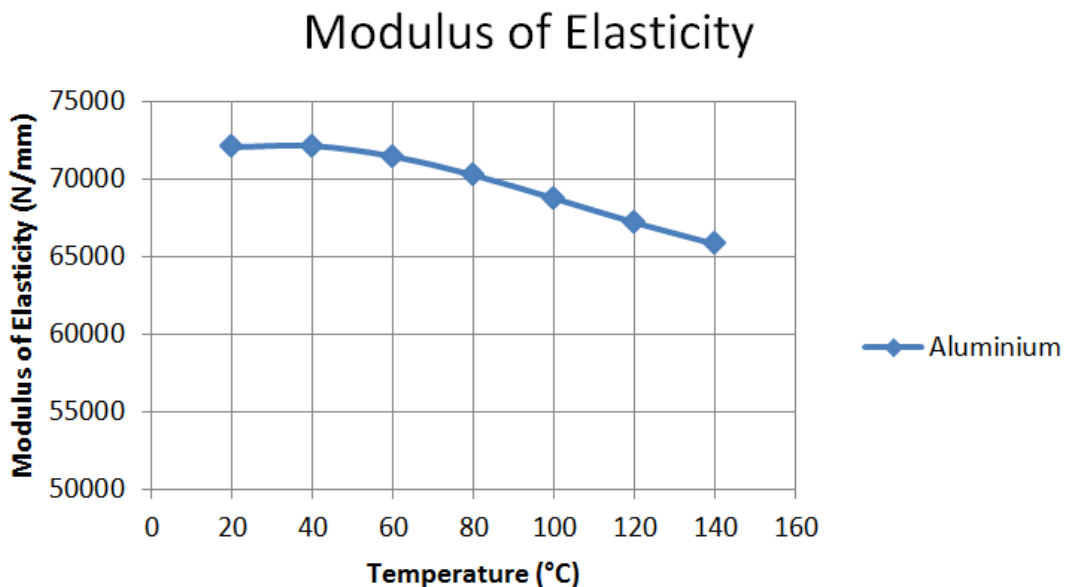
Figure 47 Modulus of Elasticity aluminium

It can be observed that the E-value at room temperature ($72 \cdot 10^3$ N/mm^2) is higher than the value known in the NEN standard ($70 \cdot 10^3$ N/mm^2). The observed higher initial stiffness value in the validation experiment is consistent with the experimental results of both of the glass rods. To have an accurate comparison of the change in Young's modulus at elevated temperatures between the standards and the analysed values from the experiment, the percentage decrease will be compared to each other.

51

4.5.3 Comparison with standards

The NEN-EN 1999-1-2 presents the Modulus of Elasticity at elevated temperatures of aluminium alloys. The relative decrease (in %) in stiffness according to the NEN and the analysed values from the test are given in Figure 48 below.
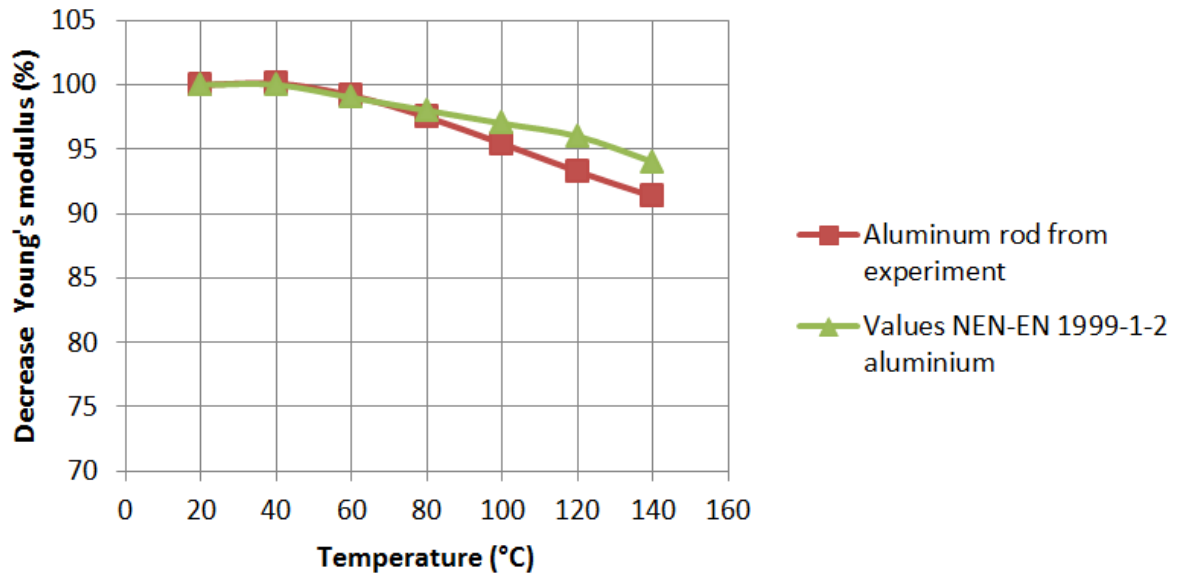
Figure 48 Decrease Young's modulus (%) over temperature

It can be noticed from the graph that the values for the percentage decrease in the beginning of the temperature range correspond to each other. However, more towards the higher temperatures the values diverge more. The percentage error between the experiment and the NEN are calculated and presented Table 7 below.

Table 7 Relative error of change in decrease between experiment and NEN

Temperature (°C)	Relative error (%)
20	0.0
40	-0.1
60	-0.2
80	0.5
100	1.6
120	2.9
140	2.8

The error at the lower temperatures is almost zero, but becomes bigger towards the higher temperatures with a maximum error of 2.9%. In addition, there is a measurement error of 2.9% based on the difference in the E-value at room temperature between the experiment and the NEN.

5. Tests on coated laminated glass panels

5.1 Theoretical background

For structural applications, laminated glass is often used to increase robustness and performance when panes crack. From the literature review it appeared that structural glass beams have the potential to withstand fire loading for a significant time, however further research has to be carried out to, among other things, the interlayers and the use of special coatings.

In this section the experiments and the results of the effect on the fire resistance of two coatings on laminated glass will be compared and elaborated. One of the coatings that will be tested is a pyrolytic low-E coating. This coating reduces the heat radiation of the glass. Debuyser et al. (2017) stated from his research that the low-E coating caused more reflectance of the specimens, which resulted in a reduction of absorptance and transmittance. This implied that the application of a pyrolytic low-E coating has advantages for the behaviour of a structural glass element in a fire.

The second coating is the intumescent coating HCA-TR from FlameGuard which was already used in the experiments of Veer et al. (2001) and Sturkenboom (2018). This coating reacts under the influence of great heat release like fire. Due to the heat, the coating expands many times the original layer thickness producing an insulating carbon char. The carbon char will protect the glass from the effects of fire.

5.2 Test set up

For this experiment laminated glass panels of 500 x 300 mm will be used. The panels consist of two panes of 6 mm thickness with a PVB layer of 1.52 mm (4 x 0.38 mm) in between. For this test thermally tempered and pyropane glass (extra thermally tempered glass, which has undergone a specific thermal treatment, resulting in glazing which prevents flames and gases from passing through for 30 minutes: E30) are used. Tempered glass proved to perform better in cases of fire, in contrast to annealed glass. The panels are provided by AGC, as well as the application of the pyrolytic low-E coating. This low-e coating is applied at both outer sides of the laminated panel.

In order to compare the effect of both of the coatings, a series of tests is carried out on the laminated glass plates. The principle for these tests is that a burner/heater will be placed on one side of the laminated glass panel to achieve the elevated temperatures. The temperature of the glass will be measured on both sides of the glass panel with thermocouples of type K. The measured temperatures at each side will be compared as well as the time until the interlayer starts to form gas bubbles.

In order to support the laminated glass panels, four piles of stacked bricks are used in the manner shown in Figure 49. In the first instance, two heaters were placed at a constant distance under the laminated glass panel to create a high heat output. The heaters were both set to 500 °C. The thermocouples are placed a little bit above the target point of the heaters, to prevent the thermocouples measuring directly the temperature of the heaters. Besides, the thermocouples are protected by a small aluminium strip, which should shield them from direct heating. In this way the temperature of the glass should be measured more accurately. A heat resistant paste is used to glue the aluminium strip with the thermocouple on the glass. In addition, a camera is placed above the glass panel to capture the formation of the gas bubbles in the PVB interlayer.

Figure 49 Test set up laminated glass panels with stacked bricks and a heater

During the experiments on a test piece it soon became apparent that the temperature at the side of the heaters was hard to control. Due to different air flows, the maximum temperature that could be reached was not always sufficient enough. To solve this problem extra bricks are used to create an enclosed space under the glass panel. This resulted in a more controllable "small oven" as is shown in Figure 50.
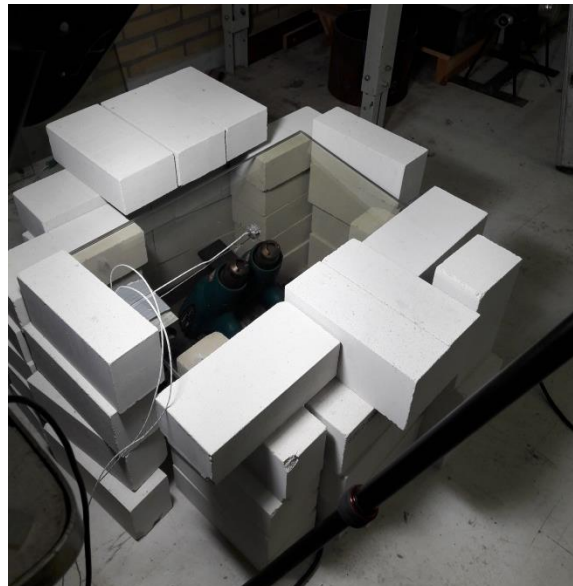

Figure 50 Test set up laminated glass panels creating a small "oven"

The configuration of the laminated glass panels that is tested in this test set up is as follows:

Glass type	Interlayer	Coating	Amount
Fully tempered	PVB	-	1
Fully tempered	PVB	HCA-TR	1
Pyropane	PVB	low-E	2
Pyropane	PVB	HCA-TR	2

However, the heat coming from the heaters did not really create the desired effect to simulate a fire situation. The heaters only heated the glass by convection: heat flow via a gas of liquid, in this case air. The effect of radiation could therefore not be measured. Hence, the setup was improved with the use of a propane/butane gas burner instead of the heaters. The test setup was built at an area with a good extraction and the burner was placed at a constant distance of the glass pane as could be seen in Figure 51. The maximum temperature of the flame was estimated to be 1100 °C.

Figure 51 Test set up laminated glass panels with stacked bricks and a burner

The configuration of the laminated glass panels that is tested in this test set up is as follows:

Table 9 Configuration laminated glass panels test with burner

Glass type	Interlayer	Coating	Amount
Fully tempered	PVB	-	1
Fully tempered	PVB	HCA-TR	1
Pyropane	PVB	low-E	2
Pyropane	PVB	HCA-TR	1

5.3 Results

In this section the measurement results of the thermocouples will be discussed as well as the observations regarding the formation of bubbles in the PVB interlayer. In Appendix C: Temperature-Time curves laminated glass panels, the results of the measurements of the thermocouples on both sides of the glass are presented for each laminated glass panel. Also the average temperature is added to the time – temperature curve for each panel. Note: this temperature should not be confused with the temperature of the interlayer. The interlayer temperature was not measured.

5.3.1   Test with heaters

In Table 10, the results and observations regarding the formation of the gas bubbles are presented.

Table 10 Results and observations tests laminated glass panels with heaters

Glass type	Interlayer	Coating	Formation bubbles after (s):	Corresponding temperature heated side (°C)	Corresponding temperature unheated side (°C)	Average temperature (°C)
Fully tempered	PVB	-	840	182.8	128.9	155.9
Fully tempered	PVB	HCA-TR	1870	212.5	118.6	165.6
Pyropane	PVB	low-E	430	181.1	93.7	137.4
Pyropane	PVB	low-E	560	182.2	99.6	140.9
Pyropane	PVB	HCA-TR	1590	206.8	122.9	164.9
Pyropane	PVB	HCA-TR	1490	198.3	125.6	162.0

What can be noticed directly from the table is the difference in time after which the gas bubbles in the PVB interlayer arise. Remarkable is that the formation of the gas bubbles occurs the fastest for the pyropane panels with low-e coating. This happens even faster than for the fully tempered panel without coating. The panels which are coated with the intumescent coating show a significantly longer time before the gas bubbles arise.

The formation of the bubbles takes place at a temperature of 180-210 °C at the heated side and around 120 °C at the unheated side, except for the low-e coated panels. The temperature at the unheated side lays between 90-100°C.

If the temperature-time curve (Figure 52) of the fully tempered glass panel without coating is compared with the curves for the pyropane panel with low-e coating, no extreme differences in the curve in temperature over time are noticed. Noteworthy, is that the temperature of the first pyropane low-e panel remains stable at 100 degrees Celsius for a significant time. This result will be discussed later in this section.
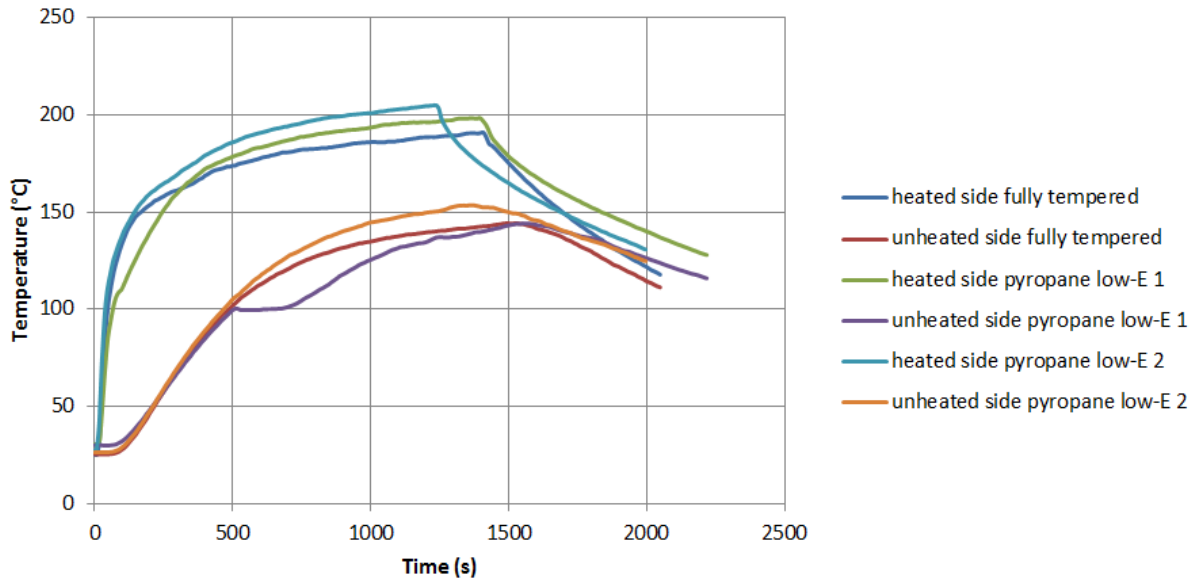
Figure 52 Comparison temperature-time curves fully tempered and pyropane low-E

If the curve for the fully tempered glass panel without coating is compared to the fully tempered and pyropane panel with HCA-TR coating, some interesting results can be observed (Figure 53). It can be seen that the temperatures at the heated side for the panels with coating are higher than those of the fully tempered panel without coating. However, the temperatures at the unheated side remain lower, indicating a bigger difference in temperature between the heated and unheated side of the panels with intumescent coating. This might refer to a delay in the heat transmission, meaning that the coating will slow down the heating of the glass.
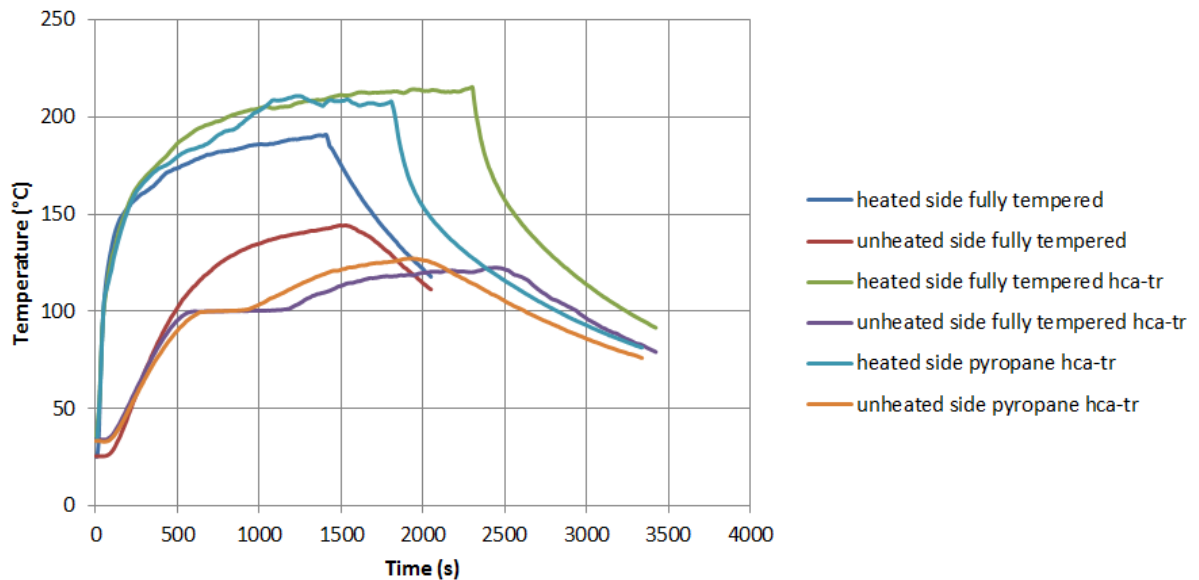

Figure 53 Comparison temperature-time curves fully tempered with and without hca-tr and pyropane hca-tr

5.3.2 Test with burner

In Table 11, the results and observations regarding the formation of the gas bubbles are presented.

Table 11 Results and observations tests laminated glass panels with burner

Glass type	Interlayer	Coating	Formation bubbles after (s):	Corresponding temperature heated side(°C)	Corresponding temperature unheated side(°C)	Average temperature (°C)
Fully tempered	PVB	-	950	206.9	112.6	159.8
Fully tempered	PVB	HCA-TR	after 2620 s still no gas bubbles			
Pyropane	PVB	low-E	530	180.6	84.1	132.4
Pyropane	PVB	low-E	760	186.9	99.0	143.0
Pyropane	PVB	HCA-TR	after 2910 s still no gas bubbles			

Similar to the test with the heaters, the time after which the gas bubbles in the PVB interlayer arise differ for the various configurations . Again, the formation of the gas bubbles occurs the fastest for the pyropane panels with low-e coating. This happens faster than for the fully tempered panel without coating. For the panels which are coated with the intumescent coating no gas bubbles were formed after a significant longer time than the other panels and therefore the test was ended after about 45 minutes.

The temperatures at the heated and unheated side are more or less comparable with those of the test with the heaters. It should be said that although the thermocouple at the heated side is protected by the aluminium, it might be higher than the actual temperature of the glass. The aluminium could be heated faster by the direct heat of the burner/heaters than the glass itself.

If a comparison is made between the temperature-time curve (Figure 54) of the fully tempered glass panel without coating and the curves for the pyropane panel with low-e coating, no extreme differences in the curve in temperature over time are noticed. However, what again is striking, is the stabilized temperature of 100 °C at the unheated side for a certain period of time. This observations will be discussed later in this section.
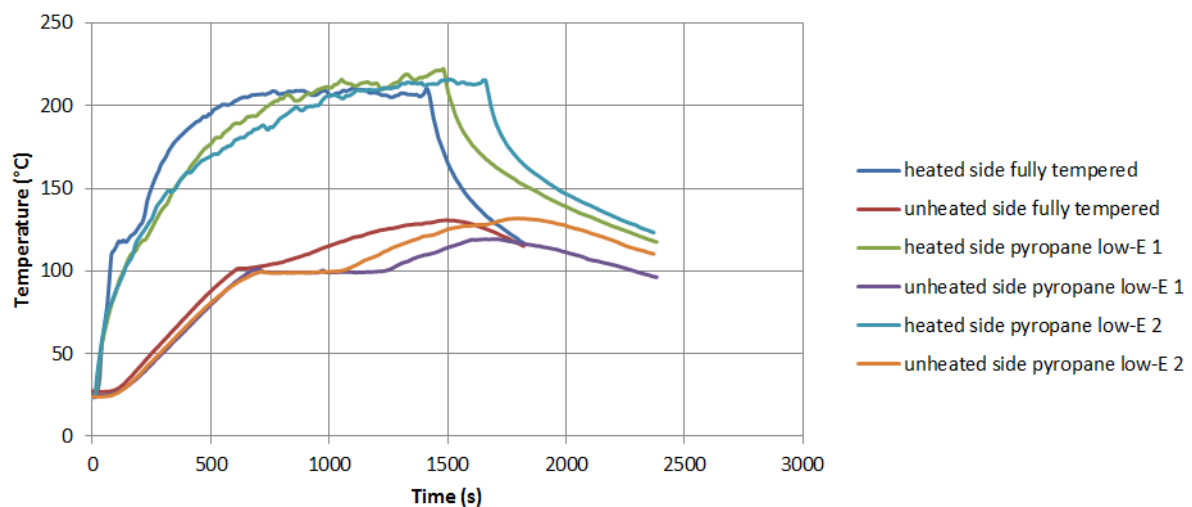

Figure 54 Comparison temperature-time curves fully tempered and pyropane low-E

If the curve for the fully tempered glass panel without coating is compared to the fully tempered and pyropane panel with HCA-TR coating, some interesting results can be observed (Figure 55). It can be seen that the temperatures at the heated side for the panels with coating are lower than those of the fully tempered panel without coating. This may indicate that the heated side is protected from heating up by the coating, resulting in a slightly lower temperature at the unheated side. It should be mentioned that also the aluminium strip which protect the thermocouples is coated. This was also done at the tests with the heaters. However, after a certain period of time the foamed coating was blown off by the heaters.
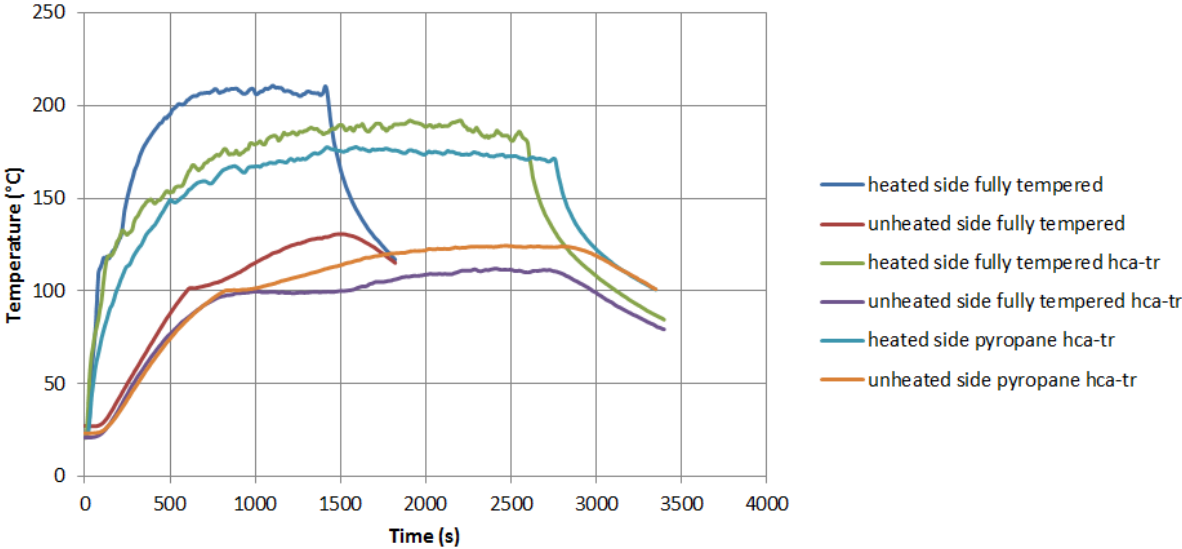

Figure 55 Comparison temperature-time curves fully tempered with and without hca-tr and pyropane hca-tr

5.3.3   Observations

Plateau at 100°C unheated side

One of the observations from the temperature-time curves was the stabilisation of the temperature at the unheated side of the panels. At almost all of the tests were this event occurred, the temperatures were observed to be stable at 100°C. The period of time were the temperature was stable differed for the various panels.

The temperature of 100°C might refer to the boiling point of water. This might indicate that some process takes place at which water evaporates. An explanation could be that the decomposition of the PVB interlayer is associated with the elimination of water.

To find out if this is an irreversible process which takes place during the heating of the panels, one of the low-e coated pyropane panels was heated up again by the burner, while the bubbles already had been formed in the previous test. In Figure 56 the comparison in temperature-time curves can be shown. It should be mentioned that this extra test was done at a different day, at which the conditions (temperature/air flows) in the room where the test was performed might have been different. This could explain the lower temperature at the heated side of the panel.
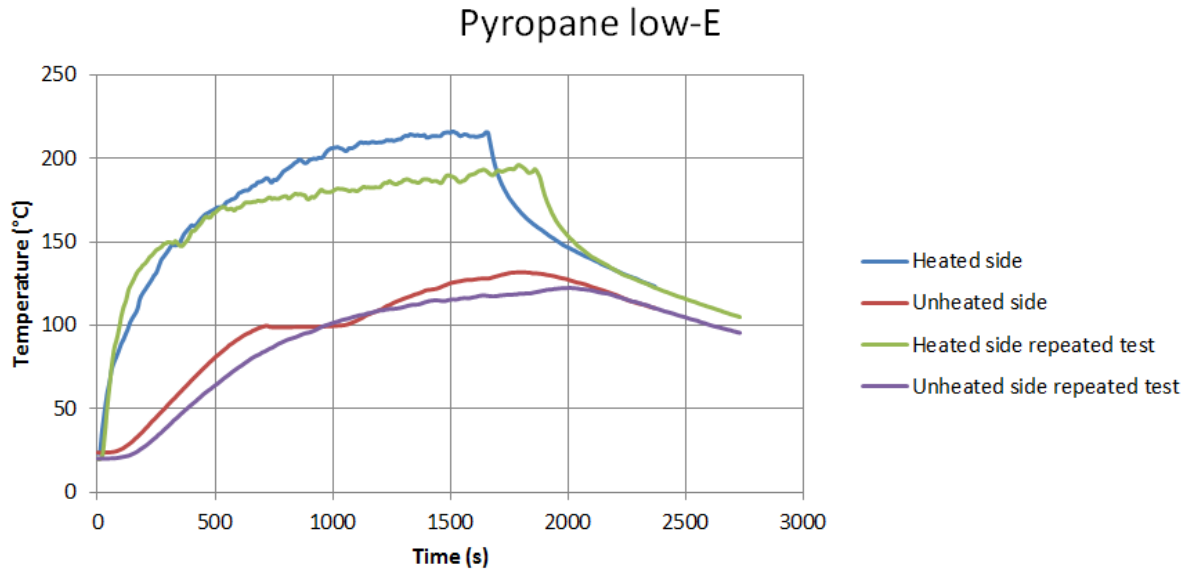
Figure 56 Comparison original test and repeated test pyropane low-E

From the graph above it can be noticed that the plateau at 100°C is not visible anymore in the curve for the repeated test. This might confirm that during the heating of the panels an irreversible process takes place. It might indicate an evaporation process of water.

Another explanation which was discovered when viewing the photos the camera made during the test has to do with the heat resistant paste. It was noticed that during heating, the paste expanded and the aluminium strip with the thermocouple was slightly lifted. The time at which this happened was equal to the time the plateau was visible in the graphs. This is a reasonable explanation for the stabilisation of the temperature.

Formation of gas bubbles

In the photos shown in Figure 57 an example of the formation of gas bubbles is presented. The time and temperature at the heated side are given for each photo. It most likely starts at the hottest point in the interlayer where suddenly one gas bubble arises. When the heating continues the gas bubble expands and new bubbles are formed around the first one. Also these bubbles expand over time with increasing temperature. When the test was ended, the gas bubbles started to shrink. However, most of the bubbles remained visible after complete cooling.
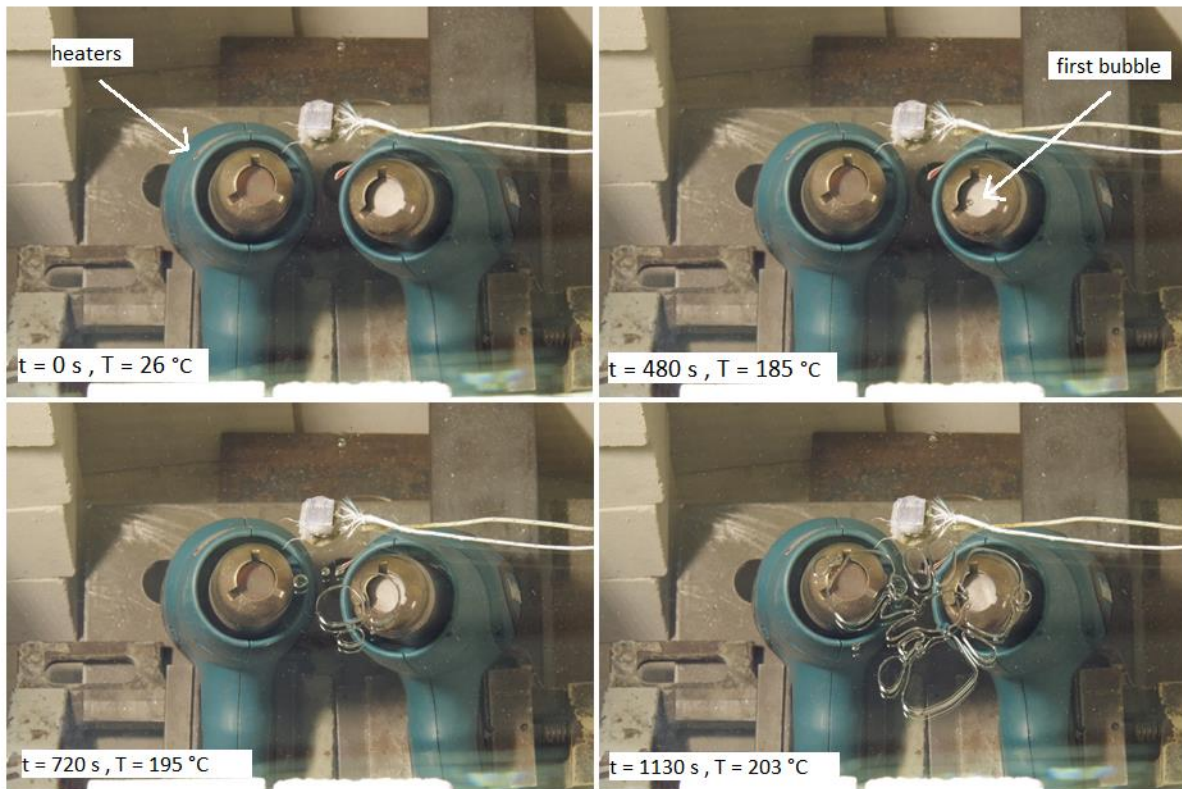
Figure 57 Formation of gas bubbles in the PVB interlayer during test with heaters

Intumescent coating

When the test started the intumescent coating almost directly reacted on the heat. This is in line with the specifications of the coating. The flash point is > 100 °C. From the graphs it can be seen that when the heaters are activated, the temperature at the bottom of the glass reached 100°C within halve a minute. The used coating already has a translucent milky white tint when applied on the glass. After several seconds the coating became opaque white and started to foam (seen by the air bubbles that arise in the coating) at the points where the heaters are aimed at. The same goes for the test with the burner. As time continues and temperature increases, the opaque white part expands and the hottest part starts to char. Also this process expands over time. The described observations are shown in Figure 58. The time and temperature at the heated side is given for each photo. The shape of the foamed coating corresponds to the shape of the formation of the gas bubbles as was observed in Figure 57.
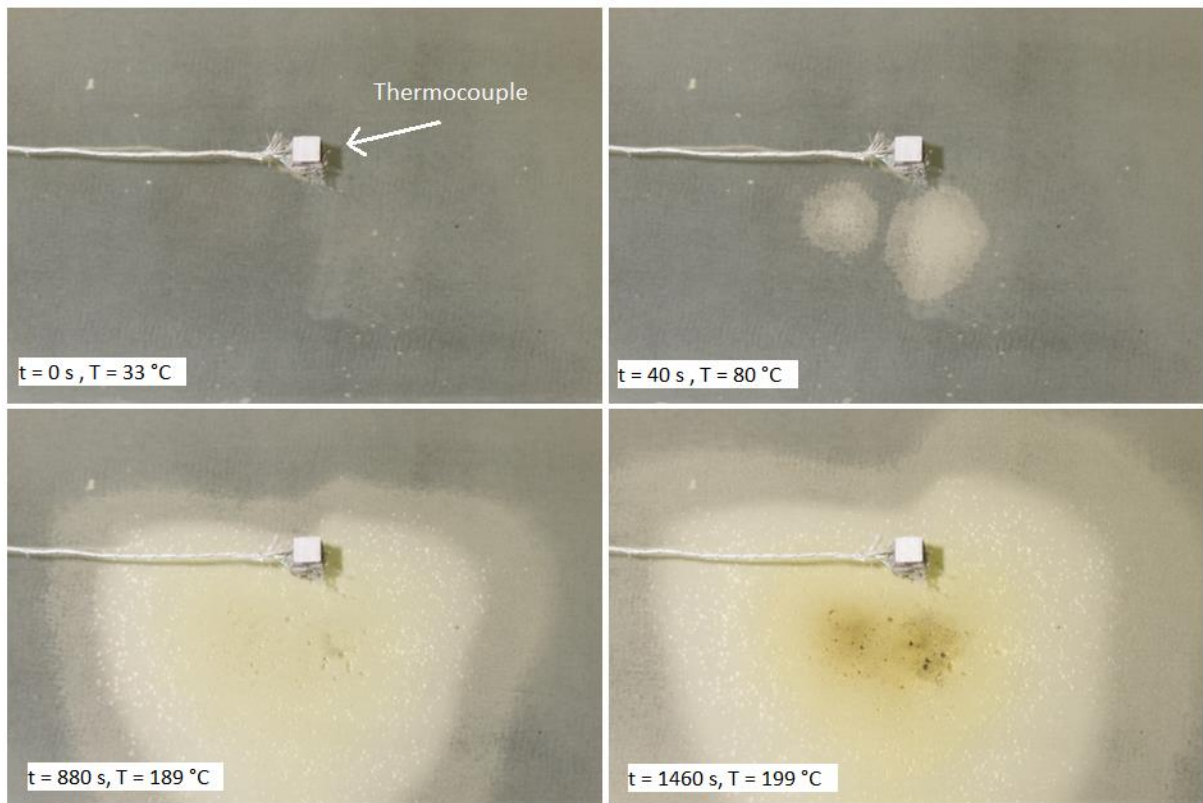
Figure 58 Effect intumescent coating during test with heaters

When the laminated glass panels were cooled down, the pattern of the intumescent coating at the heated side of the glass could be observed. Figure 59 shows the effect of the intumescent coating. At the hottest part an insulating carbon char was formed as was described in the specifications of the coating. Around the char the coating also already foamed up. It can be seen that the intumescent layer on the aluminium strip is slightly blown away by the heaters, resulting in less protection.

Figure 59 Effect intumescent coating after heating

IV
Conclusions & Recommendations

6. Discussion

In this chapter the results will be discussed, mainly with regards to the expectations, validation and limitations of the experiments.

Ultrasonic testing

The Young's modulus was determined by means of ultrasonic measurements on glass rods of Soda Lime Silica (SLS) and Borosilicate (BS).
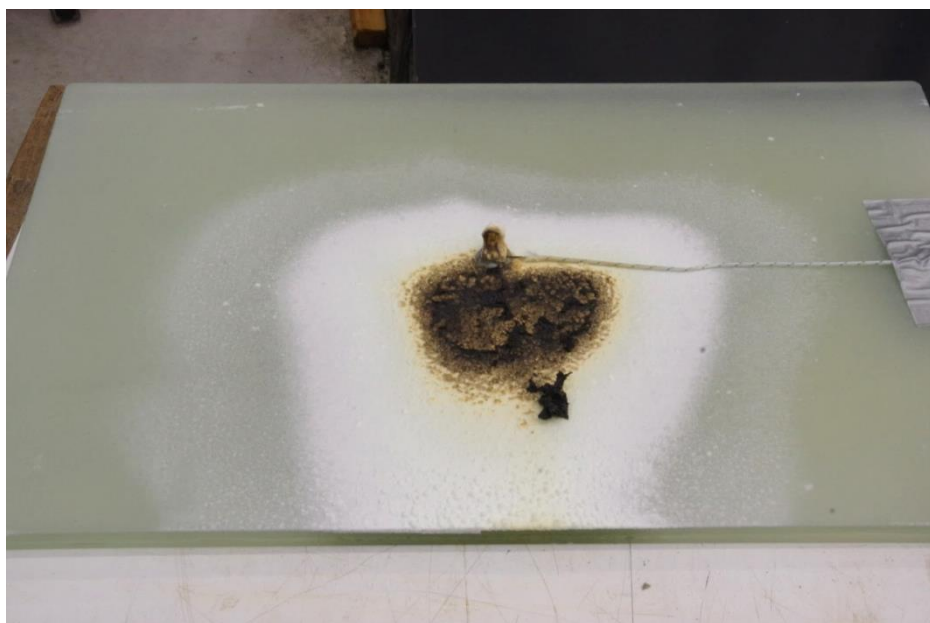
The available materials and test equipment was accompanied by limitations. Two tube furnaces were available for testing the glass rods, from which the furnace with the largest hot-zone was chosen to eliminate influence of noise. This resulted in a glass rod with a length of 1.5 m, which was also the maximum available length of the rod. Since the temperature of the glass rod was not equal over the length, additional thermocouples had to be used to accurately determine the temperature profile. As a consequence, the values of the transmission time were not directly comparable and an approximation had to be made for the longitudinal velocity of the sound wave.

Additionally, the transmission time fluctuated during the measurements. A maximum fluctuation of ± 0.4 μs (error of 0.15%) was observed. Besides, a relatively small deviation (2.7% for SLS and 1.6% for BS) of the Young's modulus at room temperature was noticed in comparison with the specifications of the manufacturer. A likely explanation is that the manufacturer used a different measurement method to determine the values. The differences lie within the measurement error of both techniques and are negligible.

The measurements were stopped at the moment the glass rods touched the bottom of the oven (between 500-600°C). The measurement corresponding to the moment the rod touched the bottom of the oven gave an unrealistic low value, indicating the soundwave chose the fastest way through the bottom of the oven. Therefore this measurement was not taken into account in the analysis.

Although the experiment was forced to stop earlier than intended, the observations provide relevant information about the behaviour of glass up to temperatures of 700 °C. For both SLS and BS glass, the deflection increased significantly (at least 10 mm) in a short time frame (several minutes) for temperatures between 500 to 600 °C. Below 500°C, no deflection of the glass was observed. However, above 500°C the glass will deform. If a structural glass element is considered at temperatures above 500°C, the structural safety of the element would not be guaranteed anymore if deformations take place as fast as was observed in the experiment. Especially when a structural glass element is subjected to loading.

This experiment was validated by an additional test on an aluminium rod under the same conditions. The approximation for the change of Young's modulus at elevated temperatures had a maximum error of 2.9%. This error is assumed to be sufficiently small to pose the presented results as valid.

Coated laminated panels

In this experiment the effect on the fire performance of a low-E coating and an intumescent coating applied to laminated glass panels at elevated temperatures is compared.

The experiment came with some limitations. To be able to observe the effect of bubble formation in the interlayer, the temperature was not measured at the exact location where the glass was heated. Therefore, the exact temperatures of the glass at the heated location will differ from the measured

temperatures. However, this will only be a systematic error. Since every single panel is measured in the same way, a relative comparison can still be made.

Additionally, it was found that the fixation of the thermocouples with the heat resistant paste was not beneficial to the results of the test. Especially at the unheated side, it was noticed that the temperature was stable at 100°C for a significant time due to the expansion of the heat resistant paste. This would not have been the case if the thermocouples were properly fixated.

Besides, due to the setting of the experiment it was hard to control the exact temperature to which the glass panel was exposed. In a set-up like an oven, the temperatures can be controlled more precisely. This makes it easier to compare results.

The amount of test specimens is also a point of discussion. The amount of panels is too small in order to be able to draw firm conclusions. Partly this was caused by the rejection of some of the produced panels, due to breakage and formation of bubbles during production. Consequently only a limited amount of panels could be tested in slightly different configurations. The amount of tests should have been increased to really draw well-founded conclusions.

The results of this test for the low-E coating were in contrast with the expectations. Initially, it was expected that the low-E would reflect a part of the heat radiation in the test with the burner, causing a delay in the heating of the exposed glass panel. However, for glass panels with low-E coating no improvement was observed compared to the glass panels without coating. This observation can be explained by the fact that the effect of the heat radiation is negligible compared to the heat caused by convection at the location where the glass is heated. The low-E coating will therefore have no effect and would have behaved differently if the heat is transferred by only radiation. In case of fire, the effect of heat radiation is only relevant with sufficiently high mass at a certain distance.

Remarkably, the panels with the low-E coating performed even worse than those without coating. The formation of bubbles in the coated panels occurred faster than for the uncoated panels. This finding was unexpected and suggests that the heat transfer coefficient might have been improved. The low-E coating gives a smooth surface of the glass, more than that of regular glass, which suggest to increase the heat transfer rate.

The results of this research also show that the PVB interlayer is the weakest link in the laminated glass panels. At temperatures of 200 °C the PVB interlayer is already completely molten, while the glass is still fully intact at 500 °C. The fire resistance can be improved by using glass without an interlayer. However, to create enough mass for, for example, a glass column, the float process would not be sufficient anymore. Cast glass might in this case be an interesting option to investigate.

7. Conclusions

The aim of this research is to investigate the performance of glass at elevated temperatures and to assess whether or not the fire resistance can be improved by applying coatings. In this section the conclusions are presented from literature study and conducted experiments on Soda Lime Silica (SLS) and Borosilicate (BS) glass rods and laminated glass panels.

Literature

- From the literature review it is concluded that much research has been carried out on the material properties of glass at elevated temperatures. A relevant structural property in these conditions is the Young's modulus, or stiffness (E) of glass. The stiffness for different types of glass is known up to 600-700 °C. One of the experiments performed in this research therefore aims to determine the values for the Young's modulus at temperatures beyond 600 degrees Celsius.

- Secondly, it is concluded that there is a lack of experimental test results for structural glass elements under fire loading. Evidence was found that laminated glass elements, such as beams, have the potential to withstand fire loading for a significant time. However still further research of other aspects, such as interlayers and the use of special coatings has to be conducted to establish a full understanding of fire resistance so the full potential of coatings can be exploited. The second experiment in this research focuses on the effect of two coatings at elevated temperatures.

Ultrasonic testing

The goal of this experiment was to determine the Young's modulus values at temperatures above 600 °C. The ultrasonic measurements proved to be a reliable method to determine the Young's modulus of glass at elevated temperatures. The following conclusions can be drawn:

- Initially a decrease of the Young's modulus for SLS glass was observed whereas an increase of the Young's modulus for BS glass was seen with increasing temperature. However, from 400 °C, both glass types show a decrease in stiffness. For SLS glass the stiffness is 100% at room temperature (20 °C) and decreases to 95% at 400 °C. At 600 °C the stiffness is still 83% of the original stiffness at 20 °C. For BS glass the stiffness increases from 100% at room temperature to 105% at 400 °C. From temperatures of 400 °C a decrease in stiffness to 94% at 600 °C and 81% at 700 °C was observed.

- Although the stiffness of the BS glass is increasing with elevated temperatures in the first part of the experiment, the stiffness does not exceed the stiffness of SLS glass within the measured temperature range.

- The experiments were stopped when the rods touched the bottom of the oven due to deformation. For SLS glass this occurred at 600 °C. The last useful value for the stiffness at this temperature was measured to be $62.3 \cdot 10^3$ N/mm^2. For BS glass it was possible to measure up to 700 °C, where the stiffness was equal to $51.7 \cdot 10^3$ N/mm^2.

- The observations provide relevant information about the behaviour of the glass up to temperatures of 700 °C. For both types of glass, the deflection increased significantly (23-25

mm) in a short time frame (several minutes) for temperatures from 500 to 600 °C. For BS glass this deflection occurred later than for SLS glass.

Coated laminated glass panels

The goal of this experiment was to investigate the effect of a low-E coating and intumescent coating applied to the laminated glass panels. Several conclusions are drawn from the experiments:

- Both during the test with the heaters and the test with the burner, low-E coating did not show to result in an improvement in terms of time before the formation of bubbles is observed. Surprisingly, the formation of the bubbles occurred even faster than for the uncoated panels. Also from the temperature – time curves the positive effect of the low-E coating could not be proven.

- The effect of the heat radiation is negligible compared to the heat caused by convection. The low-E coating therefore did not show any effect.

- The panels which were coated with the intumescent coating however showed a significant improvement in terms of time before the formation of the bubbles was observed. If for example the fully tempered panel is considered in the test with the heaters, the exposure time up to the moment the bubble formation is observed in the interlayer is almost doubled for the panel with the intumescent coating. For the panels which were heated by the burner, the formation of the gas bubbles was not even observed at all. The temperature at the heated side did not reach the temperature that cause the PVB to react.

Research conclusion

To answer the question on how glass performs at elevated temperatures and how the fire resistance can be improved, the following conclusions are drawn from the research:

- From the experiments on glass rods it is observed that glass performs well up to temperatures of 500 °C, provided that there are no distributed thermal stresses in the glass. Given this condition, the stiffness for SLS glass is still 90% and 102% for BS glass at a temperature of 500 °C. In the range of 500-600 °C a sudden deformation is observed. Therefore the structural safety of a glass element cannot be guaranteed for temperatures beyond 500 °C.

- It can be concluded that glass outperforms steel in terms of relative stiffness up to temperatures of 600 °C.

- The heating of a glass element can be delayed by the application of an intumescent coating. An improvement in fire resistance for the panels with low-E coating however is not proven in this research. Instead, a negative effect has been observed and therefore the application of low-E coating is not recommended.

- It was shown that the PVB interlayer is the weakest point. At temperatures of 200 °C the PVB interlayer is already completely molten, while at 500 °C the glass is still intact. The fire resistance can be improved without an interlayer.

8. Recommendations

From the discussion and conclusions several recommendations regarding measurements for the fire performance of glass, as well as recommendations for further research are stated.

Recommendations to increase the fire performance of glass

- The glass should be protected to postpone a rapid temperature rise of the glass. Reaching the critical temperatures of the glass beyond 500°C must be postponed. Thermal insulation will provide the highest level of protection. This could be achieved by applying an intumescent coating.

- BS glass is recommended in situations where thermal shock might occur, although the stiffness of BS glass did not exceed that of the SLS glass at the measured elevated temperatures and the production of BS glass is more expensive. If only one part of a glass element is heated, which is likely in case of fire, the thermal gradient might result in thermal shock. The low thermal expansion coefficient of BS glass causes the glass to expand less quickly at elevated temperatures.

- Produce glass elements without interlayers. The interlayer proved to be the limiting factor in a glass element. Since the float process would not be able to produce a sufficiently thick mass of glass, a glass element produced with a casting process would be interesting to investigate.

Recommendations for further research

- As was stated above, glass elements, for example, columns, produced by the cast process might be interesting to investigate for further research. In this way the weakest point in laminated glass, the interlayer, is eliminated. A sufficiently thick mass of glass could have a better fire resistance.

- An idea worth investigating for a cast glass element is the effect of texture on the surface of a glass element. The hypothesis is that a textured glass surface might result in a reduced heat transfer rate and consequently in a reduced heat transfer coefficient of the glass. This is the opposite of the smooth surface resulting from the low-E coating which suggested that a smooth surface resulted in a higher heat transfer coefficient. Additionally, the cast process provides more freedom of shape, making it easier to achieve a textured surface.

- Test the effect of the intumescent coating on loaded glass elements or full glass systems at elevated temperatures. The influence of connection details, geometry and boundary conditions (supports) on the fire performance of a glass structure cannot be neglected in the assessment.

- Perform tests in a more controlled environment in terms of temperature. In this way the results can be compared and assessed. For example, the standard temperature/time curve could be used to describe a fully developed fire in a compartment of a building.

- During experiments, ensure that the temperature of the glass is measured accurately and is not influenced by direct heat or inadequate fixation of the thermocouples.

- Increase the number of experiments to establish a more statistical reliable result.

Bibliography

Bedon, C., 2017. Structural Glass Systems under Fire: Overview of Design Issues, Experimental Research, and Developments. *Advances in Civil Engineering,* Volume 2017, Article ID 2120570, 18 pages.

Bedon, C. & Louter, C., 2018. *Thermo-mechanical numerical modelling of structural glass under fire - preliminary considerations and comparisons.* Delft, Challenging Glass Conference 6.

Bokel, R., Veer, F. & Tuisinga, L., 2003. Fire Resistance of Glass. *Proceedings of Glass Processing Days,* pp. 362-363.

Bouwbesluit , 2018. *Afdeling 2.2 Sterkte bij brand.* [Online]
Available at: https://www.bouwbesluitonline.nl/Inhoud/docs/wet/bb2012/hfd2/afd2-2
[Accessed January 2019].

Bouwen met Staal, 2019. *Materiaalgedrag staal.* [Online]
Available at: https://www.brandveiligmetstaal.nl/pag/294/1b_materiaalgedrag_staal.html
[Accessed September 2019].

Breunese, A. & Maljaars, J., 2014. *Fire Safety Design, Course reader CIE5131.* version October 2014 ed. Delft: TU Delft.

Brow, R., n.d. *Summary of Chapter 6, Viscosity, of Introduction to Glass Science and Technology by J.E. Shelby.* [Online]
Available at: http://web.mst.edu/~brow/PDF_viscosity.pdf
[Accessed 2019].

CMA, n.d. *Snelheid van geluid.* [Online]
Available at: http://www.cma-science.nl/activities/nl/natuurkunde/Geluid/Geluidssnelheid/Geluidssnelheid%20-%20Toelichting.pdf
[Accessed February 2019].

Debuyser, M. et al., 2017. Behaviour of monolithic and laminated glass exposed to radiant heating. *Construction and Building Materials,* Volume 130, pp. 212-229.

DuPont, 2018. *Building Innovations.* [Online]
Available at:
http://www2.dupont.com/Building_Innovations/zh_CN/assets/downloads/SGPintro_E.pdf
[Accessed 2019].

Haldimann, M., Luible, A. & Overend, M., 2008. *Structural Use of Glass (SED 10).* [Online]
Available at: https://app.knovel.com/hotlink/toc/id:kpSUGSED09/structural-use-glass/structural-use-glass

Huger, M., Fargeot, D. & Gault, C., 2002. High-temperature measurement of ultrasonic wave velocity in refractory materials. *15th ECTP Proceedings,* pp. 1421-1429.

Kerper, M. J. & Scuderi, T. G., 1966. Mechanical properties of chemically strengthened glasses at high temperatures. *Journal of the American Ceramic Society,* 49(11), pp. 613-618.

Kozlowski, M. et al., 2018. *Structural considerations on Timber-Glass Composites at fire scenarios.* Delft, Chanllenging Glass Conference 6.

Louter, C., 2017. *Powerpoint Structural Glass - Material Characteristic, Production, Processing & Products.* Delft: TU Delft.

Louter, C. & Nussbaumer, A., 2016. Fire Testing of Structural Glass Beams; Initial Experimental Results.

NDT Resource Center, 2014. *The speed of sound in other materials.* [Online]
Available at: https://www.nde-ed.org/EducationResources/HighSchool/Sound/speedinmaterials.htm
[Accessed February 2019].

NDT Resource Center, 2014. *Ultrasound and ultrasonic testing.* [Online]
Available at: https://www.nde-ed.org/EducationResources/HighSchool/Sound/ultrasound.htm
[Accessed February 2019].

NEN, 2002. *NEN-EN 1990:2002 - Eurocode, Basis of Structural Design,* Delft: Nederlands Normalisatie Instituut.

NEN, 2004. *- EN 1634: Fire resistance and smoke control tests for door and shutter assemblies, openable windows and elements of building hardware ,* Delft: Nederlands Normalisatie instituut.

NEN, 2011. *NEN-EN 1999-1-2+C1 Eurocode 9: Ontwerp en berekening van aluminiumconstructies - Deel 1-2: Ontwerp en berekening van constructies bij brand,* Delft: Nederlands Normalisatie Instituut.

NEN, 2012. *NEN-EN 1363-1 Fire resistance tests - Part 1: General Requirements,* Delft: Nederlands Normalisatie instituut.

NEN, 2014. *NEN-EN 1365-2: Fire resistance tests for loadbearing elements – Part 2: Floors and roofs,* Delft: Nederlands Normalisatie instituut.

NEN, 2015. *NEN-EN 1364-1: Fire resistance tests for non-loadbearing elements – Part 1: Walls ,* Delft: Nederlands Normalisatie instituut.

NEN, 2016. *NEN-EN 13501-2 Fire classification of construction products and building elements - Part 2: Classification using data from fire resistance tests, excluding ventilation services,* Delft: Nederlands Normalisatie Instituut.

Nijsse, R., 2003. *Glass in Structures.* Basel, Switzerland: Birkhäuser.

Nodehi, Z., 2016. *Behaviour of structural glass at high temperatures,* Delft: TU Delft.

Rouxel, T., 2007. Elastic properties and short- to medium-range order in glasses. *Journal of the American Ceramic Society,* 90(10), pp. 3019-3039.

Rouxel, T. & Sangleboeuf, J. C., 2000. The brittle to ductile transition in a soda-lime-silica glass. *Journal of Non-Crystalline Solids,* 271`(3), pp. 224-235.

Schipper, R., 2011. *CIE4215 - Façade design plus,* Delft: Delft University of Technoloy.

Schittich, C. et al., 2007. *Glass Construction Manual (2nd revised and expanded edition).* 2nd ed. Munich: Birkhäuser Verlag AG.

Shen, J., Green, D. J., Tressler, R. E. & Shelleman, D. L., 2003. Stress relaxation of soda lime silicat glass below the glass transition temperature. *Journal of non-crystalline solids,* 324(3), pp. 277-288.

Sturkenboom, J., 2018. *Fire Resistant Structural Glass Beams: Developing design recommendations for future development and fire certification of structural glass beams,* Delft: TU Delft.

Trosifol, 2014. *SentryGlas.* [Online]
Available at: https://www.trosifol.com/products/architecture/trosifolr-structural-security/sentryglasr/
[Accessed July 2018].

Veer, F., Van der Voorden, M., Rijgersberg, H. & Zuidema, J., 2001. Using transparent intumescent coatings to increase the fire resistance of glass and glass laminates. *Proceedings of Glass Processing Days,* pp. 392-396.

Wurm, J., 2007. *Glass Structures; Design and construction of self-supporting skins.* Basel: Birkhäuser.

V
Appendices

Appendix A: Measurement results ultrasonic testing

In this Appendix the exact values of the measured temperatures, corresponding to the measured transmission times are presented for both SLS and BS glass and aluminium.

Table 12 Measurement results Soda Lime silica glass rod

Time of measurement (s) (Start at t=0)	Set temperature oven (°C)	Real temperature oven (°C)	Temperature								Time ultrasound from A to B (µs)
			end A (°C)	TC1 (°C)	TC2 (°C)	TC3 (°C)	TC4 (°C)	TC5 (°C)	end B (°C)		
0	-	20.9	19.2	22.0	26.4	21.4	21.5	21.2	19.8		271.5
3900	120	126.3	24.7	44.2	78.9	98.4	74.0	40.4	22.6		272.1
8100	230	233.0	31.9	82.0	167.4	213.9	157.1	74.0	27.5		272.0
12350	320	322.3	38.3	110.9	242.2	309.1	229.1	99.8	30.5		272.6
16500	415	416.5	43.1	137.7	325.2	407.7	308.8	123.6	32.6		275.3
20680	505	505.0	47.6	162.1	403.9	499.2	386.7	145.0	37.4		276.0
21870	605	605.3	53.0	161.5	455.7	570.9	432.6	144.4	39.2		278.6
22400	605	605.0	51.4	157.7	463.8	590.2	438.1	139.9	38.0		279.5

Table 13 Measurement results Borosilicate glass rod

Time of measurement (s) (Start at t=0)	Set temperature oven (°C)	Real temperature oven (°C)	Temperature								Time ultrasound from A to B (µs)
			end A (°C)	TC1 (°C)	TC2 (°C)	TC3 (°C)	TC4 (°C)	TC5 (°C)	end B (°C)		
0	-	20.9	19.0	20.1	21.0	20.3	20.2	20.4	19.2		278.0
3900	120	122.6	21.5	44.8	78.5	99.2	77.0	40.3	20.4		276.8
8000	230	232.5	29.7	84.2	169.7	215.1	164.2	73.7	24.8		275.2
12250	330	332.3	34.4	118.6	257.6	322.8	248.3	102.7	27.3		274.4
16400	415	415.7	38.4	145.3	332.5	411.5	322.1	125.4	29.4		273.2
20600	505	505.0	39.9	171.0	413.2	502.6	402.6	148.4	32.5		273.6
23500	605	605.0	40.2	179.8	489.5	601.9	465.3	156.7	33.6		275.4
24750	605	605.0	40.7	183.6	494.5	603.1	465.5	154.5	33.0		275.1
26477	705	705.1	40.9	196.3	573.8	693.6	548.7	159.1	33.2		280.0

Table 14 Measurements results aluminium rod

Time of measurement (s) (Start at t=0)	Set temperature oven (°C)	Real temperature oven (°C)	Temperature								Time ultrasound from A to B (µs)
			end A (°C)	TC1 (°C)	TC2 (°C)	TC3 (°C)	TC4 (°C)	TC5 (°C)	end B (°C)		
0	-	20.6	20.2	20.5	25.9	20.7	23.7	20.7	20.1		290.0
1950	40	46.4	21.5	23.2	29.6	28.5	28.0	23.0	21.3		290.4
3900	60	62.8	24.4	28.5	36.4	37.5	34.6	27.9	24.0		290.1
5950	100	103.2	29.9	37.5	51.1	55.0	48.3	36.0	28.7		290.2
8100	150	151.6	44.1	54.7	77.5	87.9	71.6	52.0	41.9		292.2
10100	180	188.3	54.0	70.7	98.7	114.9	92.4	66.8	50.7		294.8
12150	210	213.6	63.4	85.8	120.6	141.0	113.0	80.8	59.8		297.7

Appendix B: Young's modulus values at elevated temperatures

In this Appendix the Young's modulus values resulting from the ultrasonic measurements are listed, along with the relative decrease in percentages.

Table 15 Young's modulus Soda Lime Silica glass from tests

Temperature (°C)	E-modulus ($\cdot10^3$ N/mm^2)	Decrease (%)
20	75.2	100
100	74.8	99
200	74.7	99
300	74.0	98
400	71.9	96
500	67.3	89
600	59.6	79

Table 16 Young's modulus Soda Lime Silica glass from tests including change of length rod

Temperature (°C)	E-modulus ($\cdot10^3$ N/mm^2)	Decrease (%)
20	75.2	100
100	75.0	100
200	74.7	99
300	73.7	98
400	71.6	95
500	67.9	90
600	62.3	83

Table 17 Young's modulus Borosilicate glass from tests

Temperature (°C)	E-modulus ($\cdot10^3$ N/mm^2)	Decrease (%)
20	64.0	100
100	64.7	101
200	66.1	103
300	67.3	105
400	67.3	105
500	65.2	102
600	60.1	94
700	51.7	81

Table 18 Young's modulus aluminium from tests

Temperature (°C)	E-modulus ($\cdot 10^3$ N/mm^2)	Decrease (%)
20	72.0	100
40	72.1	100
60	71.4	99
80	70.2	97
100	68.7	95
120	67.2	93
140	65.8	91

Appendix C: Temperature-Time curves laminated glass panels

In this Appendix the results of the measurements of the thermocouples on both sides of the glass are presented for each laminated glass panel. Also the average temperature is added to the temperature-time curve for each panel. Note: this temperature should not be confused with the temperature of the interlayer. The interlayer temperature was not measured.
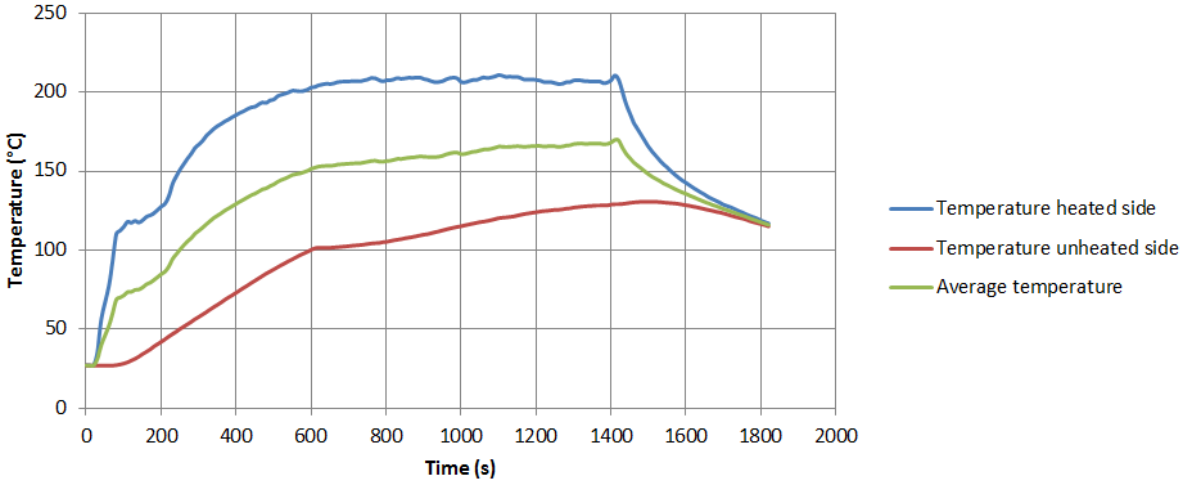
Tests with heaters
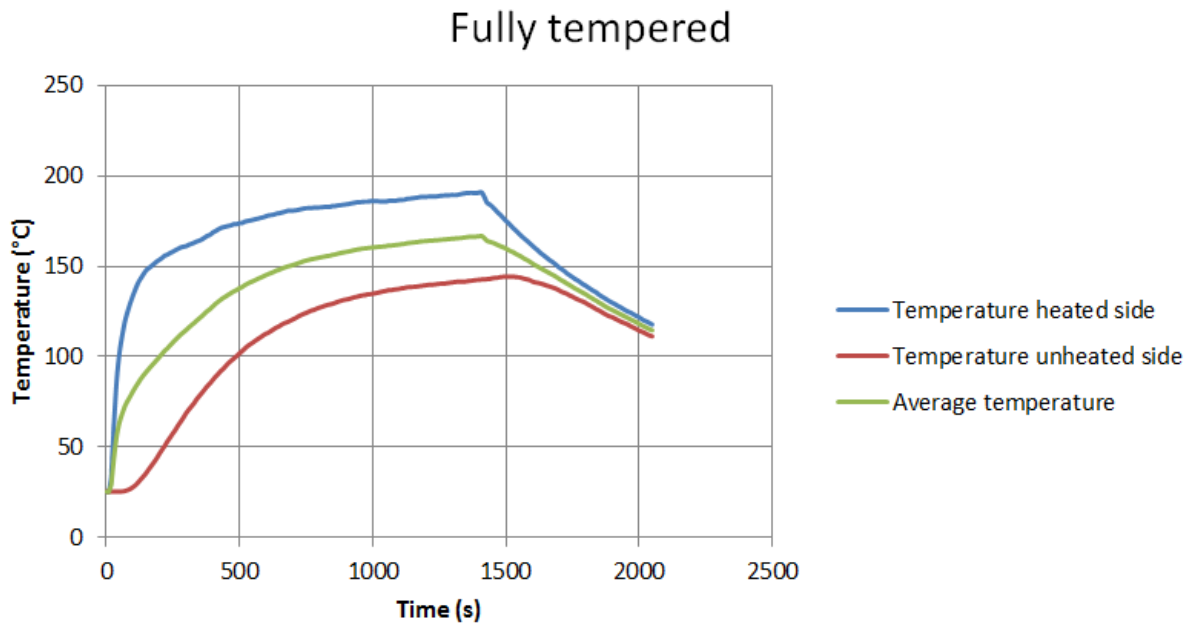
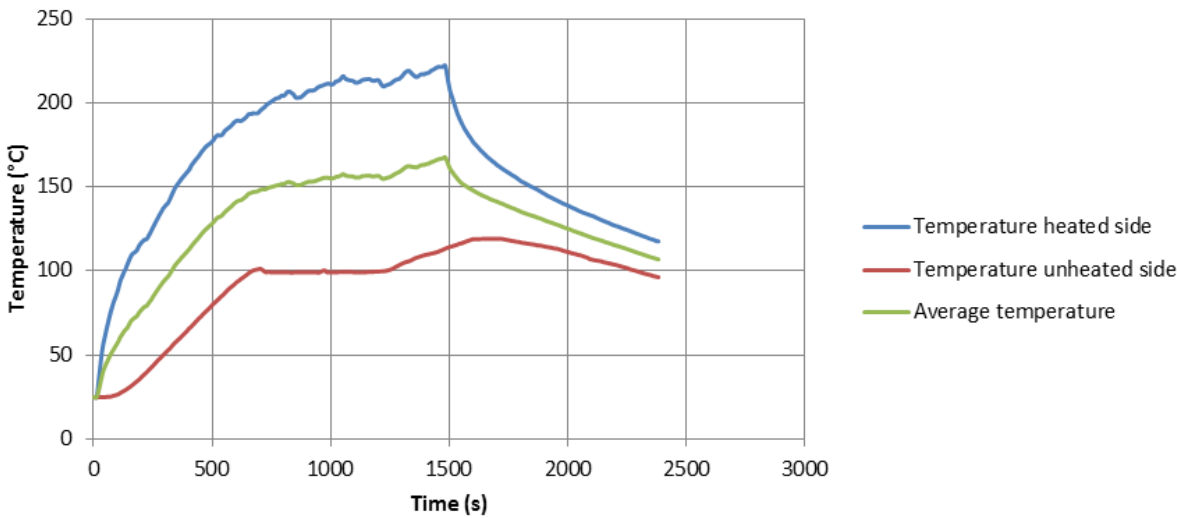Figure 60 Temperature-time curve fully tempered glass
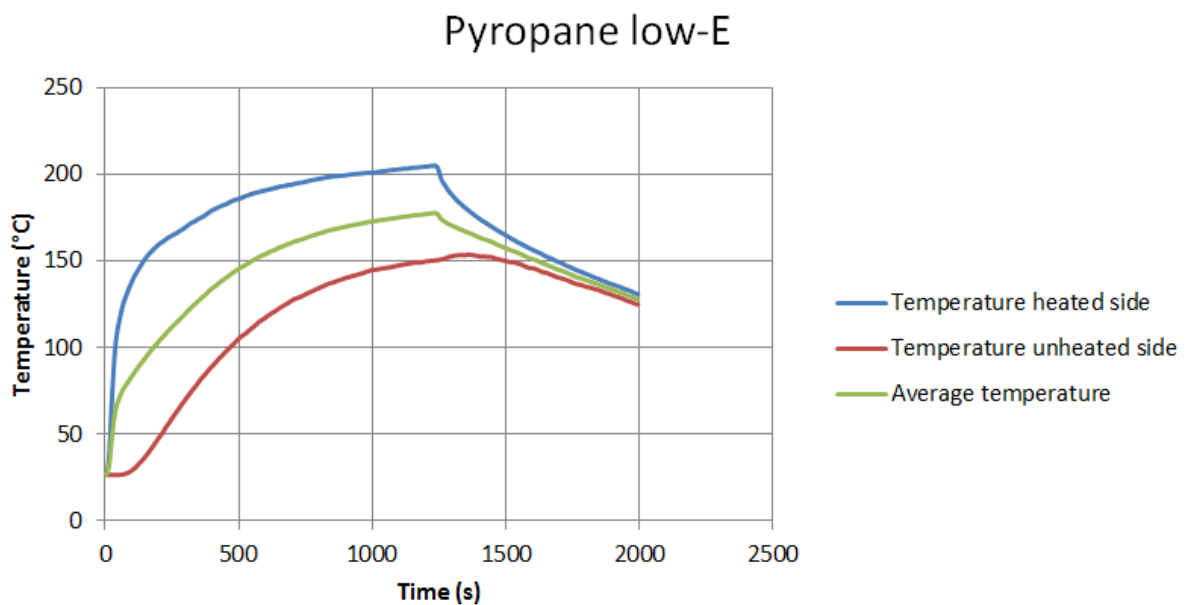
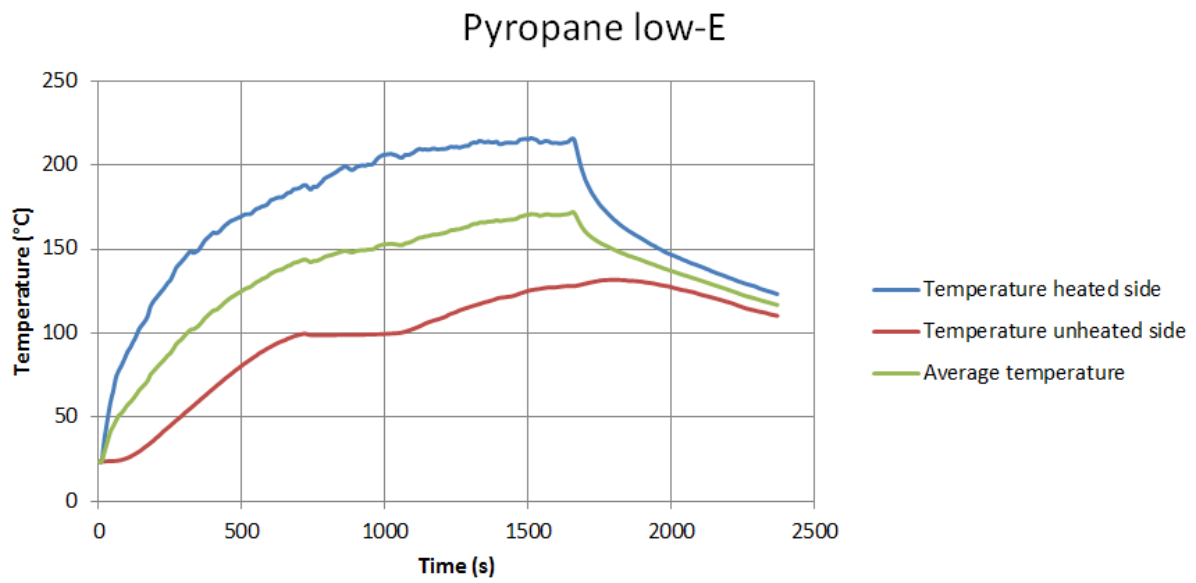Figure 61 Temperature-time curve pyropane low-E coating
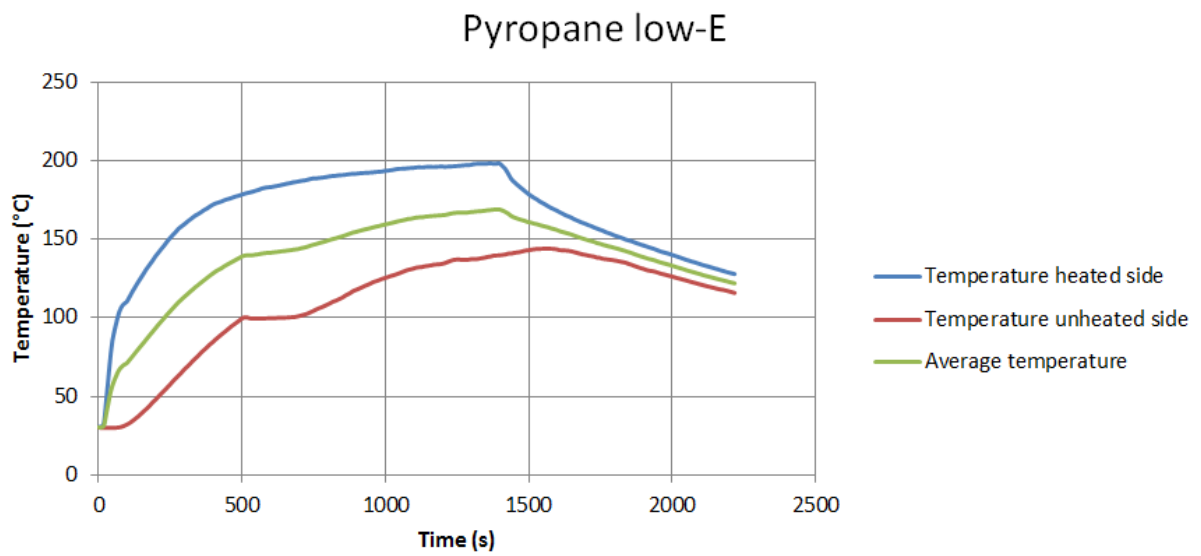
Figure 62 Temperature-time curve pyropane low-E coating
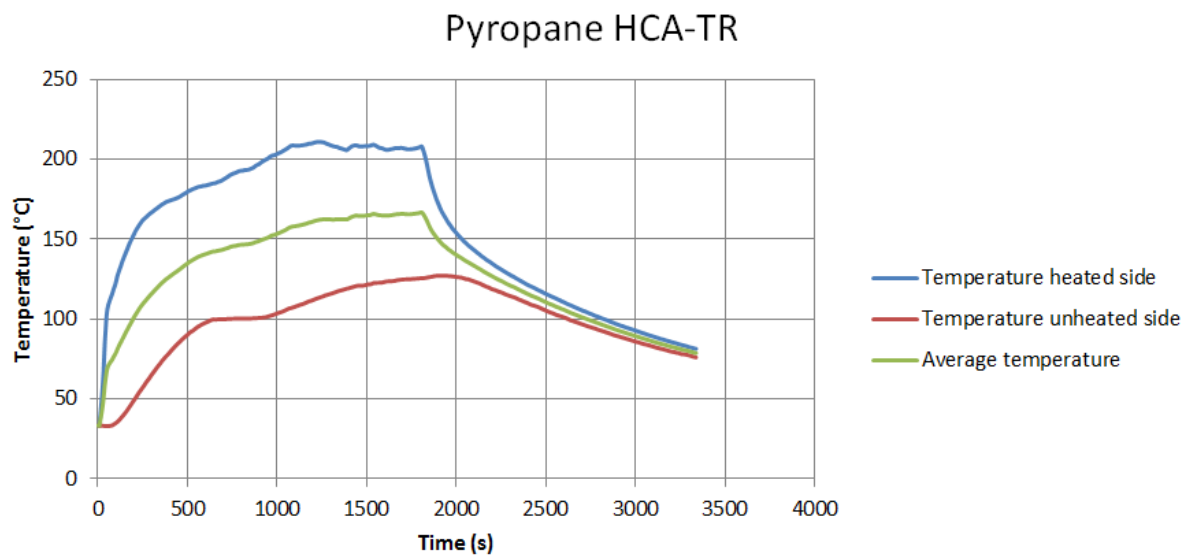
Figure 63 Temperature-time curve pyropane HCA-TR coating
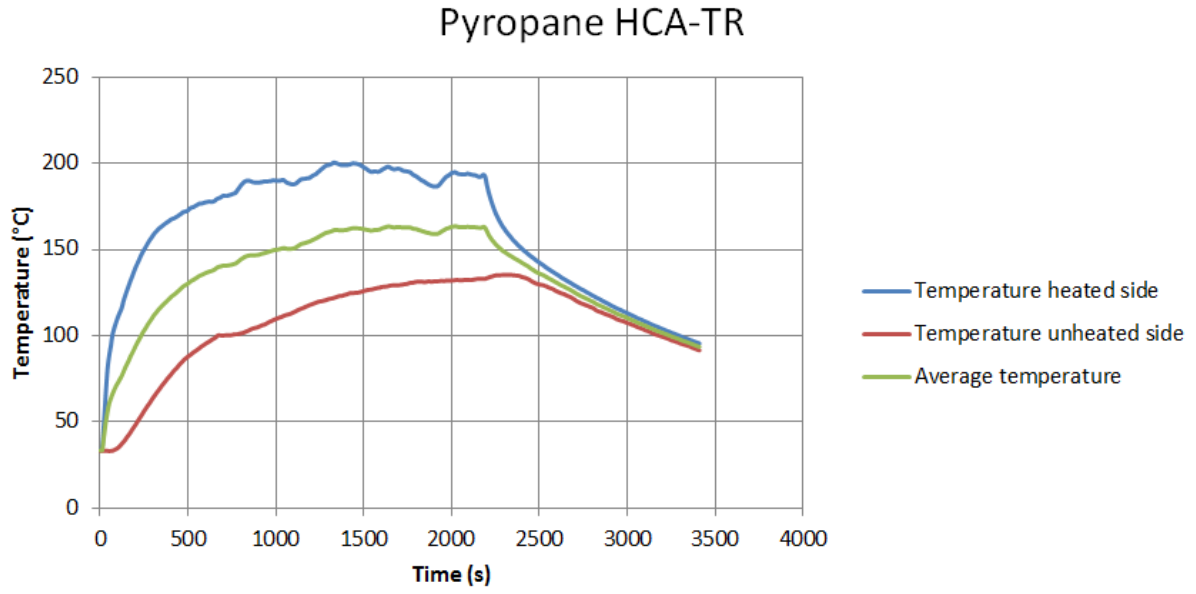
Figure 64 Temperature-time curve pyropane HCA-TR coating
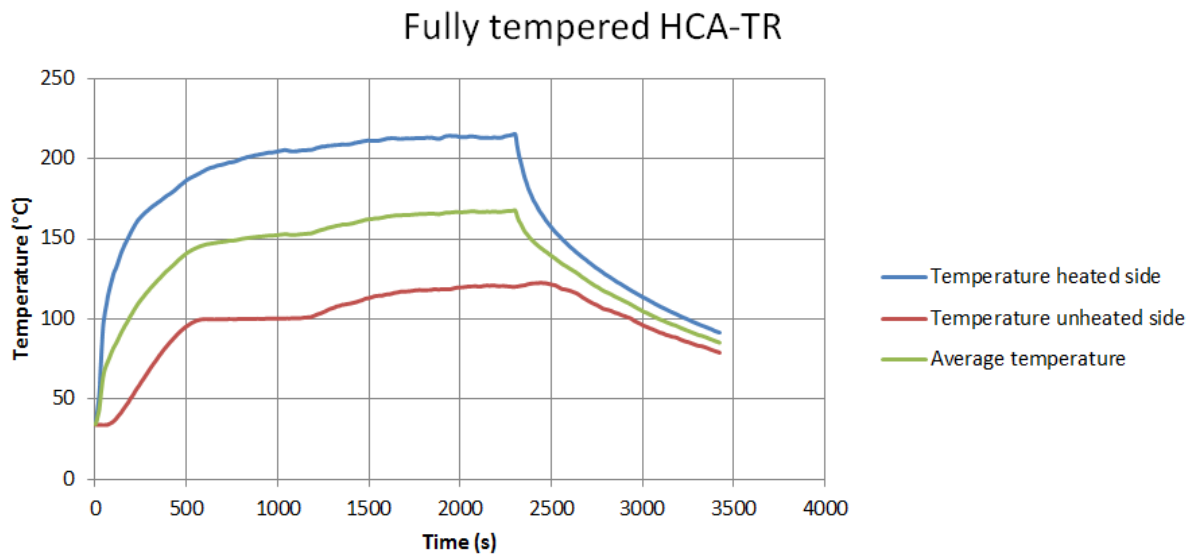
Figure 65 Temperature-time curve fully tempered HCA-TR coating

80

Tests with burner

Figure 66 Temperature-time curve fully tempered glass

Figure 67 Temperature-time curve pyropane low-E coating
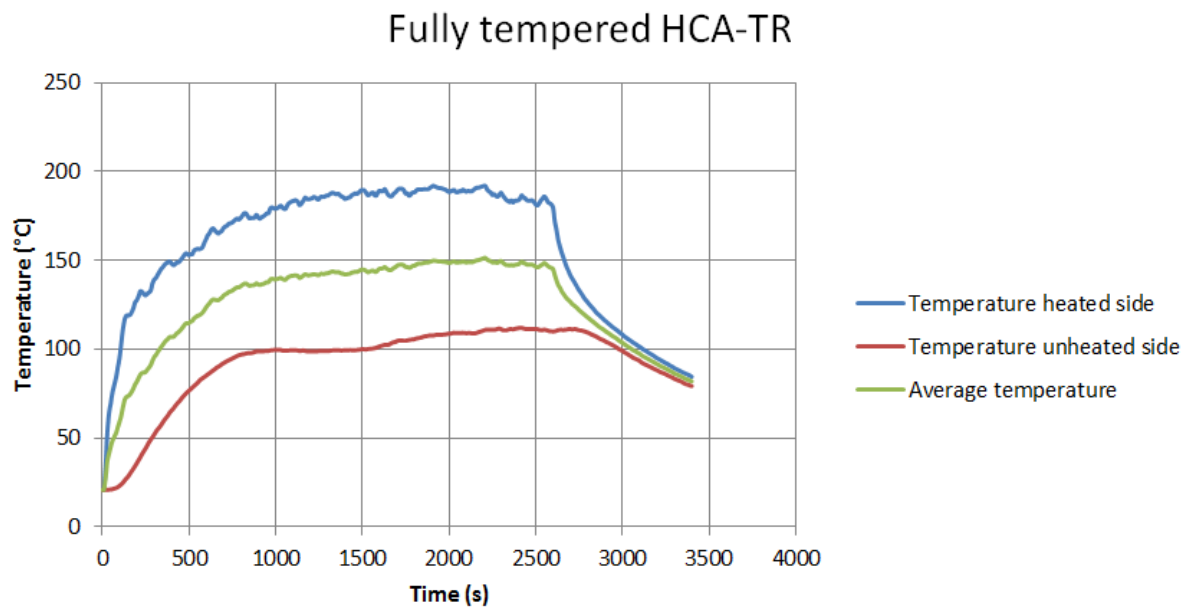
Figure 68 Temperature-time curve pyropane low-E coating

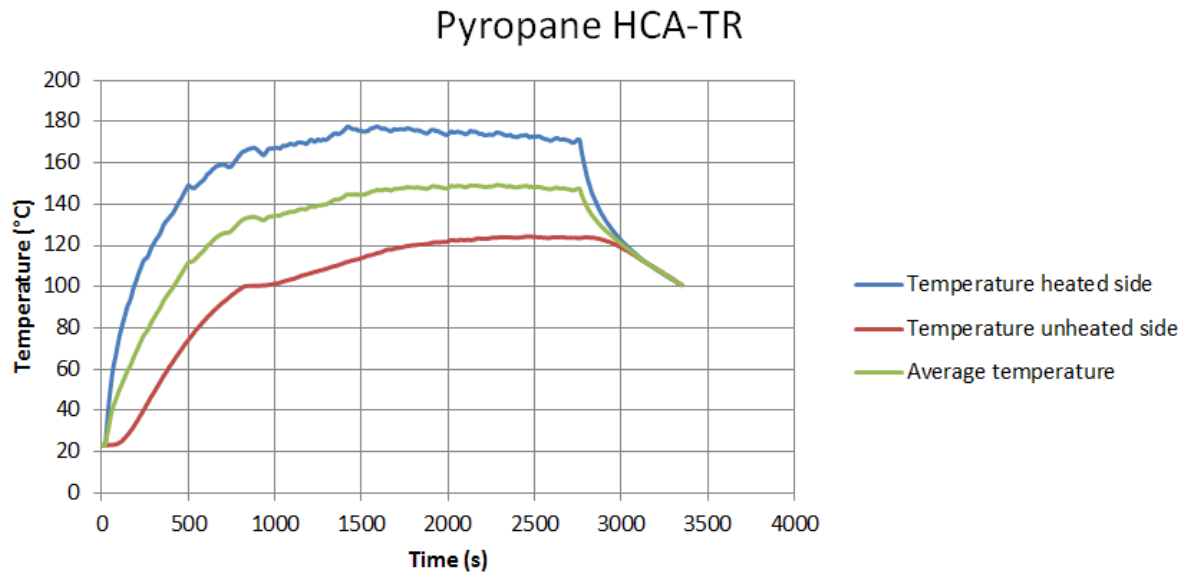**Figure 69 Temperature-time curve fully tempered HCA-TR coating**

82

Figure 70 Temperature-time curve pyropane HCA-TR coating

Appendix D: Thermal transmittance glass panels

Prior to the experiments with the laminated glass panels described in section 5, the thermal transmittance of the glass panels was determined. The thermal transmittance is the rate of heat transfer through matter and is expressed as a U-value. The unit for the U-value is W/(m²·K). The value indicates the degree of thermal conductivity of the glass: a high U-value means thermally poor insulating glass, a low U-value the opposite.

The U-value was determined by measuring the heat flux (flow of energy per unit of area) of the glass panel in W/m². Therefore the glass panels were placed at the opening of a box, thereby closing of the space within the box. A light bulb was hanging in the box with a temperature of approximately 45°C. Due to the heat of the light bulb, the temperature within the box increased and resulted in a temperature difference at both sides of the panel. This difference is measured for both the glass and the air. The set-up can be seen in Figure 71.

Figure 71 Thermal transmittance test set-up

From the heat flux, the R-value (in m²·K/W) can be determined from the following equation:

$$q = \frac{\Delta T}{R}$$

Where q is the average heat flux measured and ΔT is the temperature difference of the glass. With the value for R the U-value can be calculated according to:

$$U = \frac{1}{R + 0.17}$$

When the measured heat fluxes on both sides of the glass were stable and equal to each other, the measured values for the temperature and heat flux could be read.

For the fully tempered panels this resulted in a U-value of 4.1 W/(m^2·K) and 3.9 W/(m^2·K) for the pyropane panels with low-e coating. The difference between the panels is very low. It was concluded that the effect of the low-e coating could not be tested with this set-up. Also there was a difference with the given U-values from the manufacturer. Furthermore, not all glass panels were delivered due to rejection, so not every configuration could be tested. The amount of tested panels was also too low to base conclusions on these results. Therefore these measurements were not incorporated in the results.